UDK 62
DOI: http://doi.org/10.21857/9xn31cv46y

ISSN 1848-8935 (Online)
ISSN 1330-0822 (Tisak)

RAD

HRVATSKE AKADEMIJE
ZNANOSTI I UMJETNOSTI

549

TEHNIČKE ZNANOSTI
21

ZAGREB, 2022.

RAD HRVATSKE AKADEMIJE ZNANOSTI I UMJETNOSTI
KNJIGA 549

HRVATSKA AKADEMIJA ZNANOSTI I UMJETNOSTI
RAZRED ZA TEHNIČKE ZNANOSTI

CROATIAN ACADEMY OF SCIENCES AND ARTS
DEPARTMENT OF TECHNICAL SCIENCES

Razred za tehničke znanosti
Trg Nikole Šubića Zrinskog 11, 10000 Zagreb
kim@hazu.hr

Elektronička inačica svih tekstova objavljenih u časopisu dostupna je na središnjem portalu hrvatskih znanstvenih i stručnih časopisa HRČAK na e-adresi http://hrcak.srce.hr/rtz

The electronic versions of all texts published in the journal are available on HRČAK, the central portal for Croatian scientific and expert journals. Link http://hrcak.srce.hr/rtz

UDK 62
DOI: http://doi.org/10.21857/9xn31cv46y

ISSN 1848-8935 (Online)
ISSN 1330-0822 (Tisak)

R A D

HRVATSKE AKADEMIJE
ZNANOSTI I UMJETNOSTI

549

TEHNIČKE ZNANOSTI

21

ZAGREB, 2022.

CONTENTS / SADRŽAJ

DOI: 10.21857/90836c72vy

Pregledni članak / Review paper
Prihvaćeno / Accepted: 14. listopada 2021.

ADVANCED TECHNICAL SOLUTIONS FOR MARINE POLLUTION CONTROL IN THE ADRIATIC SEA

Maja Perčić, Nikola Vladimir, Ivana Jovanović, Marija Koričan, Andro Bakica

Summary

The major environmental problems within the maritime sector are atmospheric pollution due to the extensive use of fossil fuels in ship power systems, as well as seawater pollution from various sources (e.g. oil spills, microplastic, acidification, etc.). Due to their negative effect on the environment, human health and marine ecosystem, they should be carefully controlled. The studies on environmental problems of the maritime sector are more focused on atmospheric pollution, mainly thanks to the Paris Agreement. The ships are mostly powered by conventional power systems (diesel engines), and their negative effect on the environment would be lower with the implementation of some measures for emission reduction. In this paper, the outcomes of the research into the advanced technical measures for maritime pollution control are summarized, where the emphasis is put on ro-ro passenger ships engaged in the Croatian short-sea shipping sector. The results of the performed Life-Cycle Assessment (LCA) and Life-Cycle Cost Assessment (LCCA) suggested that conventional power systems should be modernized by ship electrification. This solution is represented as the most cost-effective and the most environmentally friendly solution regarding air pollution reduction. Furthermore, regarding seawater protection, several aspects of the advanced early warning system, that is being developed by the authors, are discussed. Finally, in line with the global trends in the maritime sector, a review on increasing the degree of autonomy of ships is given, as one of the most important topics for the near future.

Keywords: marine pollution; emission reduction; ro-ro passenger ship; alternative fuels; energy-saving device; early warning system.

1. ENVIRONMENTAL PROBLEMS IN THE MARITIME SECTOR

Nowadays, the effect of marine transportation on the maritime environment has become a very important issue for all parties involved in the shipping sector, i.e. shipbuilders, ship owners and operators, public authorities, policymakers, etc. Marine exhaust gas generated by the combustion of fossil fuel in marine engines can be considered one of the major causes of marine environment pollution. Another environmental problem inherent to the maritime sector is seawater pollution, which represents a direct impairment of the marine ecosystem triggered from a variety of sources [1]. Air pollution negatively affects the environment with global warming and acidification on global basis, while the seawater pollution effect on the environment is locally oriented, and affects the ecosystem and the human health for people nearby the pollution source, which is especially destructive if the sea is enclosed, as is the case with the Adriatic Sea.

The environmental protection of the Adriatic Sea needs to be addressed through a dual approach. The first one is air protection by the reduction of the shipping emissions released during the combustion of fossil marine fuel in a ship power system, which refer to the harmful emission of nitrogen oxides (NO_X), sulphur oxides (SO_X), carbon monoxide (CO), carbon dioxide (CO_2), particulate matter (PM), and hydrocarbons [2]. The environmental trends are nowadays moving toward the electrification of the shipping sector, which could ensure zero-emission shipping (at least in the ship operation stage), i.e. navigation without tailpipe emissions.

The second approach in the environmental protection of the Adriatic Sea should be focused on the development of the early warning protection system, which would continuously monitor the real-time data of the seawater quality. Such systems enable on-time actions, which prevent further pollution accidents [3].

Although seawater pollution is a very important problem that needs to be resolved, the current trends and research are focused on the emissions reduction from which the ship exhaust gas is comprised and contributes to the atmospheric pollution, while seawater pollution is mainly investigated from the biological point of view, as a factor affecting marine life.

As mentioned above, the reduction of emissions in all kinds of waterborne transportation (long-distance shipping, short-sea shipping and inland shipping), as well as seawater protection, are very important research topics, and there is a number of projects worldwide targeting particular ship types, navigation areas or the implementation of different technical and operative measures to achieve environmental benefit in a particular sector. This work brings an overview of the research results obtained at the Chair of Marine Engineering of the Faculty of Mechanical Engineering and Naval Architecture,

University of Zagreb, within several competitive ongoing research projects. They are dedicated to the improvement of ship energy efficiency and environmental friendliness for vessels operating in the Adriatic Sea, as well as to the seawater protection in this area.

2. AIR PROTECTION IN THE ADRIATIC SEA

2.1. General about the reduction of CO_2 emissions in the shipping industry

One of the important environmental problems that the global community is facing nowadays is global warming, caused by the increased concentration of anthropogenic Greenhouse Gases (GHGs) in the atmosphere. These GHGs refer to the emission of CO_2, methane (CH_4), nitrous oxide (N_2O) and fluorinated gases in very low concentrations. The GHGs in the atmosphere form a thick layer that prevents energy from the Sun to escape into space. Furthermore, the Earth is warming, which causes various climate changes [4], [5]. The relevant legally binding international treaty on climate change is the Paris Agreement, which entered into force in 2016. It aims at keeping the global temperature rise below 2°C compared to preindustrial levels, requiring a sharp decrease in the global amount of CO_2 emissions, since it is the main GHG [6]. With the UN holding that each sector should reduce the GHGs, the shipping sector is being pushed towards reduction of its Carbon Footprint (CF), which represents a measure of the total amount of CO_2 or CO_2-eq emissions caused by indirect or direct activity, or is accumulated over the life-cycle of a product [7]. The reduction of the CF refers to representing an environmental trend that is the main focus of number of studies on emission reduction in the maritime sector.

In order to reduce the CF of the maritime sector, different technical and operational measures can be implemented [8], [9], Figure 1. Most of these measures refer to the reduction of fossil fuel consumption. In that way, not only CO_2, but also other pernicious emissions released during fuel combustion are reduced.

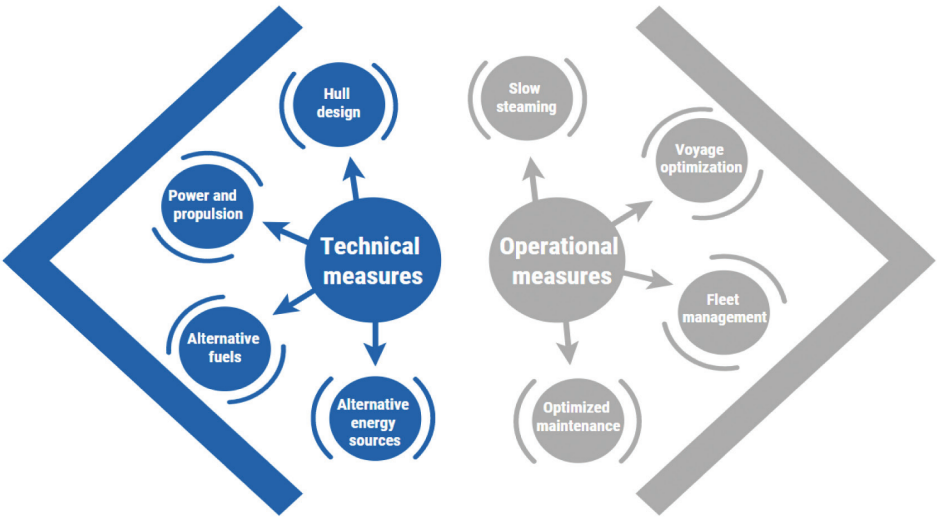

Figure 1. Measures for the CF reduction of the maritime sector [10]
Slika 1. Mjere smanjenja ugljičnog otiska u pomorskom sektoru [10]

Technical measures can be divided into four groups: hull design, propulsion and power, alternative fuels, and alternative energy sources. While some measures refer to the optimization of propeller/trim/hull or the implementation of Energy-Saving Devices (ESDs), the most significant technical measure that might result in a great reduction of shipping emissions is the replacement of conventional ship power system with an alternative one that is powered by cleaner fuel with lower carbon content, or alternative powering options, such as Renewable Energy Sources (RESs) [11].

Among different alternative fuels for maritime purposes, Liquefied Natural gas (LNG) is the most used. Even though it is of fossil origin, it has lower carbon content than diesel fuel, and its use in a dual-fuel engine regularly results in lower CO_2 emissions [12]. Methanol [13] and biofuels [14] are also thoroughly investigated for maritime purposes. However, the ultimate game-changer for the CF reduction of the maritime sector is the implementation of zero-carbon fuels, such as electricity [15] and hydrogen [16]. Their application in a ship power system results in no tailpipe emissions [17].

The potential RESs for maritime purposes include wind energy (e.g. sails, fixed wings, rotors, kites, and wind turbines), solar energy (Photovoltaic (PV) cells), wave energy, etc. [18]. Renewable energy solutions can be used for the ship propulsion or satisfying ship's auxiliary energy needs. The integration of the RESs in the ship power

system is a rather case-specific task that should be performed for each vessel separately, simultaneously taking into account its technical characteristics and operating profile (highly dependent on the navigation area and the climate factors, i.e. wind density, insolation, etc.).

Operational measures for the CF reduction include speed reduction, voyage optimisation, fleet management, optimised maintenance, etc. [19]. Among them, slow steaming, i.e. voluntary reducing the operational speed well below the design speed, is highlighted as the most effective and popular measure to reduce fuel consumption, which consequently leads to a reduction in fuel cost and released emissions [20].

Another set of measures form market-based measures. Among them, the implementation of carbon allowance is thoroughly investigated. The carbon allowance refers to a permit for emitting 1 ton of CO_2 [21]. Even though it still has not been implemented in the maritime sector, this additional cost would represent an incentive toward the emission reduction and the implementation of some technical or operative measures to reduce fossil fuel consumption, or completely replace it with alternative fuel with lower carbon content.

The IMO's strategy on the reduction of the GHG emissions represents three levels of ambition for achieving the goal of reduction of the GHGs from international shipping by 50% up to 2050, compared to the 2008 levels [22], Figure 2.

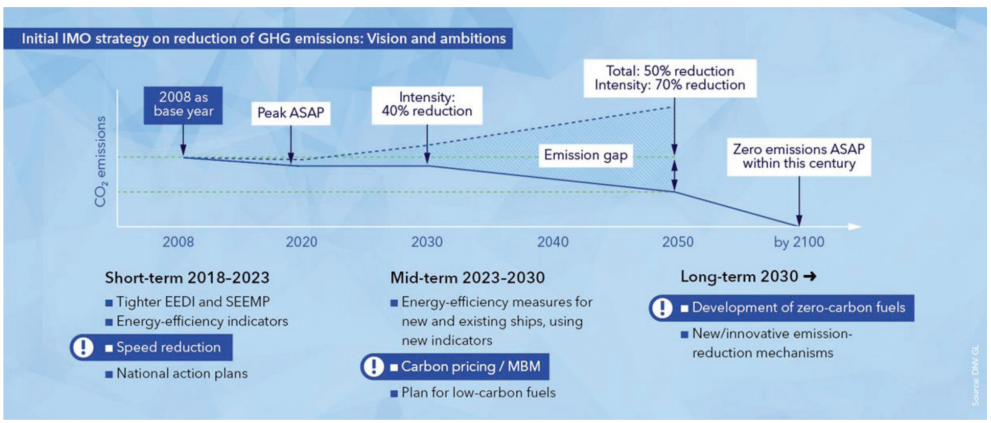

Figure 2. The IMO strategy on the reduction of the GHG emissions [23] (reproduced with permission of Det Norske Veritas (DNV))

Slika 2. IMO-va strategija za smanjenje emisija stakleničkih plinova [23] (slika je preuzeta iz literature uz dopuštenje klasifikacijskog društva Det Norske Veritas (DNV))

The short-term ambition (2018–2023) represents measures for the beginning of reducing the GHGs either by the introduction of energy efficiency regulation (Energy Efficiency Design Index (EEDI) and Ship Energy Efficiency Management Plan (SEEMP)) or by the implementation of an operative measure of speed reduction. The mid-term ambition (2023–2030) includes the measures of increasing the energy efficiency of ship power system, the implementation of low-carbon fuels and the implementation of carbon allowance in the shipping sector. The long-term ambition (2030–) refers to the development of zero-carbon fuels and innovative emission reduction technology that could achieve the 2050 goal and further zero-emission goal within this century [23].

2.2. The Croatian short-sea shipping sector

Croatia is situated on the East Adriatic coastline, which is very indented and has many islands. Since the islands need to be connected with the mainland by ships, the short-sea shipping fleet counts a great number of ships. The term short-sea shipping fleet refers to the ships that operate between national ports and between a country's ports and the ports of the neighbouring countries [24].

The released emissions during ship operation negatively affect the environment and human health; this is more pronounced for the ships that spend a lot of time near inhabited areas and in ports, which is the case for ships engaged in the short-sea shipping sector (e.g. ro-ro passenger ships) [25], [26]. Ro-ro transport refers to roll on – roll off transport for vehicles transported on and off the ship on their own wheels [27], while ro-ro passenger ship refers to a ship that transports both passengers and vehicles. A typical example of such a ship is a ferry. A major part of the Croatian ro-ro passenger fleet includes outdated vessels with an average age of 29 years powered by diesel engines. A total of 44 ro-ro passenger ships have been identified that operate on the Croatian side of the Adriatic Sea on 27 ferry lines, out of which 24 domestic and 3 international ferry lines, connecting Croatia to Italy and vice versa [10]. In order to determine which ferry lines have a major contribution to atmospheric pollution, the analysis has been performed by following steps presented in Figure 3.

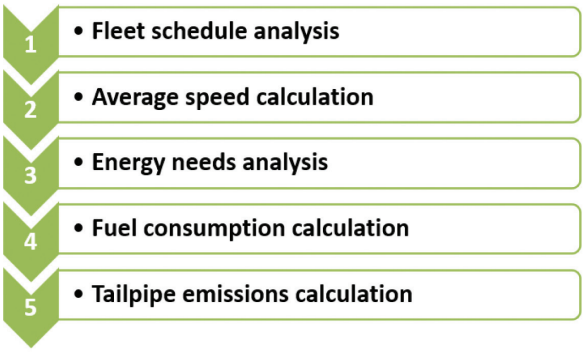

Figure 3. Analysis procedure of the emissions released from the Croatian ro-ro passenger fleet
Slika 3. Postupak analize emisija ispušnih plinova hrvatske ro-ro putničke flote

The mathematical model of the analysis is presented in the study by Perčić et al. [28]. The results are presented in Figure 4 and Figure 5, where annual tailpipe emissions of CO_2, NO_X, SO_X and PM of considered ferry lines are calculated.

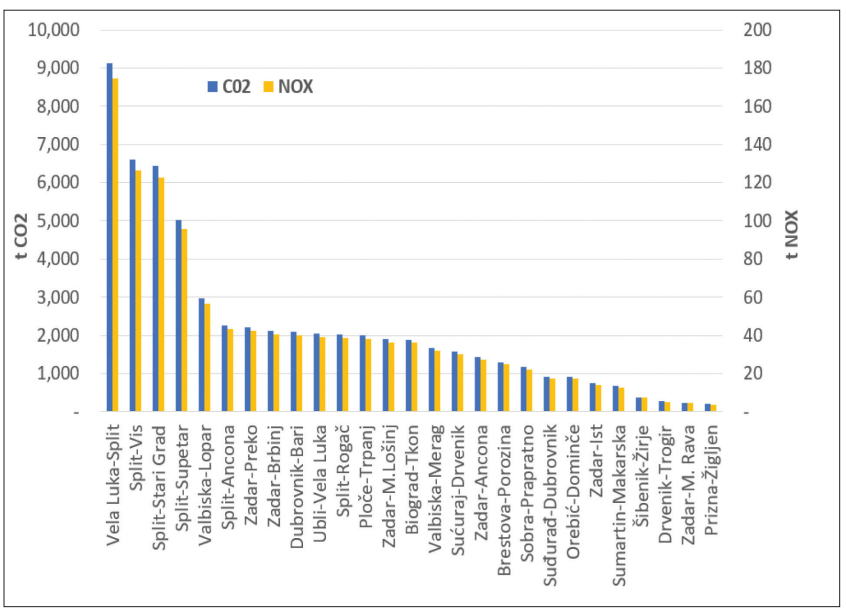

Figure 4. Annual CO_2 and NO_X emissions [29]
Slika 4. Godišnje CO_2 i NO_X emisije [29]

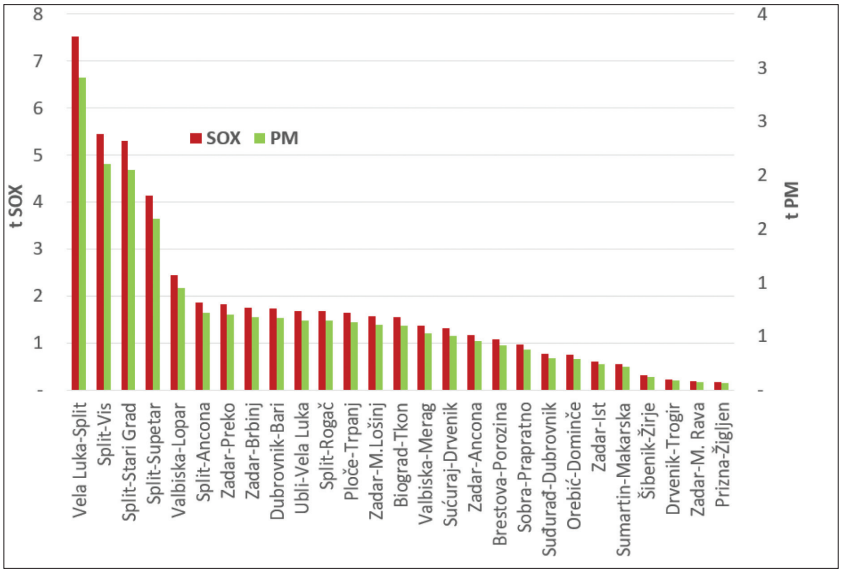

Figure 5. Annual SO_x and PM emissions [29]
Slika 5. Godišnje SO_x i PM emisije [29]

Calculated annual emissions indicated which ships, operating on specific ferry lines, contribute more to the atmospheric pollution and more negatively affect human health. With the application of the CF reduction measures, the tailpipe emissions would be reduced. The implementation of zero-carbon fuels in a ship power system does not generate tailpipe emissions during ship operation, but a great number of emissions are released during the production of such fuels. Since the main aim of the climate policy is to reduce the GHGs at global level, the emissions released through the entire life-cycle of fuel should be investigated by performing the Life-Cycle Assessment (LCA).

This paper illustrates some of the available technical solutions that can be implemented for the CF reduction of the Croatian short-sea shipping sector, whereby the emphasis has been put on the replacement of conventional diesel power systems installed on board selected ro-ro passenger ships.

2.3. Illustrative examples of the selected technical measures

The selected technical measures that offer a reduction of shipping emissions are the replacement of a conventional power system (i.e. diesel engine) with an alternative one, either powered by alternative and cleaner fuel or alternative powering options, such as the implementation of the RESs. Furthermore, the implementation of the ESD has been outlined as a technical measure of CO_2 emission reduction.

2.3.1. The application of alternative fuels in a ship power system

The analysis of the application of alternative marine fuels (electricity, methanol, dimethyl ether (DME), natural gas, hydrogen and biodiesel) has been performed in [28] for three ro-ro passenger ships that operate in the Adriatic Sea. They have been selected based on the route length, i.e. Ship 1 operates on a very short route (Prizna-Žigljen), while Ship 2 (Ploče-Trpanj) and Ship 3 (Split-Vis) operate on medium and long routes, Figure 6.

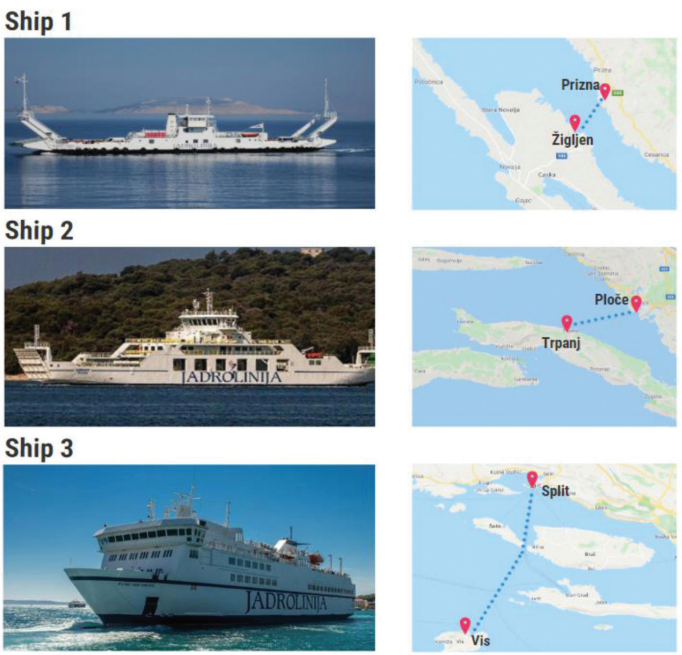

Figure 6. Selected ro-ro passenger ships and their routes [28]
Slika 6. Odabrani ro-ro putnički brodovi i njihove rute [28]

The most environmentally friendly fuel was identified with an LCA, considering the CO_2-eq emission released during the life-cycle of a power system. The investigated emissions are divided into three groups: Well-to-Pump (WTP) emissions refer to the emissions related to the fuel cycle (raw material extraction, production of fuel and its distribution to the refuelling station), Pump-to-Wake (PTW) emissions refer to the emissions released during the use of the fuel in a ship power system, i.e. ship operation, while Manufacturing emissions refer to the manufacturing of the main element of a power system. Each LCA is performed by means of the LCA software GREET [30], Figure 7.

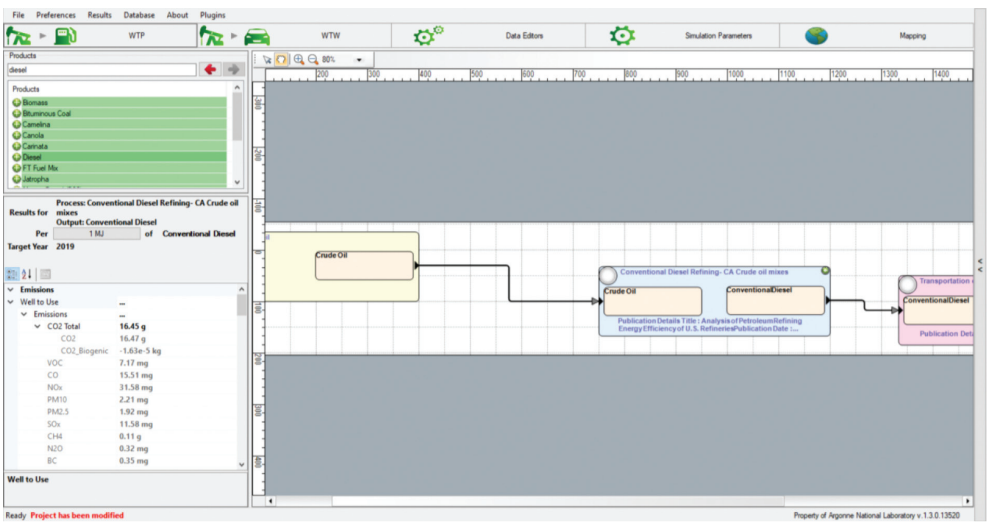

Figure 7. The interface of the LCA software GREET

Slika 7. Sučelje LCA programa GREET

The most cost-efficient power system is indicated by performing the Life-Cycle Cost Assessment (LCCA), which gathers the total costs of a power system, i.e. investment cost, fuel cost, maintenance cost, etc. In this research, the market-based measure of carbon allowance implementation is observed, where the most rigorous implementation scenario, i.e. the Sustainable Development (SD) scenario, is considered.

Both economic and environmental assessments are performed from the lifetime point of view of 20 years. Mathematical models are presented in [28], while the results of the research are shown in Figure 8, whereby D denotes diesel, E denotes electricity, M refers to methanol, the LNG refers to liquefied natural gas, the CNG denotes compressed natural gas, the DME denotes dimethyl ether, the RH represents renewable hydrogen, the FH represents fossil hydrogen, and the BD refers to biodiesel-diesel blend.

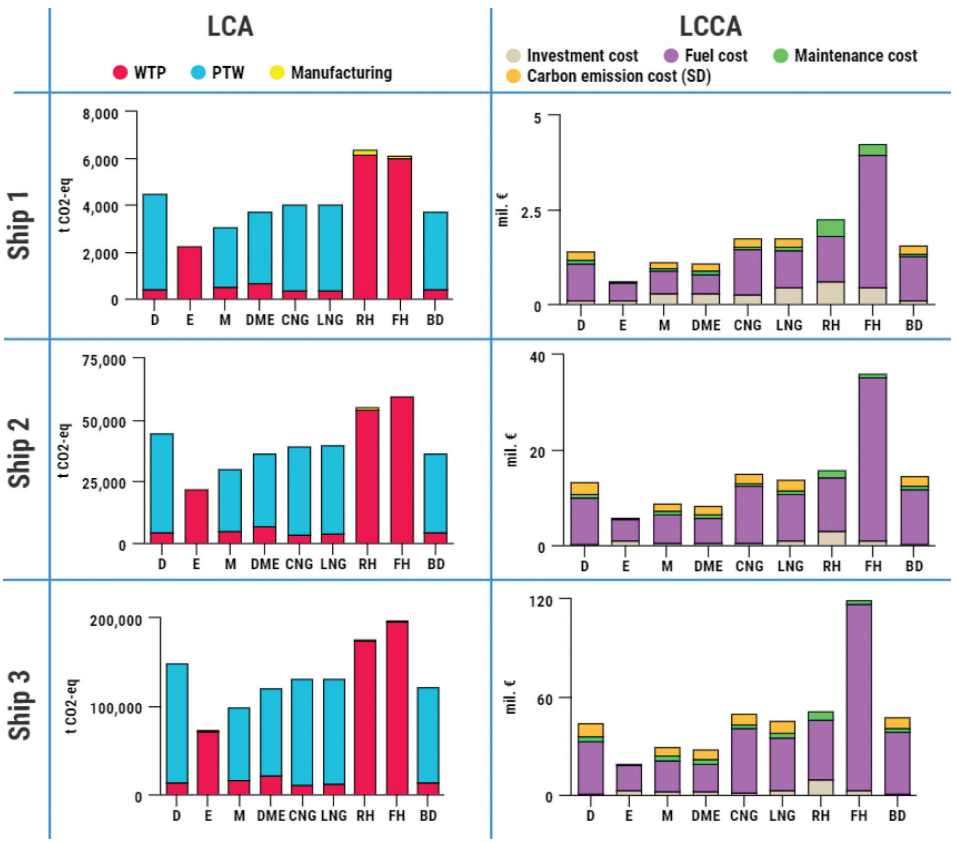

Figure 8. The environmental and economic assessment of different alternative fuels [28]

Slika 8. Ekološka i ekonomska analiza različitih alternativnih goriva [28]

The results indicate that for each considered ship, an electricity-powered ship with only a battery as power source is the most environmentally friendly and the most cost-efficient power system among those considered. On the other hand, a power system constituted of low-temperature fuel cell powered by fossil hydrogen represents the worst alternative option to be implemented in a ship power system.

2.3.2. The utilization of solar energy for ship energy needs

The analysis of different ship power systems (diesel-powered ship, battery-powered ship and PV cells-battery-powered ship) is performed and presented in [31], where the results relate to the ship that operates on the Ploče-Trpanj route, i.e. Ship 2 from Figure 6.

The utilization of solar energy for ship energy needs is accomplished by the installation of the PV cells on the ship deck. However, the selected ship cannot be powered only by solar power. Therefore, a PV system is incorporated into a power system with a battery. Such as in the previous illustrative example, in this research, the LCA and the LCCA are also performed to highlight the most ecological and economic power system. The mathematical model is presented in [31], and the results of the research are presented in Figure 9 and Figure 10.

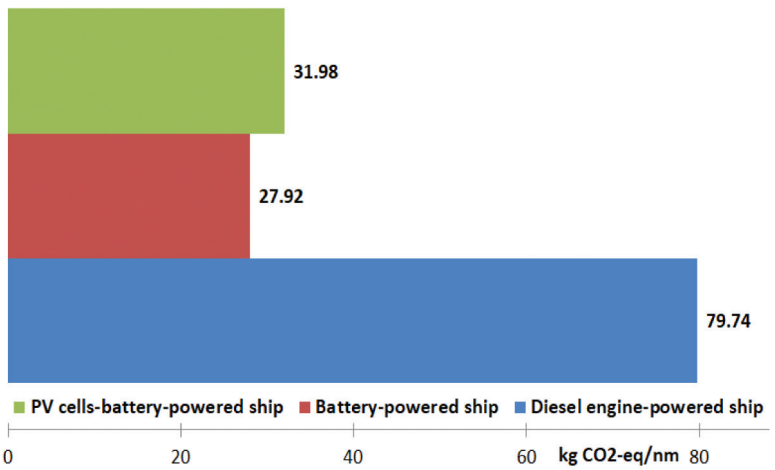

Figure 9. The LCA comparison of selected power systems [31]

Slika 9. Usporedba cjeloživotnih emisija odabranih energetskih sustava [31]

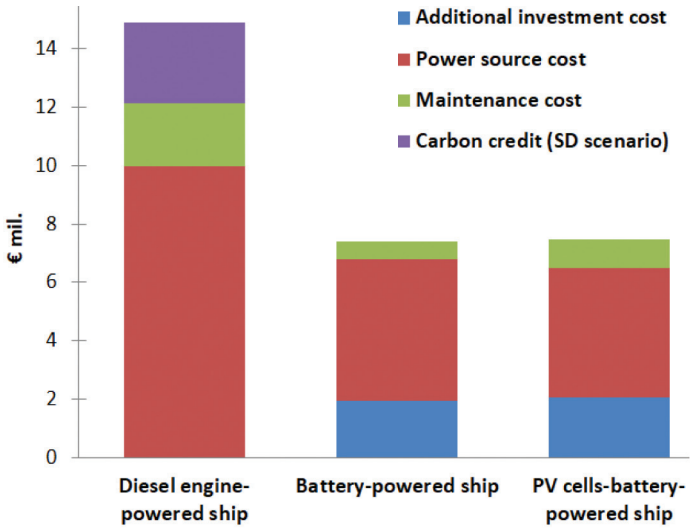

Figure 10. The LCCA comparison of selected power systems [31]
Slika 10. Usporedba cjeloživotnih troškova odabranih energetskih sustava [31]

Both considered alternative power system configurations are presented as a more ecological and cost-effective option than the existing power system configuration with diesel engine installed on board ro-ro passenger ship. Even though the PV cells-battery-powered ship satisfies some of its energy needs with solar energy, which is generated without released emissions, due to the emissions released within the process of PV system manufacturing, the battery-powered ship has a slightly lower CF and slightly lower total costs than the PV cells-battery-powered ship.

2.3.3. The installation of energy-saving devices

Recently, the ESDs have become an attractive and cost-effective measure not only in reducing fuel consumption in the shipping sector, but consequently also in reducing the carbon footprint. The ESDs can be installed both on new buildings and existing vessels in an attempt to increase its fuel efficiency. Compared to all possible improvements with respect to marine propulsion, the ESDs provide one of the least expensive alternatives, although it should be clearly stated that not every ESD can be beneficial for a specific type of ship. Essentially, these devices recover energy losses at the vicinity of the propeller, so for each device to operate properly, there must be a specific type of energy loss present in order for the ESD operational profile to be effective [32], [33].

The commonly accepted classification of ESDs is according to their location with respect to the propeller plane [34], as shown in Figure 11. Zone I (behind the propeller) devices alter the flow before it reaches the propeller by enhancing a radial uniform velocity distribution (duct type) or by adding an additional rotational component to reduce the amount of kinetic energy losses in the propeller wake (pre-swirl stator and other fin type ESDs), or by combining the benefits of both the duct and the fin typed ESD (e.g. Mewis duct). Zone II devices refer to the non-conventional propeller designs, such as contracted and loaded tip propellers, contra-rotating propeller or propeller hub improvements (propeller boss cap fins), which effectively reduce the hub vortex. Finally, Zone III devices aim at recovering energy losses in the propeller slipstream. This usually includes rudder modifications or the unconventional free-to-rotate wheel retrieving rotational kinetic energy from the propeller.

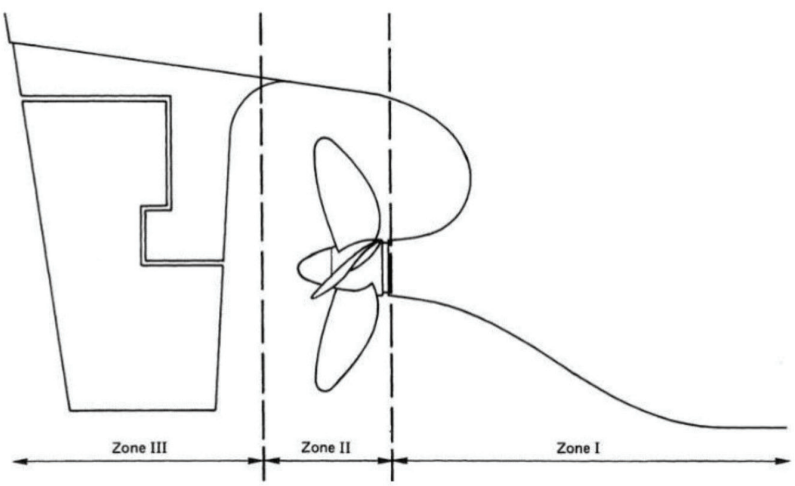

Figure 11. The classification of energy saving devices [34]
Slika 11. Klasifikacija uređaja za uštedu energije [34]

Currently, the most widespread and investigated devices for standard merchant fleet belong to Zone I. One of the first devices is the Wake Equalizing Duct (WED). Numerous authors investigated WED by using numerical methods [35] or experimental analysis [36], with estimated savings ranging even up to 9% in propulsive efficiency. Even commercially available designs are available with the authors in [37], stressing optimum effectiveness if the ship design speed lies between 12 and 18 knots, with a block coef-

ficient larger than 0.6. Similarly, the ESD designed by Mewis [38] – a combination of the duct and Pre-Swirl Stator (PSS) – reports suitable vessel speed under 20 knots, with high block coefficient as the most beneficial with savings from 3 to 9%. Obviously, these ship parameters favour the bilge vortex creation, hence creating necessary energy losses in the ship hydrodynamics, for which these ESDs can be beneficial. Similar savings of 3 to 6% are reported by Kim et al. [39] for the PSS and the PSS-duct combination. There furthermore exist the so-called vortex generators [40], but their benefit should yet be investigated in detail. Overall, devices in Zone I should not be optimized independently, but only together with both the hull and the propeller, while minimizing the flow separation at the ESD surface to reduce the drag from the installation of the device and possible vibration issues.

From the Zone II ESDs, the ongoing development is dedicated to contracted and loaded tip (CLT) propellers. These devices are theoretically explained and investigated in [41]. The CLT propellers shift the load distribution to the propeller tip; this improves the efficiency, but has a negative effect of increasing the pressure pulses on the ship stern surface, which is directly correlated to vibration and noise transmitted to the hull structure. Propeller Boss Cap Fins (PBCF) offer a simple advantage of reducing the hub vortex. The PBCF fuel savings range from 1 to 2% according to recent works in [42]; their safety and simple installation make them one of the prominent ESDs for ship owners. To the contrary, Contra-Rotating Propellers (CRPs) drastically reduce the rotational losses, but their high complexity and cost of maintenance make them suitable for specialized ship types only.

In Zone III, there are numerous rudder modifications to decrease the rotational energy loss, such as Z-twisted rudder with and without the bulb [43], placement of thrust fins on the rudder [44], X-twisted rudder [45], and even bio-mimicking wavy twisted rudder [46]. The range of savings for this type of rudder improvement lies between 2 and 5% in propulsion efficiency. Besides the rudder modifications, one of the most unusual ESDs is the Vane Wheel (VW). The VW is free to rotate after the propeller plane and designed as a turbine on the bottom part of the wing, while the geometry slowly transitions to a propeller blade shape on the outermost part. However, obvious complexities in design, maintenance and cost have not brought this device to prominence [47].

A combination of devices is possible for the optimum fuel consumption, but it should be clear that savings from a single device will not have the same efficiency when combined with another type of the ESD, having in mind their mutual interaction. Furthermore, devices reducing the same kind of energy losses should be assessed in detail before deciding whether their interaction is beneficial – for example, the PBCF combined with the rudder bulb, both of which reduce the hub vortex, is likely to reduce the

efficiency of their independent employment. Nonetheless, the evaluation of any ESD still remains an open subject due to scaling effects and uncertain estimation of interaction between the ESD, hull and propeller in real ship operation. Complementary data between experimental analysis and numerical simulations become important here. Due to high turbulence in the region near the propeller plane (i.e. wake field), the use of potential flow models is not recommended. In recent years, substantial progress in the field of the ESDs is owed to the Computational Fluid Dynamics (CFD) simulations. An example of a CFD simulation with propeller and the PSS is shown in Figure 12. Another subject still not fully addressed is the structural integrity of the ESDs. Given their novel design and the relatively complex flow field in which they operate, classification societies do not offer straightforward rules and regulations for their ultimate strength analysis, as well as fatigue. The lack of a clear design procedure initiated a joint project GRIP [48] featuring a thorough investigation of the PSS and the duct type ESD. Overall, given the current increasing regulations on harmful gases, the ESDs design will continue to mature and develop from the perspective of both the hydrodynamic design and the structural safety, while keeping in mind their promising benefit in terms of reduced fuel consumption.

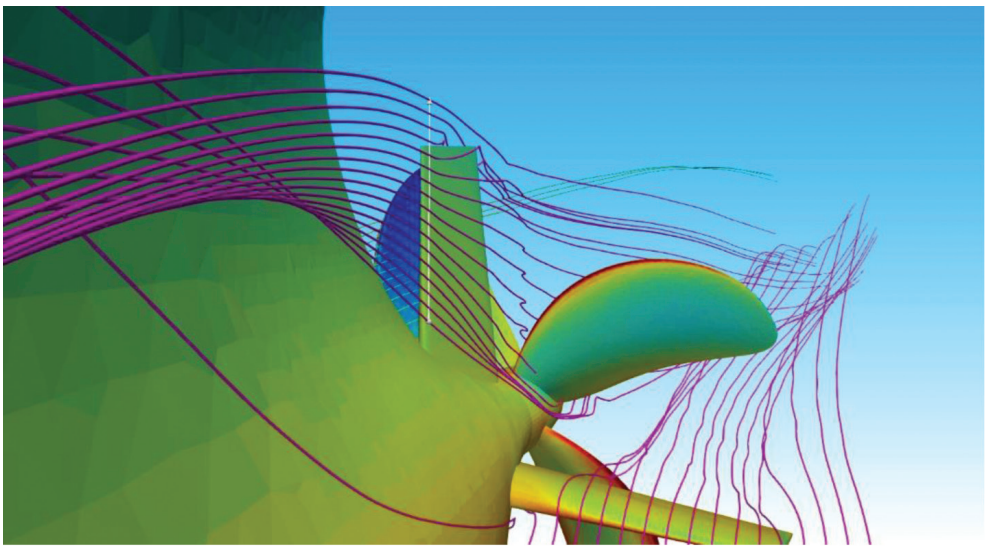

Figure 12. An example of the CFD simulation of flow around the ESD
Slika 12. Primjer CFD simulacije opstrujavanja uređaja za uštedu energije

The illustrative examples of the selected technical measures indicated that an electricity-powered ship with only a battery as a power source is the most ecological and the most cost-effective alternative power system that might replace the diesel engine power system configuration. By implementing the carbon pricing policy in the shipping sector, an electricity-powered ship appears more cost-effective due to the absence of tailpipe emissions.

Similar research as presented in this paper was performed for the Inland navigation fleet in Croatia. In that study, Perčić et al. [49] performed the LCA and the LCCA comparisons of different alternative fuels; the results are illustrated on three different types of ship: cargo ship, passenger ship, and dredger. The study showed that an electricity-powered ship with only a battery as power source represents the most ecological solution for each type of ship. However, the LCCA comparison indicated that an electricity-powered ship is the only cost-effective solution for a passenger ship, while for cargo ship and dredger, the methanol and diesel represent the most ecological solution, while for them, an electricity-powered ship results in very high costs. It is evident that the implementation of alternative fuels depends greatly on the area of navigation, as well as on the type of ship and its exploitation characteristics.

The main limitations of this research are:

- The assumption that the ship is powered by only one power source, and not with two or more power sources included in a hybrid power system. This may be thoroughly investigated by the means of an analysis of such a system and the individual shares of power sources included in it. Its environmental performance and cost-effectiveness can be assessed with optimization methods.
- The focus of the research is only on the atmospheric pollution due to emissions released through the life cycle of a power system. Replacing conventional fossil fuel with alternative fuel represents a feasible measure for the reduction of shipping emissions. While considering different alternative fuels, the toxicity of the fuel for the marine ecosystem in case the ship has an accident and the fuel ends up in the sea should be borne in mind. Therefore, with the replacement of diesel fuel with alternative and non-toxic fuel with low carbon content, seawater pollution and atmospheric pollution would be reduced.
- With respect to the ESDs, it is fair to say that their applicability was not investigated in detail for the Croatian coastal fleet, because at this stage, the emphasis of the research is on the development of hydro-structure mathematical models that will provide full insight into their structural design as a prerogative, while the techno-economic aspects will be addressed in future investigations.

3. SEAWATER PROTECTION IN THE ADRIATIC SEA

In addition to the harmful effect on the marine ecosystem, each seawater pollution problem negatively affects human health and the economy of the considered country as well. Current trends in the area of marine pollution prevention have led to the development of early warning systems with the installation of the multi-parameter probe on-site, and collecting the real-time data of several parameters. The process of establishment of an early warning system contains several steps. The first step is to conclude which parameters give valuable information about water quality level and setting up a repository that will receive and store data from various sources. The network of multi-parameter probes represents one source, a scientific set of data that can be analysed and understood by highly educated personnel. As a future challenge, the goal is to develop an application that can be used by the general public, and therefore raise the awareness of marine pollution issues [3], Figure 13.

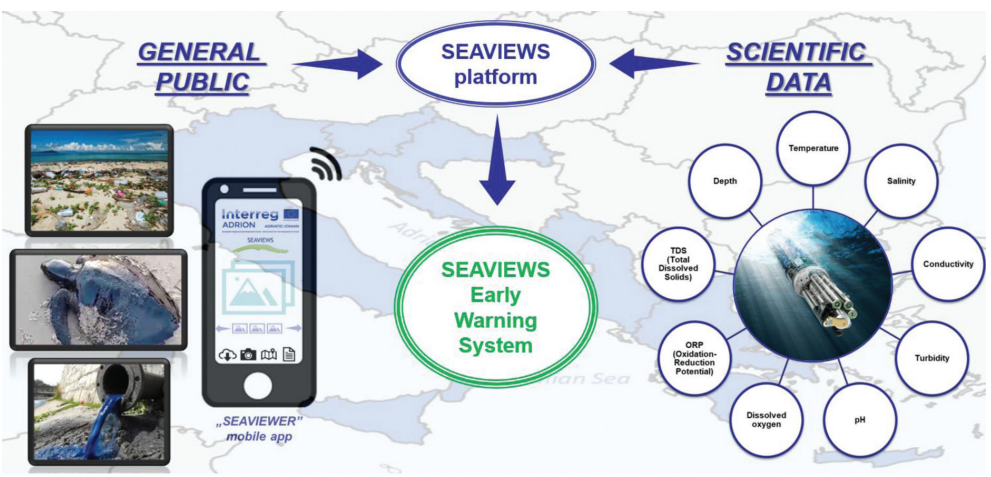

Figure 13. The preview of the early warning system developed within the SEAVIEWS project
Slika 13. Sustav ranog upozoravanja na zagađenje razvijen u okviru projekta SEAVIEWS

Some of the tracked parameters include salinity, temperature, pH, dissolved oxygen, total dissolved solids, etc., whose values can indicate that marine pollution occurred. The rise of water temperature can increase the risk of water-borne diseases, as well as contribute to the appearance of oxygen-depleted zones, i.e. "dead zones", which cause the mortality of marine organisms. Salinity variations due to the inflow of freshwater

can also affect the development of marine organisms, especially crustaceans. As a result of the absorption of a larger amount of CO_2 in the ocean and the production of carbonic acid, the acidification affects the photosynthesis of marine plants and prevents crustaceans from developing a strong exoskeleton [50].

4. FUTURE CHALLENGES IN THE COASTAL NAVIGATION – AN INCREASE OF SHIP AUTONOMY

Rapid technological development, wireless communication and monitoring, growing environmental awareness, alternative fuels, and stringent regulations are continuously present in maritime transportation and shipbuilding. The maritime sector is exploring ways to reduce cost and emissions, but at the same time to increase safety and energy efficiency. Autonomous shipping is an emerging topic, where technical, economic, safety, and environmental aspects are still not mature enough to significantly increase the percentage of autonomous vessels in the global fleet. The technologies needed for autonomous navigation already exist, and it is necessary to find the optimal way to combine their safety, reliability, feasibility, and cost-effectiveness. It is also important to investigate what types of ships and which trades are suitable for autonomous shipping.

The autonomous ship contains some form of autonomy, which means that certain tasks are executed without human interference [51]. Autonomy degree increases while human involvement decreases. A fully autonomous ship can perform all the needed tasks by itself. A fully autonomous merchant ship is not likely to be seen in the coming future, but transferring some assignments from crew to autonomous systems and shore is the way to achieve this goal [52]. The path from manned to autonomous ship is shown in Figure 14, indicating that remote control enables unmanned shipping.

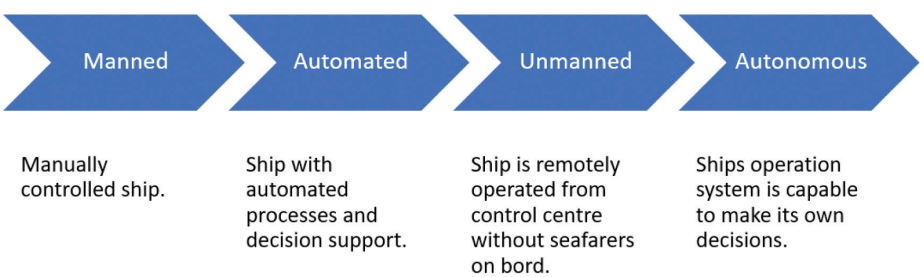

Figure 14. The path from manned to autonomous ship

Slika 14. Put od broda s posadom do autonomnog broda

The transition from manned to unmanned and autonomous shipping is expected to be gradual, with a lot of alternations, testing, and simulations [53]. It is important to precisely define the levels/classes of autonomy. Currently, there are a few classifications of ship autonomy, and they are shown in [53].

The International Maritime Organization has defined the following four Degrees of Autonomy (DoA) related to Maritime Autonomous Surface Ships (MASS) [54]:

1. DoA1, ships with automated processes and decision support, where the seafarers are on board for the operation and control. Some operations may be automated and at times be unsupervised, but with seafarers on board, ready to take control.
2. DoA2, a remotely controlled ship with seafarers on board. The ship is controlled and operated from another location. Seafarers are available on board for taking control and operating the shipboard systems and functions.
3. DoA3, a remotely controlled ship without seafarers on board. The ship is controlled and operated from another location. There are no seafarers on board.
4. DoA4, a fully autonomous ship. The operating system of the ship can make decisions and determine actions by itself.

With the increase in ship automation, the number of crew members has decreased significantly. It is now 18-22 crew members on board commercial ocean-going ships. Although the number of members was constantly decreasing, it is not known whether the number reached the lower boundary or can it be eliminated for most of the vessels with the implementation of an autonomous ship's crew. Apart from human casualties and equipment/vessel damage, maritime accidents cause environmental disasters [55]. In the period from 2011 to 2018, 65.8% of maritime accidents were attributed to human error [56], indicating that if the human action is less involved in ship operations, the number of accidents will probably decrease. An autonomous ship will find its successful commercial usage when it is shown that they are at least as safe as conventional ships [57].

Shore Control Centre (SCC) allows for the transition of the crew from ship to shore. The crew in the SCC supervises and remotely operates a ship; when needed, it takes full control. Sensor fusion on ships is crucial for reliable remote operation. Data collected by multiple cameras, RADAR (Radio detection and ranging), LIDAR (Light detection and ranging), and sonars are transmitted to the SCC to gain situation awareness [58].

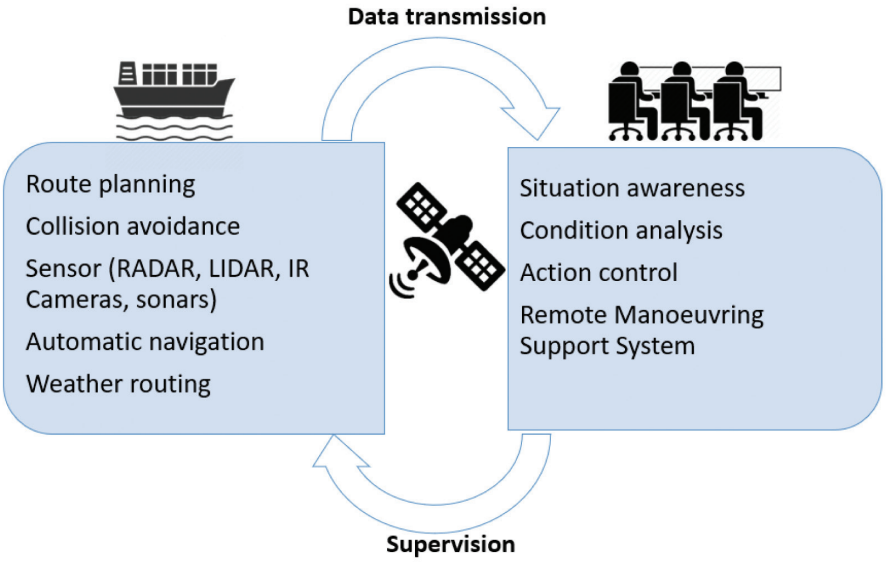

Figure 15. Relation between ship and remote control centre
Slika 15. Veza između broda i centra za daljinsko upravljanje

Essential components needed for autonomous operations are guidance, navigation, and control systems, which are connected and dependable on each other [59]. The guidance system can be classified in path planning [60], [61] (global and local) and replanning, and collision avoidance [62]. Advanced sensing technologies enable a safe navigation system that is classified in state estimation, environmental perception, and situation awareness.

Kretschmann et al. [63] conducted a cost comparison between an autonomous and a conventional Panamax bulk carrier for three scenarios, taking into consideration reduced crew, new port services, improved energy efficiency, and additional capital costs, pointing out that autonomous shipping has the potential to increase profitability and reduce emissions. The application of such a solution in the Croatian coastal navigation is a subject of ongoing research activities, where the authors are developing mathematical models to assess the effect of the increase of autonomy degree on ship total costs and safety.

5. CONCLUSION

The control of marine pollution is mainly focused on air pollution caused by emissions released from the combustion of fossil fuel in a marine engine. By replacing conventional marine fuel, i.e. diesel, with alternative and cleaner fuel, shipping emissions can be reduced. The research presented in this paper refers to the application of some advanced technical solutions, illustrated on ro-ro passenger ships engaged in the Croatian short-sea shipping fleet. The analyses of different alternative fuels and power systems are performed from the environmental and economic points of view. The presented LCA and LCCA comparisons indicated that an electricity-powered ship, i.e. a ship powered by a power system that consists of only a battery as power source that is charged onshore, is the most cost-effective and environmentally friendly solution to replace the conventional power system with diesel as fuel.

Current technological developments have brought significant changes to the shipping industry, encouraging digitalization and automation, which will result in increased autonomy levels and make the shipping sector energy efficient. There is a large number of research projects currently conducted on these topics, bringing autonomous shipping closer to commercial applications.

In this paper, the outcomes of several research projects dedicated to the protection of the Adriatic Sea are summarized. The investigations of the CF reduction of vessels operating in the Adriatic Sea is a mature topic, already offering viable options and guidelines for the modernization of the ro-ro passenger fleet. The investigations of seawater protection and an increase of the level of autonomy are currently in the intermediate stage. Precise modernization directions can be expected in near future.

Future research projects dedicated to the protection of the Adriatic Sea should be oriented toward the increase of energy efficiency and environmental friendliness of other ship types, as for instance fishing vessels, as well as to the development of intelligent solutions for sustainable and environmentally friendly aquaculture.

Acknowledgements

This research was supported within several competitive projects: "Green Modular Passenger Vessel for Mediterranean (GRiMM)", (Project No. UIP-2017-05-1253), funded by the Croatian Science Foundation; "Structural Integrity of the Energy Saving Devices (ESD) of Pre-Swirl Stator (PSS) and Flow Control Fin (FCF) type", funded by the Hyundai Heavy Industries Co., Ltd., Korea; "Sector Adaptive Virtual Early Warning System for marine pollution (SEAVIEWS)", (Project No. ADRION-951), co-funded by a European transnational programme INTERREG V-B Adriatic-Ionian ADRION Programme 2014-2020; "Autonomous Auxiliary Fishing Vessel (APROPO)", funded by the European Maritime and Fisheries Fund of the European Union and approved by the Ministry of Agriculture, Directorate of Fisheries, Republic of Croatia (Award No. 324-01/19-01/968); Croatian-Chinese bilateral project "Energy efficient and environmentally friendly power system options for inland green ships" within the University of Zagreb, Faculty of Mechanical Engineering and Naval Architecture (Croatia), and Wuhan University of Technology (China). Also, Maja Perčić and Ivana Jovanović, Ph.D. students, are supported through the "Young researchers' career development project – training of doctoral students" of the Croatian Science Foundation, funded by the European Union from the European Social Fund.

The LCA analysis in this study was performed using GREET software produced by UChicago Argonne, LLC under Contract No. DE-AC02-06CH11357 with the Department of Energy.

Finally, some contributions included in this work were presented in earlier papers by the same authors; they are properly cited within the text and included in the reference list.

References

1. Riechers, M, Brunner, BP, Dajka, J-C, Duşe, IA, Lübker, HM, Manlosa, AO, Sala, JE, Schaal, T, Weidlich S. "Leverage points for addressing marine and coastal pollution: A review", *Marine Pollution Bulletin*,167, 2021, 112263.
2. Monteiro, A, Russo, M, Gama, C, Borrego, C. "How important are maritime emissions for the air quality: At European and national scale", *Environmental Pollution*, 242, 2018, 565–75.
3. Sector Adaptive Virtual Early Warning System for marine pollution – SEAVIEWS, https://seaviews.adrioninterreg.eu/; (accessed 23 June 2021).
4. United Nations Framework Convention Climate Change, Climate Change Information kit, https://unfccc.int/resource/iuckit/cckit2001en.pdf (accessed 24 June 2021).

5. Environmental Protection Agency, Understanding Global Warming Potentials, https://www.epa.gov/ghgemissions/understanding-global-warming-potentials; (accessed 22 June 2021).
6. United Nations Framework Convention Climate Change, The Paris Agreement, https://unfccc.int/process-and-meetings/the-paris-agreement/the-paris-agreement; (accessed 22 June 2021).
7. Wiedmann, T, Minx J. "A Definition of Carbon Footprint", In: "Ecological Economics Research Trends", 2008. 1–11.
8. Bouman, EA, Lindstad, E, Rialland, AI, Strømman, AH. "State-of-the-art technologies, measures, and potential for reducing GHG emissions from shipping – A review", *Transportation Research Part D: Transport and Environment*, 52, 2017, 408–421.
9. Xing, H, Spence, S, Chen, H. "A comprehensive review on countermeasures for CO2 emissions from ships", Vol. 134, *Renewable and Sustainable Energy Reviews*, 134, 2020, 110222.
10. Ančić, I, Perčić, M, Vladimir, N. "Alternative power options to reduce carbon footprint of ro-ro passenger fleet: A case study of Croatia", *Journal of Cleaner Production*, 271, 2020, 122638.
11. Hansson, J, Månsson, S, Brynolf, S, Grahn, M. "Alternative marine fuels: Prospects based on multi-criteria decision analysis involving Swedish stakeholders", *Biomass and Bioenergy*, 126, 2019, 159–73.
12. Wan, C, Yan, X, Zhang, D, Yang, Z. "A novel policy making aid model for the development of LNG fuelled ships", *Transportation Research Part A: Policy and Practice*, 119, 2019, 29–44.
13. Ammar, NR. "An environmental and economic analysis of methanol fuel for a cellular container ship", *Transportation Research Part D: Transport and Environment*, 69, 2019, 66–76.
14. Mohd Noor, CW, Noor, MM, Mamat, R. "Biodiesel as alternative fuel for marine diesel engine applications: A review", *Renewable and Sustainable Energy Reviews*, 94, 2018. 127–142.
15. Gagatsi, E, Estrup, T, Halatsis, A. "Exploring the Potentials of Electrical Waterborne Transport in Europe: The E-ferry Concept", *Transportation Research Procedia*, 14,2016, 1571–1580.
16. van Biert, L, Godjevac, M, Visser, K, Aravind, PV. "A review of fuel cell systems for maritime applications", *Journal of Power Sources*, 327, 2016, 345–364.
17. Nuchturee, C, Li, T, Xia, H. "Energy efficiency of integrated electric propulsion for ships – A review", *Renewable and Sustainable Energy Reviews*, 134, 2020, 110145.

18. International Renewable Energy Agency, Renewable energy options for shipping, https://www.irena.org/-/media/Files/IRENA/Agency/Publication/2015/IRENA_Tech_Brief_RE_for-Shipping_2015.pdf; (accessed 24 June 2021).
19. Wan, Z, el Makhloufi, A, Chen, Y, Tang, J. "Decarbonizing the international shipping industry: Solutions and policy recommendations", *Marine Pollution Bulletin*, 126, 2018, 428–435.
20. Armstrong, VN. "Vessel optimisation for low carbon shipping", *Ocean Engineering*, 73, 2013, 195–207.
21. EU Emissions Trading System, https://ec.europa.eu/clima/policies/ets_en; (accessed 24 June 2021).
22. International Maritime Organization, Fourth IMO GHG Study Executive Summary, 2020.
23. DNV, Achieving the IMO decarbonization goals, https://www.dnv.com/expert-story/maritime-impact/How-newbuilds-can-comply-with-IMOs-2030-CO2-reduction-targets.html; (accessed 24 June 2021).
24. Arof, AM. "Decision Making Model for Ro-Ro Short Sea Shipping Operations in Archipelagic Southeast Asia", *Asian Journal of Shipping and Logistics*, 34 (1), 2018, 33–42.
25. Gobbi, GP, Di Liberto, L, Barnaba, F. "Impact of port emissions on EU-regulated and non-regulated air quality indicators: The case of Civitavecchia (Italy)", *Science of the Total Environment*, 719, 2020, 134984.
26. Sofiev, M, Winebrake, JJ, Johansson, L, Carr, EW, Prank, M, Soares, J, Vira, J, Kouznetsov, R, Jalkanen J-P, Corbett JJ. "Cleaner fuels for ships provide public health benefits with climate tradeoffs", Nature Communications, 9(1), 2018, 406.
27. Torbianelli, VA. "When the road controls the sea: a case study of Ro-Ro transport in the Mediterranean", *Maritime Policy & Management*, 27 (4), 2000, 375–389.
28. Perčić, M, Vladimir, N, Fan, A. "Life-cycle cost assessment of alternative marine fuels to reduce the carbon footprint in short-sea shipping: A case study of Croatia", *Applied Energy*, 279, 2020, 115848.
29. Perčić, M, Vladimir, N, Fan, A., Koričan, M, Jovanović, I. "Towards environmentally friendly short-sea transportation via integration of renewable energy sources in the ship power systems", *Proceedings of the Applied Energy Symposium: Low carbon cities and urban energy systems (CUE 2020) – Part 2*, Tokyo, Japan, 2020, D-171, 6.
30. GREET, https://greet.es.anl.gov/; (accessed 30 June 2021).
31. Perčić, M, Ančić, I, Vladimir, N. "Life-cycle cost assessments of different power system configurations to reduce the carbon footprint in the Croatian short-sea shipping sector", *Renewable and Sustainable Energy Reviews*, 131, 2020, 110028.

32. Vladimir, N, Bakica, A, Malenica, Š, Im, H, Senjanović, I, Cho, D.S. "Numerical Method for the Vibration Analysis of Pre-Swirl Stator", *Ships and Offshore Structures*, Vol. 16, No. Sup1, 2021., pp. S256-S265.
33. Bakica, A, Vladimir, N, Gatin, I, Jasak, H. "CFD simulation of loadings on circular duct in calm water and waves", *Ships and Offshore Structures*, Vol. 15, No. Sup1, 2020., pp. S110-S122.
34. Carlton, J. "Marine Propellers and propulsion", 3rd edition, 2012.
35. Çelik, F. "A numerical study for effectiveness of a wake equalizing duct", *Ocean Engineering*,34, 2007, 2138-2145.
36. Dang, J, Chen, H, Guoxiang, D, Van Der Ploeg, A, Hallmann, R, Mauro, F. "An Exploratory Study on the Working Principles of Energy Saving Devices (ESDs)". *Symposium on Green Ship Technology*, 2011.
37. Schneekluth, H. "Wake equalizing duct", *The Naval Architect*, 103, 1986, 147–150.
38. Mewis, F. "A Novel Power-Saving Device for Full-Form Vessels", *First International Symposium on Marine Propulsors*, 2009.
39. Kim, JH, Choi, JE, Choi, BJ, Chung, SH, Seo, HW. "Development of Energy-Saving devices for a full Slow-Speed ship through improving propulsion performance", *International Journal of Naval Architecture and Ocean Engineering*, 7, 2015, 390–398.
40. Dymarski, P, Kraskowski, M. "Numerical and Experimental Investigation of the Possibility of Forming the Wake Flow of Large Ships by Using the Vortex Generators", *Second International Symposium on Marine Propulsors*, 2011.
41. Gaggero, S, Gonzalez-Adalid, J, Sobrino, MP. "Design of contracted and tip loaded propellers by using boundary element methods and optimization algorithms", *Applied Ocean Research*, 55, 2016, 102–129.
42. Mizzi, K, Demirel, YK, Banks, C, Turan, O, Kaklis, P, Atlar, M. "Design optimisation of Propeller Boss Cap Fins for enhanced propeller performance", *Applied Ocean Research,* 62, 2017, 210–222.
43. Kim, JH, Choi, JE, Choi, BJ, Chung, SH. "Twisted rudder for reducing fuel-oil consumption", *International Journal of Naval Architecture and Ocean Engineering*, 6, 2014, 715–722.
44. Hai-Long, S, Obwogi, EO, Yu-Min, S. "Scale effects for rudder bulb and rudder thrust fin on propulsive efficiency based on computational fluid dynamics", *Ocean Engineering*, 117, 2016, 199– 209.
45. Ahn, K, Choi, GH, Son, DI, Rhee, KP. "Hydrodynamic characteristics of X-Twisted rudder for large container carriers", *International Journal of Naval Architecture and Ocean Engineering*, 4, 2012, 322–334.

46. Shin YJ, Kim, MC, Lee, JH, Song, MS. "A numerical and experimental study on the performance of a twisted rudder with wavy configuration", *International Journal of Naval Architecture and Ocean Engineering*, 11(1), 2019, 131-142.
47. Lee, KJ, Bae, JH, Kim, HT, Hoshino, T. "A performance study on the energy recovering turbine behind a marine propeller", *Ocean Engineering*, 91, 2014, 152–158.
48. Prins, HJ, Flikkem, MB, Schuiling, B, Xing-Kaeding, Y, Voermans, AA, Müller, M, Coache, S, Hasselaar, TW, Paboeuf, S. "Green retrofitting through optimisation of hull-propulsion interaction - GRIP", *Transport Res Proc*., 14, 2016, 1591–1600.
49. Perčić, M, Vladimir, N, Fan, A. "Techno-economic assessment of alternative marine fuels for inland shipping in Croatia", *Renewable and Sustainable Energy Reviews*, 148, 2021, 111363.
50. European Environmental Agency, https://www.eea.europa.eu/; (accessed 24 June 2021).
51. Peeters, G, Kotzé, M, Afzal, MR, Catoor, T, Van Baelen, S, Geenen, P, Vanierschot, M, Boonen R, Slaets, P."An unmanned inland cargo vessel: Design, build, and experiments", *Ocean Eng*ineering, 201, 2020, 107056.
52. Rødseth, ØJ, Burmeister, HC. "Developments toward the unmanned ship", *Proc. Int. Symp. Inf. Ships--ISIS,* no. MUNIN (Maritime Unmanned Navigation through Intelligence in Networks), 2012, 16.
53. Gu, Y, Goez, JC, Guajardo, M, Wallace, SW. "Autonomous vessels: state of the art and potential opportunities in logistics", *International Transactions in Operational Research*, 28(15), 2020, 1–34.
54. Rødseth, ØJ, Håvard, N, Åsa, H. «Characterization of autonomy in merchant ships», *In 2018 OCEANS-MTS/IEEE Kobe Techno-Oceans (OTO),* 2018, 1-7.
55. Wahlström, M, Hakulinen, J, Karvonen, H, Lindborg, I. "Human Factors Challenges in Unmanned Ship Operations – Insights from Other Domains", *Procedia Manufacturing*, 3, 2015, 1038–1045.
56. EMSA, Annual Overview of Marine Casualties and Incidents 2019.
57. Porathe, T, Home, A, Rødseth, H, Fjørtoft, K, Johnsen, SO. "At least as safe as manned shipping? Autonomous shipping, at least as safe as manned shipping? autonomous shipping, safety and "human error"", Saf. Reliab. - Safe Soc. a Chang. World - Proc. 28th Int. Eur. Saf. Reliab. Conf. ESREL 2018, 417–426.
58. Porathe, T, Prison, J, Man, Y. "Situation awareness in remote control centres for unmanned ships" *In Proceedings of Human Factors in Ship Design & Operation,* February 2014, 26-27.

59. Liu, Z, Zhang, Y, Yu, X and Yuan, C. “Unmanned surface vehicles: An overview of developments and challenges.” *Annual Reviews in Control*, 41, 2016, 71-93.
60. Chen, P, Yamin, H, Papadimitriou, E, Mou, J, van Gelder, P. “Global path planning for autonomous ship: A hybrid approach of Fast Marching Square and velocity obstacles methods.” *Ocean Engineering*, 214, 2020, 107793.
61. Woo, J, Chanwoo, Y, Nakwan, K. “Deep reinforcement learning-based controller for path following of an unmanned surface vehicle”, *Ocean Engineering,* 183, 2019, 155-166.
62. Woo, J, Kim, N. “Collision avoidance for an unmanned surface vehicle using deep reinforcement learning.” *Ocean Engineering,* 199, 2020, 107001.
63. Kretschmann, L, Burmeister, H-C, and Jahn, C. “Analyzing the economic benefit of unmanned autonomous ships: An exploratory cost-comparison between an autonomous and a conventional bulk carrier.” *Research in transportation business & management*, 25, 2017, 76-86.

NAPREDNA TEHNIČKA RJEŠENJA ZA KONTROLU ONEČIŠĆENJA POMORSKOG SEKTORA U JADRANSKOM MORU

Sažetak

Glavni ekološki problemi u pomorskom sektoru su onečišćenje atmosfere zbog upotrebe fosilnih goriva u brodskom energetskom sustavu te onečišćenje morske vode iz različitih izvora (npr. izlijevanje nafte, mikroplastika, zakiseljavanje itd.). Zbog njihovog negativnog utjecaja na okoliš, ljudsko zdravlje i morski ekosustav, treba ih pažljivo kontrolirati. Studije o ekološkim problemima pomorskog sektora više su usredotočene na onečišćenje atmosfere, što je uglavnom posljedica Pariškog sporazuma prema kojem bi svaki sektor trebao doprinijeti smanjenju stakleničkih plinova. Brodovi su uglavnom pogonjeni konvencionalnim energetskim sustavima s dizelskih motorima, čiji bi negativan učinak na okoliš bio manji provedbom nekih mjera za smanjenje emisija. U ovom radu prikazana su istraživanja o naprednim tehničkim mjerama za kontrolu pomorskog onečišćenja, a rezultati su ilustrirani na ro-ro putničkim brodovima hrvatske priobalne plovidbe. Analize cjeloživotnih emisija i troškova potiču modernizaciju konvencionalnih energetskih sustava elektrifikacijom broda. Ovo je rješenje predstavljeno kao najisplativije i ekološki najprihvatljivije. Uz spomenute mehanizme za smanjenje onečišćenja zraka, u radu je dan osvrt na određena rješenja za nadzor i očuvanje morske vode s naglaskom na sustav ranog upozoravanja razvijen od strane autora u okviru kompetitivnog međunarodnog projekta. Naposljetku, u skladu sa svjetskim trendovima u pomorskom sektoru, dan je osvrt na povećanje stupnja autonomnosti brodova, kao jedne od važnijih tema u bližoj budućnosti.

Ključne riječi: onečišćenje pomorskog sektora; smanjenje emisija; ro-ro putnički brod; alternativna goriva; uređaj za uštedu energije; sustav ranog upozoravanja.

Maja Perčić
University of Zagreb
Faculty of Mechanical Engineering and Naval Architecture
Ivana Lučića 5, 10002 Zagreb
Croatia
e-mail: maja.percic@fsb.hr

Ivana Jovanović
University of Zagreb
Faculty of Mechanical Engineering and Naval Architecture
Ivana Lučića 5, 10002 Zagreb
Croatia
e-mail: ivana.jovanovic@fsb.hr

Andro Bakica
University of Zagreb
Faculty of Mechanical Engineering and Naval Architecture
Ivana Lučića 5, 10002 Zagreb
Croatia
e-mail: andro.bakica@fsb.hr

Nikola Vladimir
University of Zagreb
Faculty of Mechanical Engineering and Naval Architecture
Ivana Lučića 5, 10002 Zagreb
Croatia
e-mail: nikola.vladimir@fsb.hr

Marija Koričan
University of Zagreb
Faculty of Mechanical Engineering and Naval Architecture
Ivana Lučića 5, 10002 Zagreb
Croatia
e-mail: marija.korican@fsb.hr

DOI: 10.21857/9xn31cop7y

Pregledni članak / Review paper
Prihvaćeno / Accepted: 14. listopada 2021.

THE EUROPEAN AIRSPACE FRAGMENTATION: A COST-EFFICIENCY BASED ASSESSMENT

Sanja Steiner, Zvonimir Rezo, Ružica Škurla Babić, Cristiana Piccioni

Summary

Due to the ANSPs' (Air Navigation Service Providers') unit rates variability in different European airspace areas, the AUs (Airspace Users) pay different financial amounts for the same ANS (Air Navigation Service) provision. The AUs' interest is to achieve the lowest possible operational costs, so it is often the case that the aircraft, if there is an alternative, fly on longer but economically more acceptable routes through cheaper charging zones. Over the time, the application of such practice has led to the creation of different business interests – that is a critical issue hindering further air transport development in Europe. This paper investigates the research question of whether and if so, how the European airspace is fragmented in terms of cost-efficiency features. By the application of the spatial autocorrelation methodology, i.e. by associating every ANSP's unit rate value with its spatial position within the European ATM (Air Traffic Management) system, the research question has been answered. Research findings indicate that the European airspace is fragmented from a cost-efficiency aspect and divided into several different homogeneous areas. Such areas are characterized by a certain similarity level of adjacent unit rates, whereas one charging zone represents a hotspot in terms of its dissimilarity to adjacent spatial units.

Keywords: Air Traffic Management; European airspace; Strategic planning; Fragmentation; Cost-efficiency.

1. INTRODUCTION

Since the 1950s, the European countries have hesitated to impose en-route charges to usually financially subsidized or fully state-owned airlines. However, several factors made governments re-evaluate their standpoints. Greater exploitation of jet aircraft, as well as increased traffic levels, have resulted in significantly increased costs of providing air navigation services. Governing bodies became aware that their systems did not

correspond with the ideas of the future air traffic development. Moreover, they realized that further expansion of the civil aviation market would enable the free provision of air navigation services to domestic airlines, foreign airlines and privately-owned airlines. This situation resulted in developing a more comprehensive approach to strategic air traffic planning at regional rather than national level, as it was done in the past.

The current applications of strategic air traffic planning with the "demand-oriented" option within highly fragmented European airspace design has caused an unbalanced air traffic development in Europe. This furthermore had a direct impact on the creation of different unit rate values applicable in various charging zones across the European airspace.

Airspace fragmentation is generally recognized as one of the main causes of the ATM system's inefficiency, especially from the economic point of view. In this context, the paper seeks to provide information that can ease the conduction of strategic planning of the future air transport development in Europe. More precisely, this paper aims at determining whether and how the European airspace is fragmented from the cost-efficiency aspect, thus presenting an overview of research background, in terms of literature review and research motivation, the currently applicable European ANS charging scheme, as well as the methodological framework. Furthermore, the obtained results are presented and briefly described. Lastly, before conclusion, the research findings are discussed in wider context, whereby their relevance is argued in sense of airspace fragmentation' repercussions on day-to-day operations, and in respect to some of the ideas/proposals of the future ATM system's development in Europe.

2. RESEARCH BACKGROUND

2.1 A survey of previous studies

In the domain of air traffic management, the term "fragmentation" began to be frequently used within the last two decades. Even though the problem of airspace fragmentation was recognized in the 1990s [1], little has been done to resolve this issue or to minimize associated negative impacts [2]. Various authors [3-14] are concerned with airspace design and system performances, and highlight the European airspace fragmentation as one of the main causes of the European ATM system's inefficiency and a barrier to its future development. Thereby, a null hypothesis of this research is that the European airspace is also fragmented in terms of cost-efficiency (one of four key performance areas of the future development of the ATM system in Europe). However, although the airspace fragmentation became a commonly applied term, during the past

years it was neither frequently studied nor comprehensively addressed, so that a minor progress has been made to describe this issue more in-depth [15]. To this end, this research aims at complementing the existing literature in the field.

Although significant work has been done to study design, characteristics and performances of the European ATM system, most studies do not consider all three correlated features of the ANSPs' performance data. They usually omit the spatial, and define only the temporal and value features of data. As a result of this practice, the spatial component of data set is often underutilized. Since 80% of information requirements posed by policy makers are related to the spatial location, it certainly raises many issues [16,17]. Moreover, the literature review indicates that there are no sources that spatially correlate performances of the ATM system in Europe and airspace fragmentation. Hence, it was necessary to study this issue more in-depth.

By testing the existence and determination of the level of the European airspace fragmentation in terms of cost-efficiency, the ones dealing with the strategic planning and development of the ATM system in Europe can get a clear picture of potential areas requiring improvements, and obtain information about why do the AUs "behave" as they do. Figure 1 shows a simplified view of flight trajectory in respect to spatial process that influenced flight planning in such a way that the AU flew rather through green than through yellow and red areas. Thereby, colour gradation from green to red can be observed from various performance indicators. For instance, red areas can denote areas with capacity shortfall, inadequate horizontal flight efficiency, higher en-route charges or higher airspace complexity – and vice versa for green areas. Additionally, considering that risks existence can compromise the realization of strategic goals, one of the core purposes of strategic planning is to reduce business risks. This is of great importance, because aviation is a financially intensive business environment, within which the ATM system represents a business activity with high financial turnover. Accordingly, better understanding of the European airspace fragmentation level in terms of cost-efficiency leads to a better description of business environment, and consequently reduces business risks.

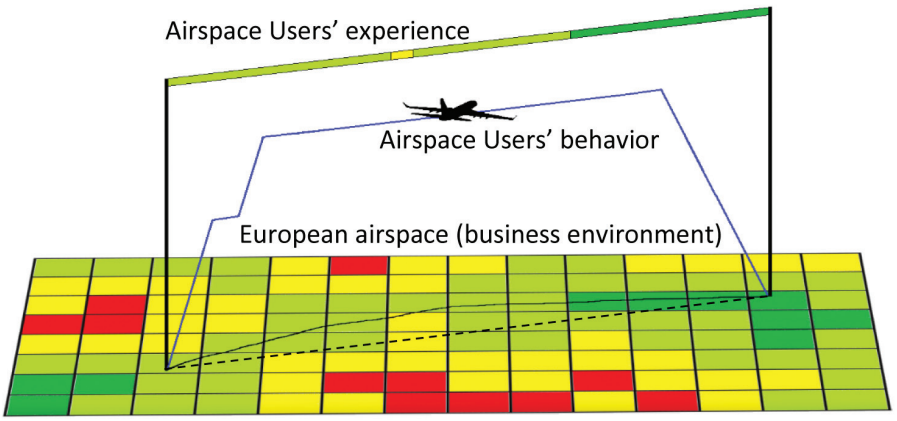

Figure 1. A simplified view of understanding Airspace Users' "behaviour" through the understanding of spatial processes [18]

Slika 1. Pojednostavljeni prikaz razumijevanja „ponašanja" korisnika zračnog prostora kroz razumijevanje prostornih procesa [18]

Considering the above-mentioned, the survey of the previous research points out that it has never been defined how to test the existence or how to measure the level of the European airspace fragmentation in terms of the ATM system performances. In order to determine this, the method of the ESDA (Exploratory Spatial Data Analysis) has been applied. It has been composed from a set of techniques aimed at describing and visualizing the spatial distribution of data, identifying "atypical localization" or outliers, detecting patterns of spatial association (e.g. clusters, hotspots, or cold spots), and suggesting spatial regimes [19-22].

2.2 Research motivation

In addition to attempting to fill the shortcomings identified by the literature review, this research is also strongly motivated by the high relevance of the covered topic in the domain of strategic planning of the ATM system development in Europe, particularly because conceptual assumptions of the currently applicable strategic planning framework have many flaws – all of which are associated with the fragmentation issue. One of them arises from the fact that the European ATM system is still mainly organized at national scale. This is problematic, because the ATM system in Europe involves a high

number of stakeholders, which may, in different areas, have greater or smaller impact on the ATM system performances [23]. In such circumstances, partial and nationally oriented development plans are not a rare occurrence, which is a critical issue, because regional planning ought not to be conditioned by individual national interests. This is compounded by the fact that there is currently no methodological framework that considers the ANSPs' performance interdependencies, trade-offs, goal conflicts, etc., or that evaluates the coherence of their development plans, performance targets, etc.

Another issue related to the above strategic planning is its individualistic approach to evaluating the achieved performance level. Whether or not an ASNP is successful is purely determined by comparing its performance achievements with those regulatory determined, e.g. Performance Scheme. This is problematic, because the spatial component of the data is completely ignored. For instance, if in the following year the ANSP achieves a reduction of 1.9% of unit rate value, according to performance targets of RP3 (3rd Reference Period) [24], this will be considered a success. However, currently, such success is at no point assessed in respect to the situation and performances achieved at local level. Given that "positions are already taken" and that in the following years, every ANSP will be obliged to respect the RP3 targets, the application of such an approach will result in the fact that future outlook will be proportionally equal to the pre-existing situation. In other words, higher and lower values will remain so, only that, within a certain time lag, their values will be reduced. Thereby, as long as individualistic approach in the evaluation of achieved performances is applicable, this will contribute to the existence of the performance-based European airspace fragmentation.

Considering that such an approach is not sustainable in the long run, strategic planning needs to be conceptually set, so that it is oriented towards achieving performances that will lead to spatial cohesion [25]. Accordingly, the first step in closing potential performance gaps is to acquire objective information about the current situation. This means the determination of whether, and if so, how fragmented the European airspace is from the cost-efficiency aspect. Hence, it can be concluded that the identification of the European airspace fragmentation in terms of cost-efficiency, by scientifically acceptable methods, is of high significance as such. Particularly, since the obtained information can later be placed in the context of the valorisation of on-going changes, ideas, discussions and regulation proposals seeking to modify, improve, optimize, etc. the performance and outlook of the European ATM system.

3. THE EUROPEAN AIR NAVIGATION SERVICES CHARGING SCHEME

The provision of air navigation services requires certain financial resources. To this end, the European Commission has established a charging system aimed at covering the ANSPs' costs. Nowadays, the ANSPs' costs are directly covered by the AUs. This includes the coverage of terminal and en-route charges charged within en-route and terminal charging zones. Thereby, the ANSPs' costs of en-route services are financed by means of en-route charges imposed to the ANS' users, while the costs of terminal services are financed by means of terminal charges. Both charges are estimated based on unit rate, so that it represents a crucial element of the European ANS charging scheme. For instance, the terminal charge for a specific flight in a specific terminal charging zone equals the product of the unit rate established for this terminal charging zone and the terminal service units for this flight. Thereby, this research deals with the en-route part of charging scheme. Accordingly, a greater emphasis is given to this aspect of the European ANS charging scheme. The value of the en-route charge is established on the yearly basis for each charging zone, and it consists of two parts – the unit rate, and the administrative unit rate. It is calculated by dividing the charging zone's forecasted en-route facility cost-base by the forecasted number of service units generated in the same charging zone. The purpose of administrative unit rate is to recover the costs of collecting route charges, and it is identical for all charging zones [26]. The ANSPs' remuneration is managed by EUROCONTROL's CRCO (Central Route Charging Office). The CRCO was established in 1971, when seven Member States of EUROCONTROL decided to adopt a common charging policy, thus creating a framework of the presently applicable charging scheme. As Figure 2 shows, 40 Member States participate in the charging scheme, thus covering an area of 18,970,200 km^2.

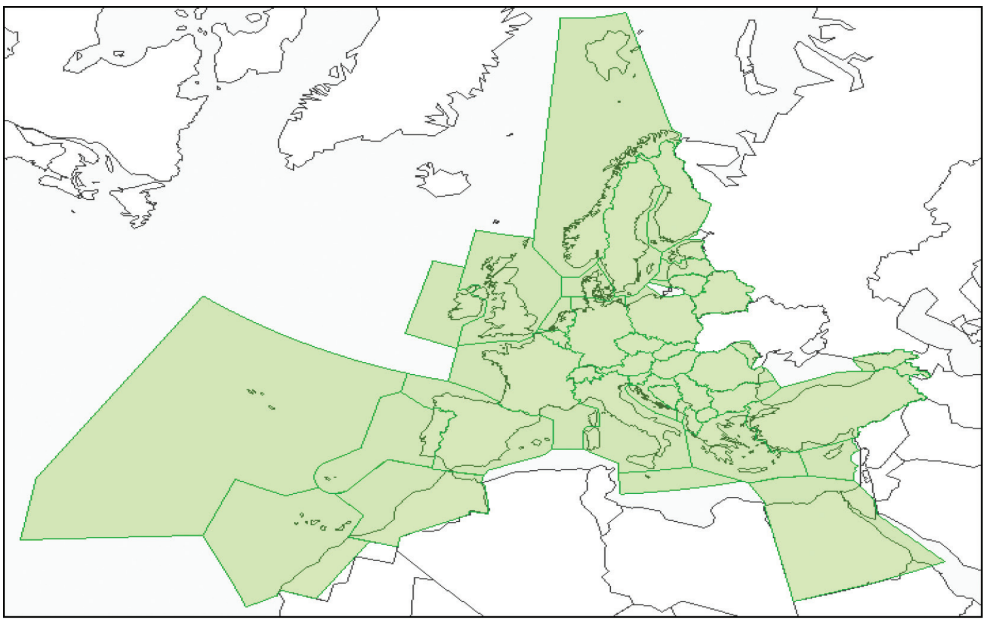

Figure 2. The spatial overview of the charging zones of the European airspace

Slika 2. Prostorni pregled naplatnih zona europskog zračnog prostora

As defined in the Commission's implementing Regulation (EC) 2019/317 [27], when an aircraft enters the charging zones of the Member States, a single *charge for en-route service* (*R*) is applied. It equals the total amount of the *individual charging zones* (r_i), which the aircraft was flying through:

$$R = \sum_{n} r_i \quad \text{[EUR]} \tag{1}$$

The fee for each individual charging zone is given by the product of the *unit rate* (t_i) and the *number of service units* (*N*) corresponding to the flight in the specific charging zone:

$$r_i = t_i \cdot N \ \text{[EUR]} \tag{2}$$

The number of service units is calculated as the *flight length factor* (d_i) multiplied by the *weight factor* (*p*) for the observed flight:

$$N = d_i \cdot p \tag{3}$$

The flight length factor is calculated by dividing by 100 the orthogonal distance between the departing aerodrome (if within the zone) or charging zone's entry point and

the first landing airport (if within the zone), or the exit point from the observed charging zone. It is worth noting that the cost calculation process also includes 20 NM (Nautical Miles) deducted for each take-off and landing within the territories of the Member States. The final element required for the cost estimation – *weight factor* (*p*) – depends on the aircraft MTOW (Maximum Take-Off Weight) as follows:

$$p = \sqrt{\frac{MTOW}{50}} \ [\text{t}] \tag{4}$$

Finally, Figure 3 shows an example from practice that best summarises the outlook of the European ANS charging scheme. More precisely, two route options between Cardiff International Airport and Corfu International Airport are given: the blue route indicates the cheapest option, while the green one represents the shortest route option between these two airports.

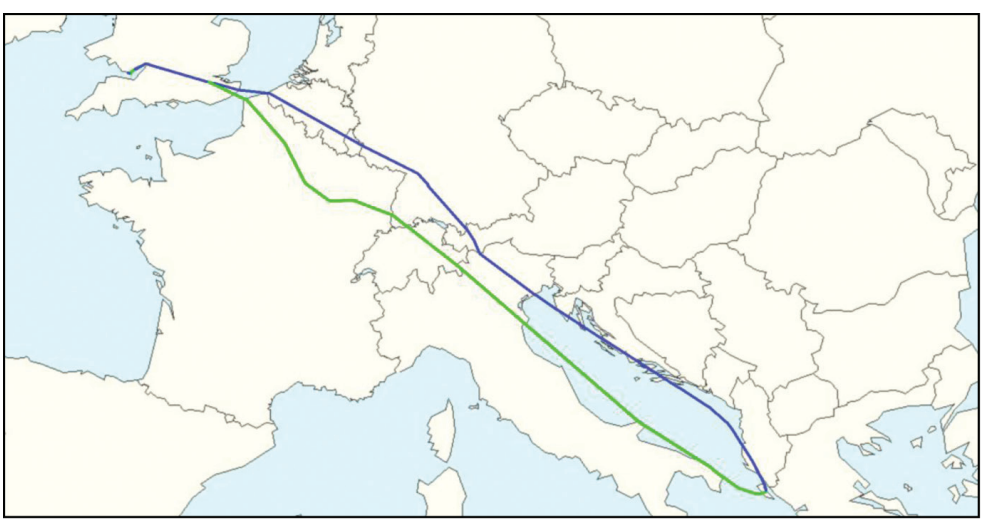

Figure 3. The repercussion of the existing charging scheme' framework on flight planning
Slika 3. Reperkusije postojećeg okvira sustava obračuna naknada na planiranje leta

As already mentioned, the AUs can choose which option suits them best. Considering that aviation is a commercial activity with thin profit margins, it is not surprising that the AUs may, if an alternative exists, prefer the cheaper (but potentially longer) to the shorter (but more expensive) route option. In this context, if the AU uses the blue route option (cheaper, but longer route), its route charges will be approximately 21.90% lower in comparison with the green route option. Moreover, if an AU uses this route/practice two times a day for return flights, by the end of the year, it can reduce its direct operating costs by EUR 543,850. Thus, it is evident that every ANSP's unit rate value in combination with the ANSPs' spatial position within the European ATM network has great importance in relation to the execution of the day-to-day operations of both the ANSPs and the AUs.

4. THE MODELLING APPROACH

In order to answer the well-defined research question, a mathematical model was developed. Such a model performed a data geo-referencing by placing unit rate values in a spatial context. Then the data processing followed, i.e. the conduction of three data analyses involving the European airspace: (1) clustering analysis; (2) spatial outliers' analysis; and (3) critical area analysis. The applied data analysis techniques are further explained in detail in the following paragraphs.

It is worth mentioning that, within the applied model, unit rate values presented in MAUR (Monthly Adjusted Unit Rates) reports have been used as input data. Since EUROCONTROL/CRCO publishes MAUR reports on the monthly basis, all unit rate values were standardized in the form of an average annual value. Thus, unified data have enabled research conduction and the presentation of main findings corresponding to the fragmentation status during 2018. This is important to emphasise because of the variability of the unit rate values both on the annual and on the monthly basis. In this respect, variability on the monthly basis is significantly lower compared to the annual variability. Figure 4 shows the comparison unit rate values in 2012 and 2018. Additionally, the forecasted unit rate values for 2023 have been included in the comparison. In this context, a comparative analysis of the CRCO's and EUROCONTROL's STATFOR (Statistic and Forecast Service) reports [28-33] clearly indicates charging zones, in which unit rate values in 2023 will vary from the given values in 2018. Furthermore, as Egypt, Belarus and Morocco are not EUROCONTROL's Member States, their unit rate values for 2023 were not accounted.

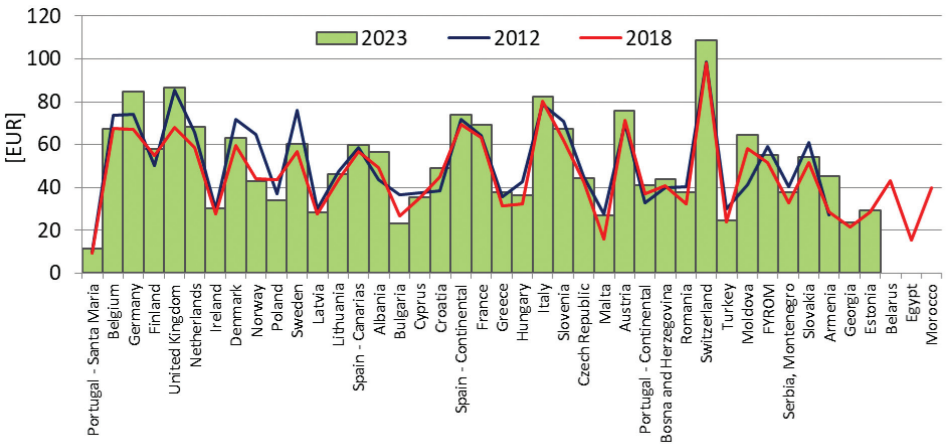

Figure 4. The value and temporal comparison of unit rate values [28-33]

Slika 4. *Vrijednosna i vremenska usporedba vrijednosti jediničnih cijena [28-33]*

4.1 The European airspace clustering analysis overview

A spatial autocorrelation method was used in the analysis of the European airspace clustering. The use of such a method in modelling spatial relations dates back to the late 1940s and 1950s. Schabenberger and Gotway defined it as a relationship among values of a single variable that comes from the geographic arrangement of the areas, in which these values occur [34]. It also corresponds to the Tobler's first law of geography that reads: "Everything is related to everything else, but near things are more related than distant things", thus spatially identifying similarities and differences between adjacent spatial units.

Spatial autocorrelation can be counted both locally (in parts of an observed area) and globally (across the whole observed area). Local spatial autocorrelation analyses are considered more accurate, because the variations are identified by focusing on close neighbourhoods. According to Fotheringham et al. [35], local Moran's indexes I_i can be measured by using the following equation:

$$I_i = \frac{(x_i - \bar{x}) \sum_{j=1}^{n} w_{ij} (x_j - \bar{x})}{\sum_{j=1}^{n} (x_j - \bar{x})^2 / n} \tag{5}$$

where the aforementioned elements designate:

x_i – the value of observed area;

$\bar{x}$ – the average value of observed dataset;

w_{ij} – spatial weight matrix;

x_j – the value of the adjacent area;

n – the number of observed values.

Global spatial autocorrelation analysis detects and measures a spatial pattern across the entire area of interest, but it does not reveal local grouping tendencies or the location of significant patterns. It is measured as an average value of all local Moran's indexes:

$$I = \frac{1}{n}\sum_{i=1}^{n} I_i \tag{6}$$

Based on the obtained local Moran's indexes I_i and resulting global Moran's index I, it is possible to determine the type of spatial autocorrelation. On the one hand, in case of obtaining a negative result of spatial autocorrelation, geographic units of similar values will be scattered over the map (observed area). On the other hand, a positive result of spatial autocorrelation indicates that geographical units of similar values tend to group on one spot. Furthermore, since spatial autocorrelation is an inferential statistic, it enables the testing of the null hypothesis. Thereby, as defined by the European Commission [36] and recommended by EUROCONTROL [37], when manipulating aeronautical data and drawing conclusions therefrom, the confidence level must be set at 95%. In order to test the null hypothesis, it is necessary to estimate the z-score. It is estimated based on global Moran's index (I), its expected value $E(I)$, and its variance $Var(I)$ as follows:

$$z - score = \frac{I - E(I)}{\sqrt{Var_{(I)}}} \tag{7}$$

In order to reject the null hypothesis, the value of the z-score needs to be higher that 1.96 or lower than -1.96. Additionally, the p-value needs to be lower than 0.05 in order to reject the null hypothesis. In case that the p-value is not statistically significant, the null hypothesis cannot be rejected. This would indicate that the spatial distribution of the unit rates is the result of random spatial process – meaning that the European airspace is fragmented from the cost-efficiency aspect. However, in case that the p-value is statistically significant, the null hypothesis can be rejected and this would indicate that

the European airspace is not fragmented. In such case, the spatial distribution of high values and low values in the dataset is more spatially clustered than would be expected if the underlying spatial process were random.

4.2 The European airspace spatial outliers' analysis overview

The research of the European airspace fragmentation is expanded by tackling the problematics of spatial outliers. Unlike the previous one, this analysis places the focus on the local level. Accordingly, it determines whether the unit rate value of every charging zone differs from the values of its neighbours. To be able to do so, Moran's I scatter plot method was applied. Anselin [38] describes Moran's I scatter plot as a useful visualization tool for conducting research as it allows to estimate the similarity of the observed value to adjacent values. As Figure 5 shows, Moran's I scatter plot is conceptualized so that the horizontal axis denotes the standard score (*z-score),* while the vertical axis marks the spatial lag (*Wz*$_i$), which is a product of the sum of the standard scores multiplied with their spatial weights:

$$W_{z\,i} = \sum_{j=1}^{n} w_{ij} y_j \tag{8}$$

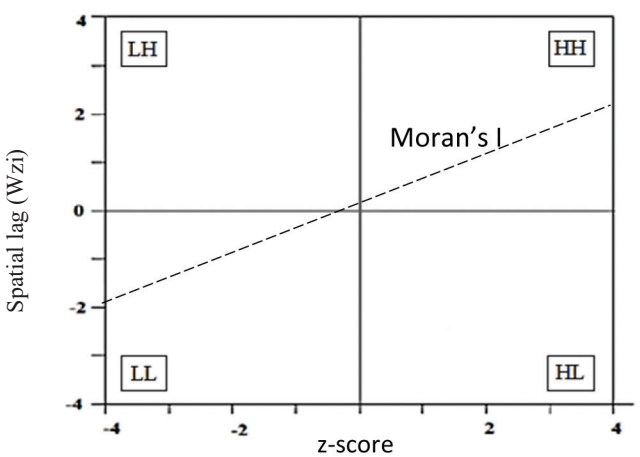

Figure 5. Moran's I scatter plot

Slika 5. Moranov dijagram rasprostiranja

In accordance with Moran's I scatter plot, four indicators have been used:

- HH (High-High) indicator, which defines the area of high neighbouring values;
- HL (High-Low) indicator, which defines a high value area with a low value neighbourhood;
- LH (Low-High) indicator, which defines a low value area with a high value neighbourhood;
- LL (Low-Low) indicator, which defines the area of low neighbouring values.

Considering that this analysis is conceptually analogous to the previous analysis, the interpretations of the results are complementary. In this context, Anselin et al. [39] argue that HH and LL areas indicate a positive spatial autocorrelation (a positive spatial association of values that are higher or lower than the samples' average). Accordingly, HL and LH areas indicate a negative spatial autocorrelation – meaning that the observed values bear little resemblance to their neighbours, and hence represent spatial outliers.

4.3 The European airspace critical areas' analysis overview

The last phase of data processing analyses where significant patterns appear. Thus, the European airspace critical areas' analysis places the focus on the national scale. It determines the significance level of every unit rate value by analysing data similarity with the rest of the dataset, as well as the significance of every unit rate value by analysing their spatial similarity with neighbouring values. The interpretation of the significance level is based on the standard score measuring the mathematical deviation of every unit rate value from the mean value of the analysed dataset (x axis), and based on the probability density function (y axis), which equals:

$$f(x) = \frac{1}{\sqrt{2\pi}} e^{\left(\frac{x^2}{2}\right)} \tag{9}$$

With respect to the aforementioned and as Figure 6 shows, seven indicators were classified and used:

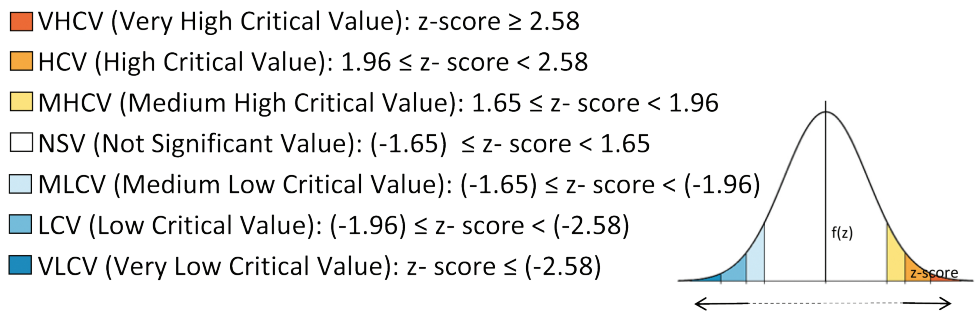

Figure 6. Overview of applied critical values criterion
Slika 6. Pregled primijenjenog kriterija kritičnih vrijednosti

Such an approach (the separation of the spatial from traditional statistics) has allowed the identification of the areas (i.e. charging zones) with significantly higher or lower unit rate values with respect to the analysed dataset, as well as with respect to the values of the adjacent spatial units. Accordingly, extreme unit rate values have been determined. Thereby, extremely high (positive) values, located at the edge of right-tail distribution, have been defined as hotspots. To the contrary, extremely low (negative) values positioned at the edge of the left-tail distribution indicate cold spots.

5. MAIN FINDINGS

5.1 The European airspace clustering analysis' results

The European airspace clustering analysis' outcomes indicate the existence of positive spatial autocorrelation (I=0.32). Keeping in mind that spatial autocorrelation ranges from 0 to 1, it can be argued that a correlation between the spatial units exists, and that geographical units of similar values tend to group on one spot. Accordingly, Figure 7 shows the charging zones composing a spatial pattern that includes 40.48% of all the analysed unit rate values, while from the spatial viewpoint, they cover 33.74% of the total studied area. Additionally, the local Moran's indexes' results show that the Swiss, Belgian, German, Austrian, Turkish, French, Georgian, Armenian and Egyptian unit rate values contribute the most to the positive value of the global Moran's index. Contrary to that, the unit rates of Portugal – Santa Maria, Malta and Ireland deviate in the other direction (areas with negative local Moran's indexes), thus lowering the overall scale of the positive value of the global Moran's index. Moreover, after running the significance test, it has been determined that the depicted spatial pattern does not represent

a spatially significant pattern (with the z-score of 0.405, and the p-value of 0.686). In other words, the spatial distribution of high values and low values in the dataset is not spatially clustered. Accordingly, the depicted spatial pattern does not represent a spatial cluster.

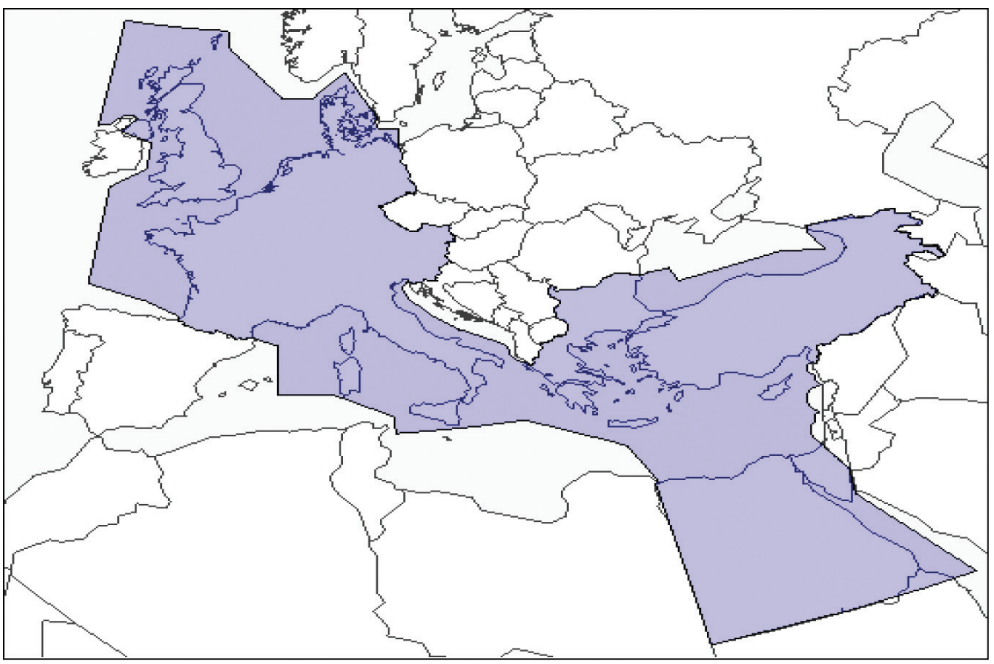

Figure 7. The spatial overview of the obtained spatial pattern
Slika 7. Prostorni prikaz dobivenog prostornog uzorka

In line with the above, the null hypothesis cannot be rejected. In other words, the spatial distribution of the unit rate values is the outcome of the random spatial process. It can thus be concluded that the European airspace is fragmented in terms of cost-efficiency. Furthermore, considering that there is no significant spatial pattern, the understanding of this outcome can be improved by studying the functional integration of spatial units at the local level. This is also required because the depicted spatial pattern does neither reveal local grouping tendencies nor where significant patterns appear. This has paved the way to further analyses aimed at overcoming the methodological limitations and providing more details about spatial processes occurring locally.

5.2 The European airspace spatial outliers' analysis results

Spatial processes that occur locally and contribute to the existence of the fragmented European airspace in terms of cost-efficiency have been identified by the conduction of the airspace spatial outliers' analysis, i.e. by comparing the unit rate value of every charging zone with their neighbours' values. Accordingly, the research findings indicate that thirteen charging zones (30.95% of overall dataset) can be classified according to the HH indicator, i.e. they are designated as areas of high neighbouring values. Fourteen charging zones are characterized as areas of low neighbouring values, and cover 33.33% of the overall analysed dataset. HL indicator, which characterizes high value areas with low value neighbourhood, includes five charging zones, and covers 11.91% of the whole analysed dataset. All the other charging zones are classified according to the LH indicator, and they constitute 23.81% of the overall analysed dataset. In general, spatial outliers are mainly located in the delimitation areas of high and low adjacent values, and represent 35.72% of the overall analysed dataset. From the spatial viewpoint, in respect to the total area under study, the European airspace is segmented as follows: HH (21.85%); LL (23.46%); HL (14.02%); LH (40.67%). Figure 8 illustrates the European airspace spatial outliers' analysis overview.

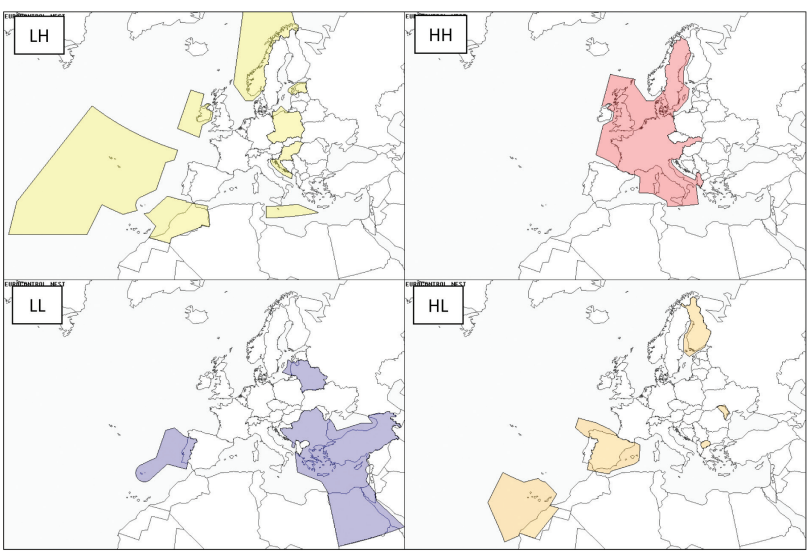

Figure 8. The spatial overview of the European airspace spatial outliers

Slika 8. Prostorni prikaz prostornih netipičnih vrijednosti u okviru europskog zračnog prostora

5.3 The European airspace critical areas' analysis results

The European airspace critical areas' analysis processed data in respect to their (*a*) value-based similarity and (*b*) spatially-based similarity. On the one hand, the value-based similarity of data distribution has been determined by means of traditional statistics, where raw data have been used as an input data. On the other hand, the spatially-based similarity of data distribution has been determined by means of spatial statistics, whereby local Moran's indexes have been used as input data. Accordingly, this approach has led to different data distributions.

Based on the application of Sturges' rule, Figure 9 shows a comparative overview of the resulting data distributions. Thereby, in order to obtain a sense of data distribution, data have been categorized into 6 bins (*x* axis). These bins have been placed in respect to frequency distribution (*y* axis) displaying the number of values in each bin. Their combination makes a histogram that enables the determination of data distribution. By comparing two distributions, it can be viewed that raw data have more uniformed distribution in respect to local Moran's indexes distribution. Furthermore, the figures of frequency distribution that categorises the charging zones according to the observed modality of studied data set indicate that raw data tend to be more dispersed than local Moran's indexes.

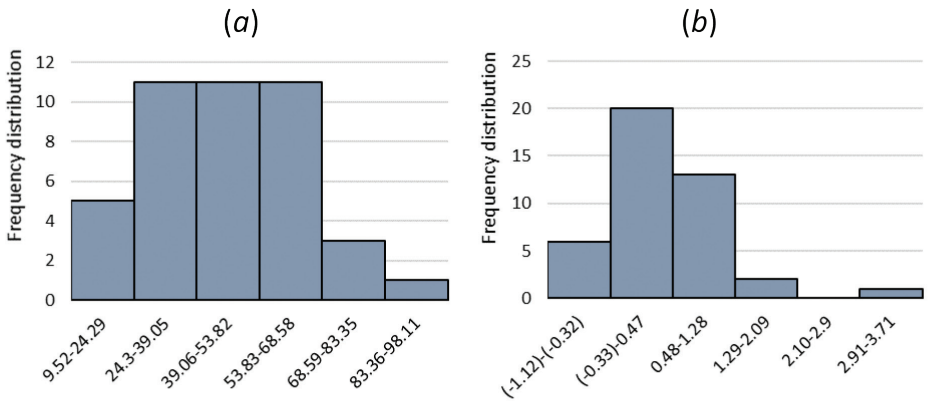

Figure 9. A comparative overview of (a) raw data and (b) local Moran's indexes' distribution

Slika 9. Usporedni pregled distribucije (a) neobrađenih podataka i (b) lokalnih Moranovih indeksa

Furthermore, in terms of the European airspace critical areas' analysis, although the results indicate approximately similar data distributions, different areas were recognized as critical ones. Figure 10 shows the distribution of the identified critical areas. Data distribution within both histograms indicates that only few charging zones can be viewed as outliers. Thereby, the left-hand side histogram and spatial overview under it depict outliers from the attributive aspect. The right-hand side histogram and spatial overview under it denote spatial outliers that differ from the neighbouring charging zones by both the attributive and the spatial aspects. As seen within the spatial overview of the studied area, different charging zones have been identified as critical areas. As such, it was possible to spot differences in the data distribution that are a result of the adoption of the methodological assumption of both independent observations and spatially-dependent observations.

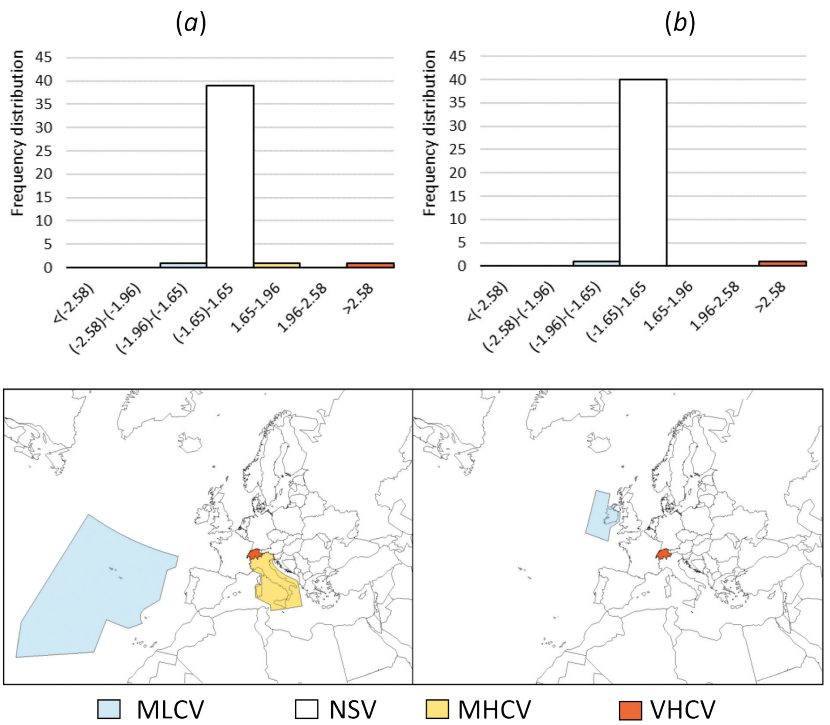

Figure 10. A comparative overview of the critical values' distribution based on the data's (a) value-based similarity and (b) spatially-based similarity

Slika 10. Usporedni pregled distribucije kritičnih vrijednosti na temelju (a) vrijednosne sličnosti i (b) prostorne sličnosti podataka

The results of the value-based data similarity indicate that the unit rate values of Portugal – Santa Maria (z-score of -1.918 indicating MLCV) and Italy (z-score of 1.832 indicating MHCV) significantly differ from the mean value of the analysed dataset, whereby 92.86% share of the dataset, i.e. 68.47% share of the overall studied area, represents an area classified as an "insignificant" one. Compared with the results of the spatially-based data similarity, the unit rate values of these two areas are spatially irrelevant. There are two reasons for this: the first one is due to the fact that the unit rate value of Portugal – Santa Maria charging zone does not significantly differ from unit rate values of neighbouring charging zones; whereas the second reason is that such a charging zone represents a boundary area, thus interacting with both the charging zones of higher and lower unit rate values.

Moreover, the results of the spatially-based data similarity indicate that the unit rate value of Ireland (with the z-score of -1.691 indicating the MLCV) differs significantly from neighbouring value. This is due to the combination of Ireland's unit rate value and its position within the European ATM network. Accordingly, it deviates from its only neighbouring value (United Kingdom), in relation to which it has a significantly lower unit rate.

Both assessments have identified the Swiss unit rate value as the VHCV (both z-score values are ≥ 2.58), meaning that it represents a hotspot. On the one hand, from a value-based data similarity viewpoint, the Swiss unit rate value differs considerably from the arithmetic mean of the analysed dataset. On the other hand, in terms of the spatially-based data similarity assessment, although it is surrounded by several adjacent charging zones, all of which have above average unit rate values, the Swiss unit rate value differs from them in a relevant manner.

6. DISCUSSION

In Europe, the air transport sector represents a complex yet unique network linking people and playing a vital role in Europe's further integration and development [40]. However, to maintain this function, certain conceptual changes need to be made in the strategic planning domain. For instance, the strategic modelling of the future air transport development should not only be indicated by the transport networks' technical elements or the handled transport volume, but rather in terms of availability or connectivity [41]. Moreover, its aim needs to be oriented towards achieving better performances that will lead to spatial cohesion. In this context, Steiner et al. [42] argue that when considering the strategic modelling of air transport development, it is necessary to bear in mind that it is influenced by different external and internal factors. Hence,

when evaluating the current state or determining projections of air traffic development, it is important to take into consideration different factors – ranging from the social to the economic impacts of air transport development [43]. For instance, despite the successful resolution of prerequisites enabling the future economic development in terms of the deregulation and implementation of three packages of market liberalisation measures [44-46], the European airspace has remained fragmented based on national borders. This clearly indicates that such an issue is more complex than it might seem, particularly when considering multiple viewpoints from which the airspace fragmentation can be defined and observed.

The airspace fragmentation problem was officially recognized by the European Commission back in 1996, arguing that the European Union "cannot keep the frontiers in the sky that it has managed to eliminate on the ground" [47]. Although much time has passed since then, recognizable constraints associated with the fragmentation problem are still seriously impeding the ability of the European air traffic market to grow sustainably and compete at the international level [48]. Besides, even though the fragmented design of the European airspace is a rather recognizable problem, there are still many assumptions and unanswered questions requiring comprehensive analyses to provide appropriate feedbacks. In this context, added value to this research is that for the first time, the fragmentation of the European airspace has been determined based on the application of the performance-based assessment. Accordingly, the performance-based fragmentation of the European airspace was studied with respect to cost-efficiency – one of four key performance areas of the further development of the European ATM system. This included fragmentation testing through the application of the top-down approach and analysis conduction at three complementary levels (regional, local and national level). Thereby, on the regional level, it was tested whether the European airspace is fragmented in terms of cost-efficiency. Furthermore, at the local level, spatial processes occurring locally were studied, i.e. the appearance areas of spatially-similar values. Lastly, at the national level, it was studied where value-based and spatially-based critical areas occur.

Besides, this research has shown that the European airspace is fragmented from the cost-efficiency aspect, as well as that homogeneous areas with similar unit rate values do exist, and that they are unevenly sized and distributed across the studied area, and finally, that one charging zone represents a hotspot. Accordingly, since the spatial distribution of unit rate values is a result of a random spatial process, the null hypothesis was rejected. However, the acquired results show that at the local level, it was possible to distinguish homogeneous areas that have equal or highly similar unit rate values. Spatial

outliers were identified as well. Thereby, since HL areas bear little resemblance to their neighbours, they can be marked as areas in which improvements are needed in near future. Contrary to this, areas that need to avoid their alignment with the adjacent values have been marked as LH areas. Lastly, it is possible to conclude that Switzerland, based on both data similarity and spatial similarity, represents a hotspot and has the highest critical value within the studied area.

In the previous years, it was possible to notice a high variability of unit rate values in different charging zones across the European airspace [49]. This is important to emphasise, because the way that the airspace has been "arranged" will have an impact on the "behaviour" of the air traffic flows / the AUs. Thus, one of the indirect ways of managing air traffic flows is through the unit rates.

The variability of the unit rate values and the spatial inconsistency of the air transport demand has resulted in the current situation, where the AUs pay different fees for Air Navigation Services across different European airspace's areas. That is problematic, because such situations lead to development based on partial and business-oriented interests. For instance, airspace fragmentation in terms of cost-efficiency results in a fact that the AUs have an option to purposely impair their flight efficiency (with the goal to make some financial savings). However, such practice is environmentally harmful, because it results in an increased fuel consumption and consequently, a higher emission level.

From the practical viewpoint, fragmentation effects from the cost-efficiency aspect can be verified by correlating spatial and economic dimensions of research findings with the two earlier presented route options. In this regard, Figure 11 clearly shows why the AUs would prefer the blue to the green route option. It is evident that the green trajectory – indicating that the shorter route (which is environmentally more acceptable, but more expensive) passes almost along its whole length through the charging zones of high neighbouring values. It additionally passes through the charging zone identified as the hotspot. Opposite to this, the blue trajectory indicating the cheaper, but longer route option, avoids the hotspot, and later enters areas marked as LH and LL – hence additionally making financial saving for the AUs. Moreover, considering the spatial position of the identified hotspot within the European ATM network, probably situations as the one shown in Figure 11 are not so rare. Thus, it can undoubtedly be concluded that the way that the European airspace is fragmented in terms of cost-efficiency will have a significant impact on the flight planning activities performed by Airspace Users.

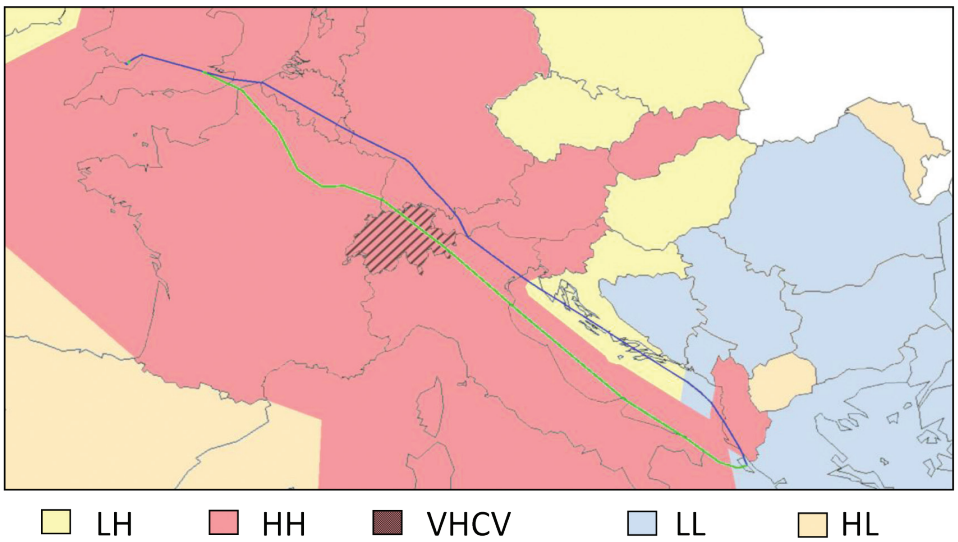

Figure 11. A comparative overview of research findings in relation to two possible flight routes
Slika 11. Usporedni pregled rezultata istraživanja u odnosu na dvije moguće rute leta

The obtained results can be placed in a wider context. For instance, Castelli et al. [50] have concluded that the unit rate values may also be used as a means for preventing further airspace congestion. It is important to note that such an approach should be taken into account with extreme caution. The increase of the unit rate value would not affect the ANSP's annual profitability level significantly, but the same conclusion cannot be drawn in relation to the profitability level of Airspace Users – which directly cover the ANSPs' costs. Profit margins of the AUs are often very low and even a small increase of operational costs will have a major impact on their annual net profit. Hence, one of the strategic goals of the future ATM system development in Europe should be oriented towards (1) the preservation of charging zones marked as LH, so that they do not become identical with their business environment, and (2) the gradual narrowing of the gap between the charging zones marked as LH with their adjacent zones – hence defragmenting the European airspace from the cost-efficiency aspect.

The research findings are also valuable to air traffic stakeholders when put in the context of new ideas and proposals for the future development of the European ATM systems. Accordingly, they can be discussed in the context of e.g. the idea of the EUA (European Upper Airspace) area, including a common route charge. In brief, the estab-

lishment of the EUA area was recommended in the report of the Wise Persons Group [51,] which was set up by the European Commission to consider recent developments in the European aviation [52]. The expectation of this idea is to achieve a higher utilisation of the shortest route options – consequently delivering benefits for the environment. However, the strategic planning of the future air transport development is influenced by several factors. The EUA idea is problematic because – as argued by Adler et al. [53] – setting a single unit rate across the entire network will result in an average price, likely to cause such a situation in which some AUs will be winning and other losing. Accordingly, over a certain period after the establishment of the EUA idea, some AUs would disappear from the market, while the "stronger ones", after the disappearance of some competitors, would (1) have the option to strengthen their position by entering markets that they have not served before; (2) in case they are already serving some market, have the option to increase their presence; or (3) have the option not to operate non-profitable routes, hence leaving some geographic areas poorly connected or isolated from other parts of Europe. If we consider research findings, we can precisely distinguish the aviation stakeholders (Member States; ANSPs; AUs) that might find the EUA idea acceptable from those that might find it unacceptable. For instance, it would be acceptable for the aviation stakeholders coming from France, Germany, Italy, Netherlands, Belgium (those mainly marked by HH indicator), and especially for Switzerland (since it is marked by the VHCV indicator). To the contrary, as research findings indicate, it is probable that aviation stakeholders coming from the less developed Member States (mainly those marked by the LL indicator) would find this idea unacceptable.

To sum up, it can be determined that the European airspace fragmentation issue, and consequently the issue of its fragmentation in terms of cost-efficiency, represents a complex problem that undoubtedly decreases the efficiency of the ATM system in Europe. Thereby, since this research provides information about every ANSP in respect to their unit rate value and position within the European ATM network, it supports the decision-making process, contributes to better understanding of business environment, and may form a basis for the future argumentative discussions in the context of strategic planning, e.g. in the context of the future development initiatives, plans, etc. Lastly, this research confirms the fact – as argued by Rezo and Steiner [54] – how difficult it is to create and implement a comprehensive and sustain air transport development plan that evenly complies with the interests of all stakeholders.

7. CONCLUSION

The problem of the fragmented design of the European airspace has been known for a long time and addressed in many different ways over the past decades. The primary reason is that airspace fragmentation negatively affects the efficiency of the European ATM system. The problem of the European airspace fragmentation in terms of cost-efficiency arises due to the fact that the ANSPs' unit rate values vary across the European airspace. This is so because they are calculated by dividing the charging zone's forecasted en-route facility cost-based by the estimated number of service units generated in the same charging zone.

The main added value of this paper is the confirmation that the European airspace is fragmented, along with the provision of the interpretation of fragmentation details in terms of cost-efficiency. By emphasising the international dimension of unit rate values impacts, it accurately shows the European airspace fragmentation level in 2018 and represents the ANSPs' competitiveness level on the economic (unit-rate) basis. The main research outcomes confirm that the European airspace is fragmented, and indicate the existence of different homogeneous areas across the European airspace, wherein one charging zone stands out as the hotspot. In addition to this, the European ATM's business environment boundaries have been clearly determined, thus framing the key issues to enhance the air market sector competitiveness. In this context, the main research findings presented within this paper will complement further research activities that will deal with airspace fragmentation from the capacitive aspect. The expected outcome of correlating the cost-efficiency and the capacitive aspect of performance-based airspace fragmentation will be the determination of where it is possible to achieve capacity-based airspace defragmentation.

Furthermore, scarcity of information supporting the European ATM community can be singled out as one of the causes for the lack of focus for collaborative initiatives addressing the European airspace defragmentation from the performance-based aspect. In this context, since it has been recognized that there are currently no unambiguous answers to the question how to test existence and measure the airspace fragmentation level, this research complements the existing literature, additionally presenting a novel approach. Its further added value is that the fragmentation has been studied by placing values of interest (unit rates) in their spatial context – which has not been the practice so far. As a result, the cost-efficiency based boundaries of the European airspace have been clearly identified, thus paving the way to further progress in terms of a performance-based airspace defragmentation.

In principle, strategic planning should provide guidance on how to improve the ATM system, so that it may become more efficient in future. In order to do so, conceptual assumptions of the strategic planning of the ATM system development in Europe need to turn to new perspectives that can contribute to the smart, inclusive and spatially-oriented development. Keeping in mind that the ATM system's most apparent flaw for the last few decades has been decision-making at the national level, this research represents one of the ways of ensuring high-quality information that might address the complex issues. Therefore, the findings shown in this paper could facilitate decision-making, and boost the future strategic air traffic planning activities.

References

[1] European Commission. Air Traffic Management; Freeing Europe's airspace; White Paper. Brussels, Belgium. 1996.

[2] Steiner S, Mihetec T, Rezo Z. Resolution of operational constraints imposed by fragmentation of European airspace. Proceedings of International Conference Science and Traffic Development (ZIRP2019), 9-10 May 2019, Opatija, Croatia

[3] Helios Economics and Policy Services. The impact of fragmentation in European ATM/CNS. EUROCONTROL. Report number: S031D019, 2006.

[4] Hartman N, Boscoianu M. Single European Sky – the transformation of the aviation industry based on the dynamic capabilities. INCAS BULLETIN. 2017;7(1): 97-109.

[5] Matsoukis E, Poulimenakos S. Air traffic management in the South East European countries. Current situation and prospects. European Transport\Trasporti Europei. 2007;37: 16-34.

[6] EUR-LEX. An Aviation Strategy for Europe [Internet]. [cited 2019 Feb 16]. Available from: https://eur-lex.europa.eu/legal-content/EN/TXT/PDF/?uri=CELEX:52015DC0598&from=EN

[7] Van Antwerpen N. Cross-Border Provision of Air Navigation Services with Specific Reference to Europe: Safeguarding Transparent Lines of Responsibility and Liability. Alphen aan den Rijn, The Netherlands: Kluwer Law International; 2008.

[8] Crespo D, Mendes de Leon P. (eds.) Achieving the Single European Sky: Goals and Challenges. Alphen aan den Rijn, The Netherlands: Kluwer Law International; 2011.

[9] O'Connell J, Williams G. Air Transport in the 21st Century: Key Strategic Developments. New York, USA: Routledge; 2016.

[10] Mihetec T, Vidović A, Rezo Z. Assessment of Single European Sky Implementation in the Functional Airspace Block Central Europe. Promet - Traffic & Transportation. 2017;29(6): 643-655.
[11] Grebenšek A, Magister T. Traffic variability in benchmarking of Air Navigation Service Providers cost-effectiveness. International Journal for Traffic and Transport Engineering. 2012;2(3): 185-201.
[12] Fox SJ. Single European Skies: Functional Airspace Blocks - Delays and responses. Air and Space Law. 2016;41(3): 201-227.
[13] Nava-Gaxiola C, Barrado C. Performance measures of the SESAR Southwest functional airspace block. Journal of Air Transport Management. 2016;50: 21-29.
[14] Young D, Pilon N, Brom L. Challenges of Air Transport 2030: Survey of experts' views. EUROCONTROL. Report number: 09/07/15-20, 2009.
[15] Rezo Z, Steiner S. European Airspace Fragmentation Typology. International Journal for Traffic and Transport Engineering. 2020;10(1): 15-30.
[16] Biggs RS, Garson GD. Analytic Mapping and Geographic Databases. Newbury Park, CA: Sage Publications Inc.; 1992.
[17] Franklin C, Hane P. An introduction to GIS: linking maps to databases.Database.1992;15(2):17-22.
[18] Rezo Z, Steiner S, Piccioni C. Potential of Geospatial Business Intelligence Solutions for Air Traffic Management. International Conference on Transport Science, 4-5 June 2020, Portorož, Slovenia
[19] Anselin L. Interactive techniques and exploratory spatial data analysis. In: Longley PA, Goodchild MF, Maguire DJ, Wind DW (eds.) Geographical information systems: principles, techniques, management and applications. Wiley, New York; 1998.
[20] Anselin L. Exploratory spatial data analysis in a geocomputational environment. In: Longley PA, Brooks SM, McDonnell R, Macmillan B (eds.) Geocomputation, a primer. Wiley, New York, 1998.
[21] Bailey T, Gatrell AC. Interactive spatial data analysis. Longman, Harlow; 1995.
[22] Ertur C, Le Gallo J. An Exploratory Spatial Data Analysis of European Regional Disparities, 1980-1995. In: Fingleton B. (ed.) European Regional Growth. Springer, Berlin, Germany. 2003. 55-97.
[23] Rezo Z, Steiner S. European airspace complexity and fragmentation correlation research. Research Workshop: Fragmentation in Air Traffic and its Impact on ATM Performance, 14-15 May 2019, Budapest, Hungary, 2019. p. 31-38
[24] EUR-LEX. Commission Implementing Decision (EU) 2019/903 of 29 May 2019 setting the Union-wide performance targets for the air traffic management network

for the third reference period starting on 1 January 2020 and ending on 31 December 2024 [Internet]. [cited 2020 Feb 20]. Available from: https://eur-lex.europa.eu/legal-content/EN/TXT/PDF/?uri=CELEX:32019D0903&from=GA

[25] Steiner S, Feletar P, Šimecki A. Transport and spatial correlation of regional development. In: Vidan P, Twrdy E, Leder N, Mulić R. (Eds.) 6th International Maritime Science Conference. 28-29 April 2014, Solin, Croatia, p. 505-517

[26] Central Route Charges Office. Guidance on the route charges system. Brussels, Belgium: EUROCONTROL; 2012.

[27] EUR-LEX. Commission implementing regulation (EU) 2019/317 of 11 February 2019 laying down a performance and charging scheme in the single European sky [Internet]. [cited 2019 Jan 20]. Available from: https://eur-lex.europa.eu/legal-content/EN/TXT/PDF/?uri=CELEX:32019R0317&from=EN

[28] CRCO. Monthly Adjusted Unit Rate - March 2012. Brussels: EUROCONTROL; 2012.

[29] CRCO. Monthly Adjusted Unit Rate - March 2018. Brussels: EUROCONTROL; 2018.

[30] STATFOR. Seven-year forecast; Flight Movements and Service Units 2017-2023. EUROCONTROL. Report number: 17/01/02-100

[31] EUROCONTROL. Information circular: Air Navigation charges in the Belarus. Brussels: EUROCONTROL; 2018.

[32] EUROCONTROL. Information circular: Air Navigation charges in the Arab Republic of Egypt. Brussels: EUROCONTROL; 2018.

[33] EUROCONTROL. Information circular: Air Navigation charges in Morocco. Brussels: EUROCONTROL; 2018.

[34] Schabenberger O, Gotway CA. Statistical Methods for Spatial Data Analysis. Boca Raton, FL: Chapman & Hall/CRC Press; 2005.

[35] Fotheringham AS, Brunsdon C, Charlton ME. Quantitative Geography: Perspectives on Spatial Data Analysis. London, England: SAGE Publications Ltd; 2000.

[36] Commission Regulation (EU) No 73/2010 of 26 January 2010 laying down requirements on the quality of aeronautical data and aeronautical information for the single European sky. Brussels, Belgium, 2010.

[37] EUROCONTROL. Guidelines for Supporting the Implementation of Commission Regulation (EU) 73/2010. Brussels, Belgium, 2017.

[38] Anselin L. The Moran Scatterplot as an ESDA Tool to Assess Local Instability in Spatial Association: Spatial Analytical Perspectives on GIS. London, England: Taylor and Francis; 1996.

[39] Anselin L, Syabri I, Kho Y. GeoDa: An Introduction to Spatial Data Analysis. Geographical Analysis. 2006;38(1): 5-22.

[40] Steiner S, Božičević A, Mihetec T. Prospects of Air Traffic Management in South Eastern Europe. Promet - Traffic & Transportation. 2010;22(4): 293-302.
[41] Steiner S, Feletar P, Šimecki A. Transport and spatial correlation of regional development. In: Vidan P, Twrdy E, Leder N, Mulić R. (Eds.) 6th International Maritime Science Conference. Solin, Croatia, 2014, p. 505-517.
[42] Steiner S, Božičević A, Mihetec T. Determinants of European air traffic development. Transport Problems. 2008;3(4): 73-84.
[43] Steiner S, Galović B, Radačić Ž. Strategic Framework of Air Traffic Development. Promet - Traffic & Transportation. 2008;20(3): 157-167.
[44] Janić M. Liberalisation of European aviation: analysis and modelling of the airline behaviour. Journal of Air Transport Management. 1997;3(4): 167-180.
[45] Button K. Deregulation and Liberalization of European Air Transport Markets. Innovation: The European Journal of Social Science Research. 2001;14(3): 255-275.
[46] Ozmec Ban M, Škurla Babić R. European air transport market under influence of cooperative arrangements. Proceedings of the 4th International Conference on Traffic and Transport Engineering. Belgrade, Serbia, 2018, p. 38-43.
[47] European Commission. Air Traffic Management - Freeing Europe's airspace. Brussels, Belgium, 1996.
[48] European Commission. Aviation: Open and Connected Europe. Brussels, Belgium, 2017.
[49] Castelli L, Ranieri A. Air Navigation Service Charges in Europe. Proceedings of the 7th USA - EUROPE ATM R&D Seminar. Barcelona, 2007.
[50] Castelli L, Labbe´ M, Violin A. A network pricing formulation for the revenue maximization of European air navigation service providers. Transportation Research Part C: Emerging Technologies. 2013;33: 214-226.
[51] Wise Persons Group. The Future of the Single European Sky. Brussels, Belgium, 2019.
[52] European Commission. Aviation: European Commission receives high-level recommendations on air traffic management in Europe [Internet]. [cited 2020 Feb 22]. Available from: https://ec.europa.eu/transport/modes/air/news/2019-04-15-recommendations-on-air-traffic-management-in-europe_en
[53] Adler N, Hanany E, Proost S. Managing European Air Traffic Control Provision. 4th SESAR Innovation Days, 25-27 November 2014, Madrid, Spain
[54] Rezo Z, Steiner S. South East Common Sky Initiative Free Route Airspace – implementation aftermath. Transport Research Procedia. 2020;45: 676-683.

FRAGMENTIRANOST EUROPSKOG ZRAČNOG PROSTORA: PROCJENA ZASNOVANA NA TROŠKOVNOJ UČINKOVITOSTI

Sažetak

Zbog varijabilnosti jediničnih cijena Pružatelja usluga u zračnoj plovidbi na različitim područjima europskog zračnog prostora, korisnici zračnog prostora za istu uslugu u zračnoj plovidbi plaćaju različite financijske iznose. Interes korisnika zračnog prostora je ostvariti što niže operativne troškove, pa je čest slučaj da zrakoplov, ukoliko postoji alternativa, leti dužim, ali ekonomski prihvatljivijim rutama kroz jeftinije naplatne zone. Tijekom vremena, primjena takve prakse dovela je do stvaranja različitih poslovnih interesa - što predstavlja kritični problem koji ometa daljnji razvoj zračnog prometa u Europi. Ovaj rad se bavi proučavanjem istraživačkog pitanja je li i ukoliko jest, kako je europski zračni prostor fragmentiran s aspekta troškovne učinkovitosti. Primjenom metodologije prostorne autokorelacije, tj. povezivanjem jediničnih cijena Pružatelja usluga u zračnoj plovidbi s njegovim prostornim položajem u okviru europskog sustava upravljanja zračnim prometom, dobiva se odgovor na postavljeno istraživačko pitanje. Rezultati istraživanja ukazuju da je europski zračni prostor fragmentiran s aspekta troškovne učinkovitosti i da je podijeljen u nekoliko različitih homogenih područja. Pri tom, takva područja karakterizirana su određenom razinom sličnosti susjednih jediničnih cijena, dok jedna naplatna zona predstavlja žarišno područje u smislu svoje neusklađenosti sa susjednim prostornim jedinicama.

Ključne riječi: Upravljanje zračnim prometom; strateško planiranje zračnog prometa; europski zračni prostor; fragmentiranost; troškovna učinkovitost.

Sanja Steiner
Hrvatska akademija znanosti i umjetnosti,
Zavod za promet
Kušlanova 2, 10000 Zagreb,
Croatia
e-mail: ssteiner@hazu.hr

Ružica Škurla Babić
Sveučilište u Zagrebu,
Fakultet prometnih znanosti, Zavod za zračni promet
Vukelićeva 4, 10000 Zagreb,
Croatia
e-mail: rskurla@fpz.hr

Zvonimir Rezo
Hrvatska akademija znanosti i umjetnosti,
Zavod za promet
Kušlanova 2, 10000 Zagreb,
Croatia
e-mail: zvonimir.rezo@gmail.com

Cristiana Piccioni
Sapienza Sveučilište u Rimu,
Faculty of Civil and Industrial Engineering,
Dept. of Civil, Constructional and Environmental Engineering,
Via Eudossiana 18, 00184 Rim, Italija
e-mail: cristiana.piccioni@uniroma1.it

DOI: 10.21857/mzvkptq359

Izvorni znanstveni članak / Original scientific paper
Prihvaćeno / Accepted: 14. listopada 2021.

FLEXIBILITY IN POWER SYSTEMS

Hrvoje Pandžić

Summary

Modern power systems rely on power generation from renewable sources, predominantly from wind and solar. However, the intermittency and variability of these sources require additional power system flexibility. Due to retirement of conventional thermal generation, the need for flexibility is increased, while the flexible resources are reduced. Thus, new flexibility resources are sought. This paper examines real-world examples of the increased flexibility requirements, identifies the new sources of flexibility in the form of batteries and demand response, presents relevant mathematical models, and provides guidelines on future research needs in this area.

Keywords: exibility; renewable energy; battery storage; thermostatically controlled loads

1. CONTEXT AND MOTIVATION

A combined system for generation, transmission and distribution of electricity is argued to be the most elaborate and most life-changing system that human kind has ever developed. Despite its complexity, the entire power system operation can be boiled down to one simple rule – electricity generation and consumption must be balanced at all times. This balance is reflected in the measured value of frequency in a power system. While North American and some countries in Asia chose the nominal frequency to be 60 Hz, the majority of countries adopted 50 Hz nominal frequency. Regardless of the nominal frequency level, the actual frequency levels should not significantly depart from this value. The main reasons for frequency deviations can be attributed to either i) poor prediction of load and variable renewable generation, e.g. wind solar power plants, or ii) failure of a generating unit or a network element, e.g. circuit breaker, transmission line, transformer. While the load prediction error is commonly within 1% of the current load [2], prediction errors related to the output of variable generating units is significantly higher, occasionally surpassing 15% [3]. Thus, the power systems with a high share of variable renewable resources might experience increased frequency deviations due to

forecast errors. The other main reason for frequency deviations are power equipment failures. Failure of a generating unit directly affects the frequency, as it disturbs the power balance. Failure of a power line, on the other hand, causes changes in the power flows and may load the surrounding lines above their thermal limits. This can cause tripping of additional lines and even eventually break the power system in multiple islands or even cause partial blackouts. On 8 January 2021, at 14:05 CET, the synchronous area of Continental Europe was separated into two parts due to outages of several transmission network elements in a very short time. The initial event was the tripping of a heavily loaded 400 kV busbar coupler in the Ernestinovo sub- station in Croatia by the overcurrent protection at 14:04:25.9 [4]. The altered power flows caused tripping of many network elements, as shown in Figure 1, and dismantled the European power system into two parts, the north-western one, with insufficient generation, and the southeastern one, with excess generation. Consequently, the north-western part experienced a frequency drop to 49.74 Hz, while the frequency in the south-eastern part increased to 50.60 Hz. To balance these two independent systems, a portion of the interruptible load was disconnected in the north-western part, while the generators in the south-eastern part reduced their power output. After the frequencies in both islanded systems were brought close to 50 Hz again, they were re-synchronized at 15:08 CET and continued the normal operation of the Continental European power system.

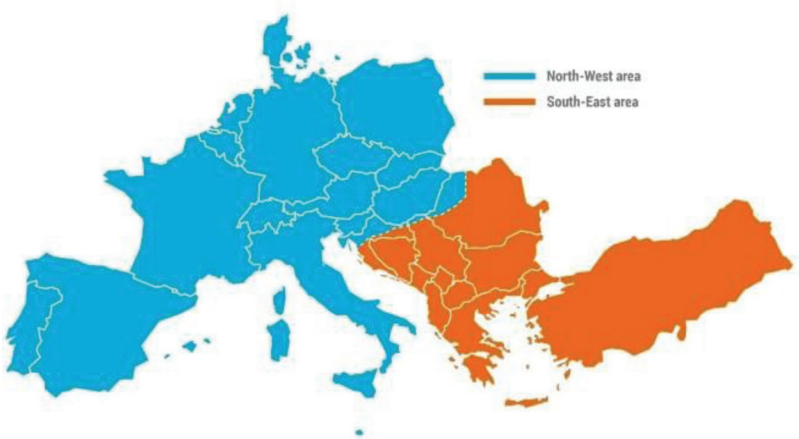

Figure 1. Separation of Continental Europe Synchronous Area on 8 January 2021 [4].
Slika 1. Razdvajanje sinkrone zone kontinentalne Europe 8. siječnja 2021.

Normal operational practice within the European power systems prescribes frequency deviations lower than 1% of the nominal value [1]. Such low frequency deviations can be achieved more easily in larger power systems. A generator failure in a system with thousands of generators is easy to deal with, as the remaining generators have sufficient regulation capacity to increase their output and jointly displace the generation of the generator under failure. Thus, large power systems are very robust to unexpected events, which was the main reason for continental Europe to be connected in a single large power system.

To address the issue of balancing the generation and the demand in power systems with a high level of variable renewable generation, and, consequently, with reduced regulation abilities from the reduced number of online controllable generators, the term *flexibility* has become important in both the scientific and technical literature recently. In one of its reports, Electric Power Research Institute defines flexibility as *the ability to adapt to dynamic and changing conditions, for example, balancing supply and demand by the hour or minute, or deploying new generation and transmission resources over a period of years [5].* Power system flexibility is becoming so important that the California Independent System Operator – CAISO introduced new market products, flexible ramp up and flexible ramp down in 2016.

Both the technical needs for flexibility and the researchers' interest worldwide in this topic are the motivation behind this paper, which aims at the following:

- Explaining the increased needs for flexibility in power systems with a high level of variable and poorly controllable renewable energy sources, i.e. wind and solar power plants (in Section 2);
- Identifying and discussing new sources of flexibility in power systems (in Section 3);
- Presenting mathematical models of new flexibility sources (in Section 4).

2. INCREASED NEEDS FOR FLEXIBILITY

Due to the load prediction errors, as well as possible failures of power system elements, power systems have been designed to operate in a way that foresees real-time adjustments in generators' power output levels. In vertically integrated power systems, as well as similarly designed US-type electricity markets, system operation is scheduled one day ahead of the operation. This process is called unit commitment, implicating that decisions are made on the commitment (on/off status) of generating units. This is highly important as thermal generators, especially nuclear and coal-fired power plants, require hours, if not days, to start up. The unit commitment problem aims at minimizing the overall operating costs of the system:

$$\text{Minimize} \sum_t \sum_i c_{i,t} \tag{1}$$

where $c_{i,t}$ denotes operating costs per generator *i* and time period *t*. The problem is primarily subject to the following technical constraints:

$$c_{i,t} = A_i \cdot x_{i,t} + \sum_k B_{k,i} \cdot p_{k,i,t} + s_{i,t} \cdot y_{i,t} \tag{2}$$

$$y_{i,t} - z_{i,t} = x_{i,t} - x_{i,t-1} \tag{3}$$

$$y_{i,t} + z_{i,t} \leq 1 \tag{4}$$

$$p_{i,t} = \sum_k B_k \cdot p_{k,i,t} \tag{5}$$

$$P^{\min} \cdot x_{i,t} \leq p_{i,t} \leq P^{\max} \cdot x_{i,t} \tag{6}$$

$$p_{i,t} - p_{i,t-1} \leq R^{\text{up}} \tag{7}$$

$$-p_{i,t} + p_{i,t-1} \leq R^{\text{dn}} \tag{8}$$

$$\sum_i p_{i,t} = \sum_l D_{l,t} \tag{9}$$

Constraint (2) calculates the hourly operating costs per generator, which consist of the fixed operating cost $A_i \cdot x_{i,t}$, the variable operating cost $\Sigma_k B_{k,i} \cdot p_{k,i,t}$ and the startup cost $s_{i,t} y_{i,t}$. The fixed operating cost is present whenever a generator is on. This is indicated by binary variable $x_{i,t}$, which takes value 1 when generator *i* is on in time period *t*, and 0 otherwise. The variable generation cost is based on a piecewise cost curve, where $B_{k,i}$ is the slope of the cost-curve segment *k,* and $p_{k,i,t}$ power produced within this segment. Finally, the startup cost is present if generator *i* is started during time period *t*, which is indicated by assigning value 1 to binary variable $y_{i,t}$. Interaction between on/

off binary variable $x_{i,t}$, startup binary variable $y_{i,t}$, and shutdown binary variable $z_{i,t}$ is modeled in constraints (3) and (4). Constraint (5) sums the generators' production per segment to obtain their overall individual outputs. Constraint (6) is used to limit the minimum and maximum production of each generator. If a generator is off, binary variable $x_{i,t}$ will have value zero and force $p_{i,t}$ to zero. Constraints (7) and (8) are ramp up and ramp down constraints. They limit the maximum change in the generator's power output in between two consecutive time periods, i.e. hours. Finally, the generation–demand balance is imposed in constraint (9). Unit commitment models also incorporate additional constraints on the generator's minimum up and down times, as well as stepwise generator startup costs and power flows [6]. In this paper, they have been omitted for brevity.

Considering the basic unit commitment model (1) – (8) in the context of the power system economics, the most relevant parameters are the ones related to the generator's costs: A_i, $B_{k,i}$ and $s_{i,t}$. However, in the context of power system flexibility, the important parameters are the minimum stable output $P^{\min}$ and the ramp limits R^{up} and R^{dn}. High values of the stable minimum output have detrimental impact on power system flexibility, as it can seriously limit the power output range of a generator. This is especially relevant for systems with a high share of photovoltaics that tend to largely reduce the net consumption curve (net load is equal to the actual load minus the generation from non-controllable renewables such as solar and wind) in the middle of the day. This phenomenon is often referred to as the duck curve (shown in Figure 2).

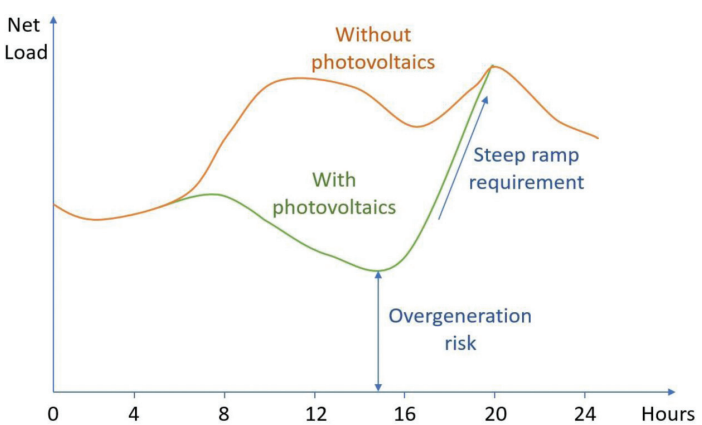

Figure 2. Visualization of a duck curve caused by high penetration of photovoltaics.

Slika 2. Prikaz tzv. krivulje patke uzrokovane visokom penetracijom fotonaponskih modula.

In systems where the online generators have high minimum output limits, the generators need to be turned off in the middle of the day, as they would otherwise cause an over-generation. However, insufficient amount of online generators in the middle of the day may not be able to meet the required steep growth of the net load caused by a simultaneous increase in the actual load and reduced generation from photovoltaics toward the end of the day. For this reason, it is required that online generators have very high ramp limits, characteristic for hydro power plants and gas-fired power plants. However, the downside of gas-fired power plants are high minimum output levels, often reaching 40% of the maximum power output. More details on the duck-curve problem is available in [7].

In order to address the duck-curve issue and sustainably increase the flexibility of the entire system, flexible energy sources need to be appropriately awarded through transparent market mechanisms. For instance, the California Independent System Operator (CAISO) introduced a flexible ramping product in 15- and 5-minute markets, which allows it to procure sufficient ramping capability via economic bids [8].

As opposed to the US-style nodal markets, the European energy markets are zonal. This means that instead of an ISO conducting the network-constrained market clearing as in the nodal markets, in Europe, a Power Exchange conducts a market clearing process without considering the network constraints. This market-clearing process can be formulated as:

$$\text{Maximize} \sum_{t} \left(\sum_{b} q_{b,t} \cdot \lambda_{b,t} - \sum_{s} q_{s,t} \cdot \lambda_{s,t} \right) \tag{10}$$

which maximizes the social welfare, defined as the sum of the producers' profit and the buyers' surplus. Variables $q_{b,t}$ and $q_{s,t}$ denote the cleared quantities of buyer b and seller s, respectively, while $\lambda_{b,t}$ and $\lambda_{s,t}$ denote the buyers' and sellers' prices offered in the market. The objective function (10) is subject to the following constraints:

$$q_{b,t} \leq Q_{b,t} \tag{11}$$

$$q_{s,t} \leq Q_{s,t} \tag{12}$$

where $Q_{b,t}$ and $Q_{s,t}$ are offered the buyers' and the sellers' quantities, respectively. The European-style markets do not include network constraints, so that after the market-clearing process, the market clearing outcome is sent to the system operator to conduct the power flow analysis and, if necessary, perform a re-dispatch of the generating units to keep the network away from an undesirable state.

Obviously, the US-style market clearing process is much more rigorous than the European-style, which is decentralized, and generators, usually combined in balancing groups, need to perform self-dispatching. In transparent European markets, the most of the energy is traded in the day-ahead market, which is cleared a day before the actual delivery of electricity. There are two markets closer to real time: the first one is the intraday market, cleared up to 30 or 5 minutes before the delivery, and the second one is the balancing market, where the system operator activates reserves to cover for the generation–demand imbalance in real time. More information on the European electricity markets is available in [9].

Since the traditional generators, i.e. coal-fired, nuclear and generally all thermal generators besides the fast-starting gas-fired plants, are not responsive enough for trading of large energy volumes in intraday and balancing markets, the flexible resources should focus on them. Since prices in those markets are usually very volatile and can reach considerably high prices in case of energy scarcity, the flexibility sources should be able to retrieve their investment cost by taking part in the intraday and balancing markets. These new flexibility sources are presented and characterized in the following chapter.

3. NEW SOURCES OF FLEXIBILITY

In close-to-fully-renewable power systems, there is no traditional controllable generation from gas, oil or coal power plants. Instead, bulk electricity is produced by variable renewable energy sources, primarily wind and solar. Thus, the burden on balancing the system has been fully transferred to hydro power plants with accumulation and renewable thermal power plants, such as biogas and biomass. However, such energy sources are generally limited and cannot satisfy the entire need for flexibility. Bearing this in mind, there are two options for increasing the flexibility. The first one is energy storage that can charge when there is excess electricity in the system, and discharge when the system lacks electricity. The second option is assigning (a part) of the balancing burden to the consumers. Although certain technologies can be used both as a bulk energy storage and at the consumers' premises, the following subsections discuss these two options individually.

3.1. Bulk Energy Storage

Currently, a vast majority of bulk energy storage in power systems is in the form of pumped hydro power plants. This technology is mature with sufficient roundtrip efficiency (app. 70%), and well represented worldwide. However, it strongly depends on the geographical conditions and requires major environmental interventions.

A recent storage technology that has a potential of being used in bulk is battery storage. Although lithium-ion battery storage owes its attractiveness and declining prices to the rollout of electric vehicles, some rather specific battery types are installed exclusively as stationary battery storage. For example, sodium-sulphur (NaS) batteries 7.2 h discharge rate make them ideal for energy-intensive services. The overall installed NaS power capacity in the world in 2016 was 365 MW. The largest installation of this storage technology is the one in Italy by the Italian transmission system operator Terna, with 34.8 MW [10].

Nevertheless, the most widely used battery technology today is lithium-ion, including a number of sub-technologies, e.g. with cobalt (LCO), nickel-cobalt- aluminum-oxide (NCA, NCR), nickel-manganese-cobalt-oxide (NMC, CGR, INR), manganese-oxide, (LMO) and ferro-phosphate (LFP, IFR). The world's largest lithium-ion battery is the one in Hornsdale Power Reserve in South Australia, with the capacity of 150 MW/193.5 MWh [11].

Lithium-ion battery storage has some very good characteristics. First, it has very high roundtrip efficiency, ranging from 80% to over 90%. Secondly, it responds instantaneously, making it suitable for very fast services. Thirdly, the degradation rate is fair, as usually lithium-ion batteries can perform a couple of thousand cycles before displaying a significant loss of capacity (20% or more of the initial capacity). Generally, they are highly reliable, but are known to perform badly at low temperatures. Additionally, the investment cost of these batteries is still quite high, which requires very elaborate business models and stacking of multiple services [12]. Generally, energy arbitrage is insufficient for achieving the required return-on-investment [13]. In order to achieve higher profits, it is required for battery storage to take part in the reserve markets. A model for optimal dispatching of lithium-ion battery energy storage in pay-as-bid secondary reserve market is presented in [14], while a joint participation of battery energy storage in the energy and reserve market was investigated in [15], [16].

3.2. Flexible Consumers

Moving the burden of power system balancing to the consumers is possible due to controllability of the demand and inclusion of power generation and energy storage at the consumers' premises, which is in line with the Fourth Energy Package known as Clean Energy for All Europeans [17].

Flexible industrial facilities can drain their flexibility from the industry process itself. Generally, pumps, ventilators, compressors, heating and cooling systems, dryers and mills can all defer their consumption in time and take part in demand response.

The US Department of Energy defines demand response as *changes in electric usage by end-use customers from their normal consumption patterns in response to changes in the price of electricity over time, or to incentive payments designed to induce lower electricity use at times of high wholesale market prices or when system reliability is jeopardized* [18]. If such facilities comprise controllable power generators, e.g. biogas power plant, or variable generation combined with battery storage, e.g. rooftop solar plant combined with battery storage, their flexibility potential is even greater. An energy use breakdown for cement industry is presented in [19]. Such analysis can serve as a great stepping stone for determining the potential of an industry facility in providing demand response. An example of an investment of industrial facilities in battery storage and photovoltaics for participation in energy markets is available in [20].

Commercial buildings have a strong potential for demand response too, mostly because of the thermostatically controlled loads, e.g. electric heating, boilers and air conditioning. An interested reader may find a comprehensive introduction to demand response control strategies in commercial buildings in [21]. A model for optimal investment of a hotel in battery storage is available in [22].

Finally, the residential sector also possesses a strong demand response potential. However, this potential is very difficult and very expensive to put in service, as the devices have rather low power capacity. This increases the cost of demand-response-ready investments, makes the measurements difficult to obtain and, consequently, reduces the economic impact of demand response. Furthermore, the perception of demand response among residential consumers is not always positive [23]. Some of the household devices with a high potential for demand response include clothes washers and dryers, air conditioners, water heaters, ovens, dishwashers and refrigerators [24]. Additionally, if many households on a specific location contain swimming pools, e.g. Florida in the USA, pool pumps can be utilized to provide demand response as well [25].

Lately, due to a serious uptake of electric vehicles, electric vehicle charging stations have been identified as a major flexibility source. An increasing number of electric vehicles can have an adverse effect on the power stability if inadequately controlled, but if the charging process is controlled in a system-aware way, they can become a valuable flexible asset. Controlled electric vehicle charging can bring high benefits to the balancing of the power system due to the electric vehicles' high storage capability [26] and availability during the day [27]. Essentially, electric vehicles are batteries whose primary aim is to serve the drivers' needs. However, they are not connected to the charging stations at all times, which reduces their availability to act according to the power system's needs. Since their battery capacity and (dis)charging power capacity is rather low as compared to the overall system needs, they are commonly aggregated by a special

entity, i.e. an aggregator that distributes the control commands to the electric vehicles, and acts in the energy and/or reserve market as one entity representing a number of electric vehicles or charging stations [28].

4. MATHEMATICAL MODEL FOR NEW FLEXIBILITY SOURCES

This section presents mathematical models for new sources of uncertainty identified in the previous section – battery storage, representing both stationary storage and electric vehicle battery storage, and thermostatically controlled loads as the most common representative of the demand response devices.

4.1. Battery Storage

Battery storage models are built upon the generic storage model presented below:

$$p_t^{\mathrm{ch}} \leq P \tag{13}$$

$$p_t^{\mathrm{dis}} \leq P \tag{14}$$

$$soe_t = soe_{t-1} + p_t^{\mathrm{ch}} \cdot \eta^{\mathrm{ch}} - p_t^{\mathrm{dis}}/\eta^{\mathrm{dis}} \tag{15}$$

$$soe_t \leq SOE \tag{16}$$

Constraints (13) and (14) limit the energy storage charging power p^{ch}, which is the power taken from the grid, and the discharging power, p^{ch}, which is the power injected into the grid. State-of-energy in each time step soe_t is calculated in (15) based on the state-of-energy in the previous time step, electricity taken from the grid multiplied with the charging efficiency η^{ch}, and electricity injected into the grid, accounting for the discharge efficiency η^{dis}. Finally, constraints (16) limits the state-of-energy of energy storage.

The generic energy storage model (13)–(16) has been widely used in the literature as the battery storage model. For instance, in [29], the authors use the generic battery storage model to optimize their deployment in a unit commitment model to reduce congestion and, consequently, reduce the system operation costs. In [30], the batteries are used in a security-constrained optimal power flow model to deal with contingencies. In the microgrid investment model presented in [31], as well as in the microgrid bidding model in [32], batteries are modeled using the generic energy storage model (13)–(16). Even when modeling the batteries in electric vehicles, the generic energy storage model

is predominantly used for modeling, see e.g. [33], [34], [35]. However, the generic energy storage model does not accurately capture the behavior of the lithium-ion batteries, which were directly or indirectly considered in the papers above. Figures 3–5 show voltage, current and power characteristics during charging for C-rate[1] levels 0.2C, 0.5C and 1C, while Figures 6–8 show the same curves for the discharging process. All the curves were captured in the SmartGrid Lab at the University of Zagreb, Faculty of Electrical Engineering and Computing [36].

The battery charging voltage curves in Figure 3 show that the battery voltage increases as the battery is charged. Comparing these curves with the corresponding ones in Figure 2 clearly shows that the charging process has two phases. In the first phase, the charging currents is constant (constant-current phase), and the voltage increases steeply. After the voltage reaches the upper threshold, the current needs to be reduced in order to avoid further increase of voltage and damage to the battery (the upper voltage threshold is set based on the battery producer's datasheet). This is known as the constant-voltage phase. Figure 3 shows the charging power, which is the most relevant quantity for power system economics models. It is obtained as a multiplication of voltage and current. One can notice that the charging power at the beginning, i.e. at low state-of-energy, slowly increases due to increase in voltage (the current is constant), but after entering the constant-voltage phase, the charging power is abruptly reduced due to the depreciation of the charging current. This is why battery charging at 1C lasts for 2.5 hours, as can be seen in Figure 1–3, instead of one hour. For the same reason, charging at 0.5C lasts three instead of two hours, while charging at 0.2C lasts six instead of five hours.

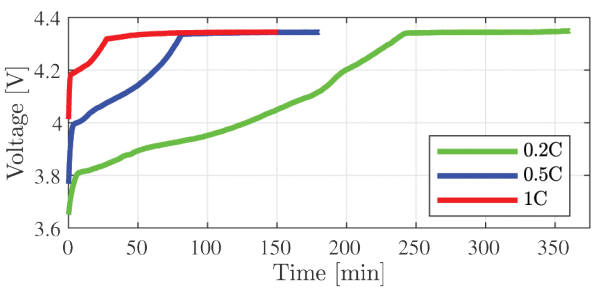

Figure 3. Charging voltage of a lithium-ion battery for three charging speeds.

Slika 3. Napon punjenja litij-ionske baterije za tri brzine punjenja

1 C-rate is a theoretical measure of the speed at which a battery is charged or discharged. For example, 1C discharge rate would deliver the battery's rated capacity in 1 hour, 0.5C in 2 hours, etc.

The discharging voltage in Figure 4 is reduced as the battery is discharged. However, the discharging current in Figure 5 is constant throughout the discharging process, resulting in almost flat discharging power shown in Figure 6. The presented laboratory tests indicate that the generic energy storage model (13)–(16) fails to capture the fact that the battery charging ability is reduced with its state-of-energy. More specifically, constraint (13) does not properly capture the physico-chemical properties of lithium-ion batteries. In literature, however, there are two linear battery models that quite accurately capture this fact; more information can be found in [37], [38].

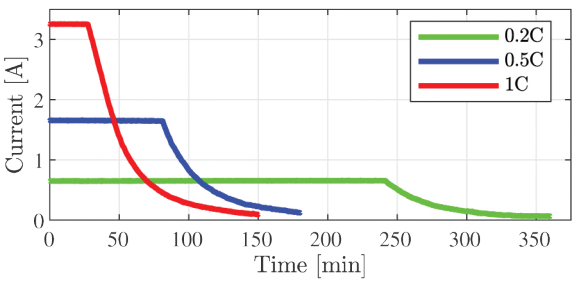

Figure 4. Charging current of a lithium-ion battery for three charging speeds.
Slika 4. Struja punjenja litij-ionske baterije za tri brzine punjenja

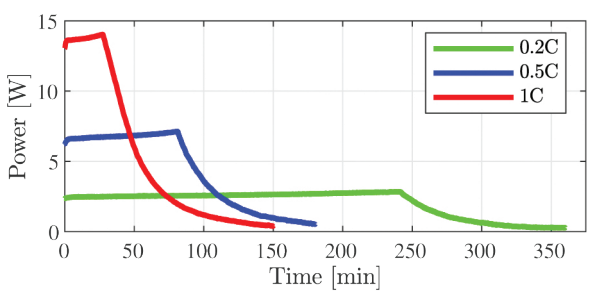

Figure 5. Charging power of a lithium-ion battery for three charging speeds.
Slika 5. Snaga punjenja litij-ionske baterije za tri brzine punjenja

4.2 Thermostatically Controlled Loads

A credible representative of thermostatically controlled loads, whose model is presented below, is a heat pump (HP) with an auxiliary heating (AH) device. These are used to provide both the space heating (SH) and hot water (HW).

$$d_t = p_t^{\mathrm{HP,SH}} + p_t^{\mathrm{HP,HW}} + p_t^{\mathrm{AH,SH}} + p_t^{\mathrm{AH,HW}} \tag{17}$$

$$p_t^{\mathrm{HP,SH}} + p_t^{\mathrm{HP,HW}} \leq P^{\mathrm{HP}} \tag{18}$$

$$p_t^{\mathrm{AH,SH}} + p_t^{\mathrm{AH,HW}} \leq P^{\mathrm{AH}} \tag{19}$$

$$\dot{q}_t^{\mathrm{SH}} = k^{\mathrm{SH}} \cdot p_t^{\mathrm{HP,SH}} + k^{\mathrm{SH}} \cdot p_t^{\mathrm{AH,SH}} \tag{20}$$

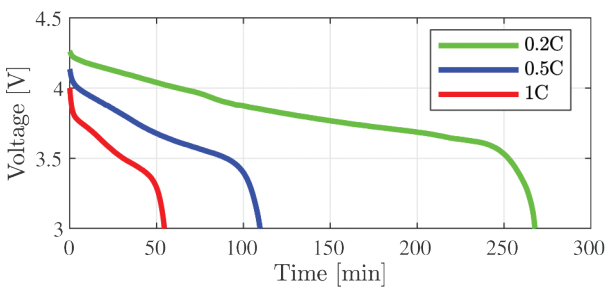

Figure 6. Discharging voltage of a lithium-ion battery for three discharging speeds.
Slika 6. Napon pražnjenja litij-ionske baterije za tri brzine pražnjenja.

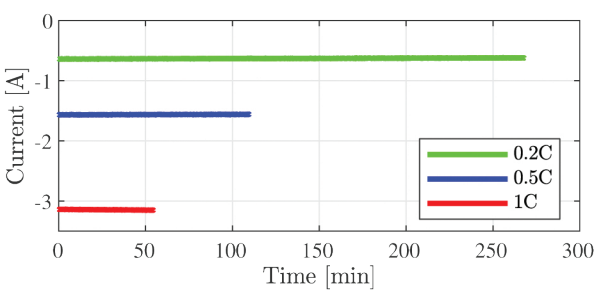

Figure 7. Discharging current of a lithium-ion battery for three discharging speeds.
Slika 7. Struja praznjenja litij-ionske baterije za tri brzine pražnjenja.

The power balance equation (17) determines the overall power demand d_t required for supplying the heat pump for space heating $p_t^{\mathrm{HP,SH}}$ and hot water $p_t^{\mathrm{HP,HW}}$, as well as supplying the auxiliary heating device for space heating $p_t^{\mathrm{AH,SH}}$ and hot water $p_t^{\mathrm{AH,HW}}$. The maximum power capacities of the heat pump P^{HP} and the auxiliary heating device P^{AH} are enforced in (18) and (19). Constraint (20) translates the electrical power consumed by the heat pump and the auxiliary heating devices to the required thermal power for space heating $\dot{q}_t^{\mathrm{SH}}$ using the space heating performance coefficient k^{SH}. Equation (21) calculates the indoor temperature based on the temperature in the previous time step, heating power $\dot{q}_t^{\mathrm{SH}}$ and thermal losses and solar gains $\mathrm{C}_{p,t}^{\mathrm{SH}}$. Coefficient matrices $\mathrm{A}_p^{\mathrm{SH}}$ and $\mathrm{B}_p^{\mathrm{SH}}$ are matrices of the linear state-space model used to simulate the indoor thermal behavior. Constraint (22) sets the upper $\mathrm{T}_{p,t}^{\mathrm{SH,hi}}$ and lower $\mathrm{T}_{p,t}^{\mathrm{SH,lo}}$ limits on the indoor temperature the inmates find comfortable. Constraints (23)–(25) model the hot water utilization in the same way constraints (20)–(22) model the space heating. Additional explanations on the model can be found in [39], [40].

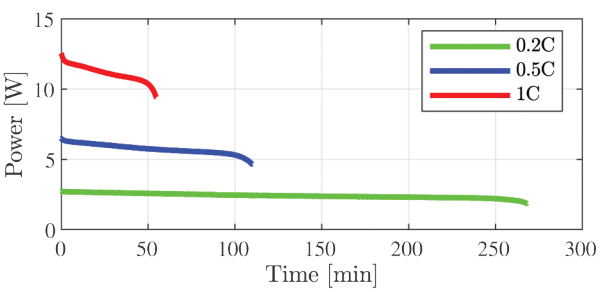

Figure 8. Discharging power of a lithium-ion battery for three discharging speeds.

Slika 8. Snaga pražnjenja litij-ionske baterije za tri brzine pražnjenja.

5. CONCLUSION

The aim of this paper was to point out the increasing needs for flexibility in modern power systems with high capacity from variable renewable sources. The technical perspective calls for new sources of flexibility in the form of deferrable loads and battery storage, both stationary and electric vehicles, whose goal is to take part in the balancing of the power systems. The paper identifies some major obstacles for a strong rollout of such devices:

1. The price of both the devices able to defer their consumption and battery storage is still rather high, and the benefits these devices bring to an investor can as yet not justify their cost. This is especially the case with countries such as Croatia, where electricity prices for consumers are relatively low (see the takeaways from [20]).
2. Control of a large number of distributed devices is not only expensive, but prone to security breaches. This is especially the case with publicly available charging stations [41]. Their high power capacity makes tampering with control systems of the electric vehicle charging stations dangerous for the power system security [42].
3. Further improvements in modeling of flexible resources is needed. This includes variable efficiency of the battery charging and discharging process (depending on the charging and discharging currents), as well as improved modeling of specific household devices with a potential for demand response.
4. Market structures need to be further developed in order to enable trading closer to real time and reward flexible sources. A good example of such market is the flexiramp product in California [8].

Acknowledgements

This work was supported in part by the Croatian Science Foundation under the project Flexibility of Converter-based Microgrids – FLEXIBASE (PZS-2019-02-7747).

References

1. Eurelectric and ENTSO-E, "Deterministic frequency deviations – root causes and proposals for potential solutions", A joint EURELECTRIC – ENTSO-E response paper, December 2011.
2. B. Hodge, D. Lew and M. Milligan, "Short-Term Load Forecast Error Dis- tributions and Implications for Renewable Integration Studies", *2013 IEEE Green Technologies Conference (GreenTech)*, Denver, CO, 2013, pp. 435– 442.
3. B. Hodge, D. Lew, M. Milligan, H. Holttinen, S. Sillanpää, E. Gómez-Lázaro, R. Scharff, L. Söder, X. G. Larsén, G. Giebel, D. Flynn, and J. Dobschinski, "Wind Power Forecasting Error Distributions: An International Comparison", *11th Annual International Workshop on Large-Scale Integration of Wind Power into Power Systems as well as on Transmission Networks for Offshore Wind Power Plants Conference*, Lisbon, Portugal, November 13–15, 2012, pp. 1–7.
4. ENTSO-E, "System separation in the Continental Europe Synchronous Area on 8 January 2021 – 2nd update", January 26, 2021. [Online] Available at: https://tinyurl.com/uvhxbm86. Accessed on February 11, 2021.
5. Electric Power Research Institute (EPRI), "Electric Power System Flexibility – Challenges and Opportunities", Technical Report, February 2016.
6. H. Pandžić, Ting Qiu and D. S. Kirschen, "Comparison of state-of-the- art transmission constrained unit commitment formulations", *2013 IEEE Power & Energy Society General Meeting*, Vancouver, BC, Canada, 2013, pp. 1–5.
7. P. Denholm, R. Margolis, and J. Milford, "Production Cost Modeling for High Levels of Photovoltaics Penetration", Technical Report, National Renewable Energy Laboratory, Technical Report NREL/TP-581-42305, February 2008.
8. California Independent System Operator. [Online] Available at: https://tinyurl.com/7rraasch. Accessed on February 11, 2021.
9. Ivan Pavić, Mateo Beus, Hrvoje Pandžić, Tomislav Capuder, and Ivona Štritof, "Electricity markets overview — Market participation possibilities for renewable and distributed energy resources", *14th International Conference on the European Energy Market (EEM)*, Dresden, Germany, June 6-9, 2017, pp. 1–5.

10. M. Andriollo, R. Benato, S. Dambone Sessa, N. Di Pietro, N. Hirai, Y. Nakanishi, and E. Senatore, "Energy intensive electrochemical storage in Italy: 34.8 MW sodium–sulphur secondary cells", *Journal of Energy Storage*, vol. 5, 2016, pp. 146–155.
11. PV Magazine. [Online] Available at: https://tinyurl.com/tcdj2fwa. Accessed on February 11, 2021.
12. M. Miletić, Z. Luburić, I. Pavić, T. Capuder, H. Pandžić, I. Andročec, and A. Marušić, "A Review of Energy Storage Systems' Applications", *Mediterranean Conference on Power Generation, Transmission, Distribution and Energy Conversion (MEDPOWER 2018)*, Dubrovnik, Croatia, November 12–15, 2018, pp. 1–5.
13. H. Pandžić and I. Kuzle, "Energy Storage Operation in the Day-Ahead Electricity Market", *European Energy Market 2015*, Lisbon, Portugal, May 19–22, 2015, pp. 1–6.
14. C. Goebel, H. Hesse, M. Schimpe, A. Jossen, and H. Jacobsen, "Model-Based Dispatch Strategies for Lithium-Ion Battery Energy Storage Applied to Pay-as-Bid Markets for Secondary Reserve", *IEEE Transactions on Power Systems*, vol. 32, no. 4, pp. 2724–2734, 2017.
15. N. Padmanabhan, M. Ahmed, and K. Bhattacharya, "Battery Energy Storage Systems in Energy and Reserve Markets", *IEEE Transactions on Power Systems*, vol. 35, no. 1, pp. 215–226, 2020.
16. K. Pandžić, K. Bruninx and H. Pandžić, "Managing Risks Faced by Strategic Battery Storage in Joint Energy-Reserve Markets", *IEEE Transactions on Power Systems*, early access.
17. European Commission: Clean energy for all Europeans package. [Online] Available at: ec.europa.eu/energy/topics/energy-strategy/clean-energy-all-europeans en. Accessed on February 12, 2021.
18. US Department of Energy: Demand Response. [Online] Available at: https://tinyurl.com/3kc7knd5. Accessed on February 12, 2021.
19. N. A. Madlool, R. Saidur, M. S. Hossain, and N. A. Rahim, "A critical review on energy use and savings in the cement industries", *Renewable and Sustainable Energy Reviews*, vol. 15, no. 4, 2011, pp. 2042–2060.
20. N. Čović, F. Braeuer, R. Mckenna and H. Pandžić, "Optimal PV and Battery Investment of Market-Participating Industry Facilities", *IEEE Transactions on Power Systems*, early access.
21. N. Motegi et al., "Introduction to Commercial Building Control Strategies and Techniques for Demand Response", Demand Response Research Center, Lawrence Berkeley National Laboratory, Berkeley, 2007.
22. Hrvoje Pandžić, "Optimal battery energy storage investment in buildings", *Energy and Buildings*, vol. 175, 2018, pp. 189–198.

23. D. Torstensson and F. Wallin, "Exploring the Perception for Demand Response among Residential Consumers", *Energy Procedia*, 2014, pp. 2797– 2800.
24. M. Pipattanasomporn, M. Kuzlu, S. Rahman, and Y. Teklu, "Load Profiles of Selected Major Household Appliances and Their Demand Response Opportunities", *IEEE Transactions on Smart Grid*, vol. 5, no. 2, pp. 742–750, March 2014.
25. S. Meyn, P. Barooah, A. Bušić, and J. Ehren, "Ancillary service to the grid from deferrable loads: The case for intelligent pool pumps in Florida", *2nd IEEE Conference on Decision and Control*, Florence, Italy, 2013, pp. 6946–6953.
26. International Renewable Energy Agency, Innovation landscape brief: Electric-vehicle smart charging, Technical Report, 2019.
27. G. Pasaoglu, D. Fiorello, A. Martino, G. Scarcella, A. Alemanno, A. Zubaryeva, an C. Thiel, "Driving and parking patterns of European car drivers – a mobility survey", European Commission Report, 2012.
28. I. Pavić, H. Pandžić, and T. Capuder, "Electric vehicle based smart e- mobility system – Definition and comparison to the existing concept", *Applied Energy*, vol. 272, 2020, 115153.
29. H. Pandžić, Y. Wang, T. Qiu, Y. Dvorkin, and D. Kirschen, "Near-optimal method for siting and sizing of distributed storage in a transmission network", *IEEE Transactions on Power Systems*, vol. 30, no. 5, pp. 2288–2300, Sep. 2015.
30. Y. Wen, C. Guo, D. S. Kirschen, and S. Dong, "Enhanced security- constrained OPF with distributed battery energy storage", *IEEE Transactions on Power Systems*, vol. 30, no. 1, pp. 98–108, Jan. 2015.
31. T. Dragičević, H. Pandžić, D. Škrlec, I. Kuzle, J. M. Guerrero, and D. S. Kirschen, "Capacity optimization of renewable energy sources and battery storage in an autonomous telecommunication facility", *IEEE Trans- actions on Sustainable Energy*, vol. 5, no. 4, pp. 1367–1378, Oct. 2014.
32. G. Liu, Y. Xu, and K. Tomsovic, "Bidding strategy for microgrid in day-ahead market based on hybrid stochastic/robust optimization", *IEEE Transactions on Smart Grid*, vol. 7, no. 1, pp. 227–237, Jan. 2016.
33. M. González Vayá and G. Andersson, "Optimal bidding strategy of a plug- in electric vehicle aggregator in day-ahead electricity markets under uncertainty", *IEEE Transactions on Power Systems*, vol. 30, no. 5, pp. 2375– 2385, Sep. 2015.
34. H. Wu, M. Shahidehpour, A. Alabdulwahab, and A. Abusorrah, "A game theoretic approach to risk-based optimal bidding strategies for electric vehicle aggregators in electricity markets with variable wind energy resources", *IEEE Transactions on Sustainable Energy*, vol. 7, no. 1, pp. 374–385, Jan. 2016.

35. M. R. Sarker, H. Pandžić, and M. A. Ortega-Vazquez, "Optimal operation and services scheduling for an electric vehicle battery swapping station", *IEEE Transactions on Power Systems*, vol. 30, no. 2, pp. 901–910, Mar. 2015.
36. Smart Grid Laboratory, University of Zagreb, Faculty of Electrical Engineering and Computing. [Online] Available at: www.fer.unizg.hr/zvne/research/research labs/sglab. Accessed on February 15, 2021.
37. S. I. Vagropoulos and A. G. Bakirtzis, "Optimal bidding strategy for electric vehicle aggregators in electricity markets", *IEEE Transactions on Power Systems*, vol. 28, no. 4, pp. 4031–4041, Nov. 2013.
38. V. Bobanac and H. Pandžić, "An Accurate Charging Model of Battery Energy Storage", *IEEE Transactions on Power Systems*, vol. 34, no. 2, pp. 1416–1426, March 2019.
39. D. Patteeuw, K. Bruninx, A. Arteconi, E. Delarue, W. D'haeseleer, and L. Helsen, "Integrated modeling of active demand response with electric heating systems coupled to thermal energy storage systems", *Applied Energy*, vol. 151, pp. 306–319, 2015.
40. K. Bruninx, H. Pandžić, H. Le Cedre, and E. Delarue, "On Controllability of Demand Response Resources & Aggregators' Bidding Strategies", *2018 Power Systems Computation Conference (PSCC)*, Dublin, Ireland, June 11–15, 2018, pp. 1-7.
41. S. Acharya, Y. Dvorkin, H. Pandžić, and R. Karri, "Cybersecurity of Smart Electric Vehicle Charging", *IEEE Access*, vol. 8, pp. 214434–214453, 2020.
42. S. Acharya, Y. Dvorkin, and R. Karri, "Public plug-in electric vehicles + grid data: Is a new cyberattack vector viable?", *IEEE Transactions on Smart Grid*, vol. 11, no. 6, pp. 5099–5113, Nov. 2020.

FLEKSIBILNOST ELEKTROENERGETSKIH SUSTAVA

Sažetak

Moderni elektroenergetski sustavi oslanjaju se na proizvodnju električne energije iz obnovljivih izvora energije, prvenstveno vjetra i Sunca. Međutim, nepravilnost i promjenjivost njihove proizvodnje električne energije uzrokuje povećane zahtjeve za fleksibilnošću sustava. Nadalje, uslijed prestanka rada konvencionalnih termalnih elektrana, koje su i same bile izvor fleksibilnosti, nedostatak iste sve je više izražen. Stoga su potrebni novi izvori fleksibilnosti. Članak izučava stvarne primjere povećanih zahtijeva za fleksibilnošću, identificira nove izvore fleksibilnosti (baterije i odaziv potrošnje), te predstavlja relevantne matematičke modele i daje preporuke za buduća istraživanja u ovom području.

Ključne riječi: fleksibilnosti; obnovljivi izvori energije; baterijski spremnici energije, termostatski upravljana trošila.

Hrvoje Pandžić
University of Zagreb
Faculty of Electrical Engineering and Computing
Unska 3, Zagreb, Croatia
e-mail: hrvoje.pandzic@fer.hr

DOI: 10.21857/9e31lhvz1m

Izvorni znanstveni članak / Original scientific paper
Prihvaćeno / Accepted: 14. listopada 2021.

EXPERIMENTAL MODELING OF BORA WIND LOADS ON ROAD VEHICLES

Hrvoje Kozmar, Ahsan Kareem

Summary

The Bora is a very strong and gusty downslope wind that blows from the northeast across the coastal mountain ranges on the eastern coast of the Adriatic Sea. It creates substantial difficulties for engineering infrastructure, traffic, and life in general. While the effects of the quasi-steady turbulent atmospheric boundary layer flow on road vehicles are currently fairly well known, the Bora wind also creates unsteady aerodynamic loads on these vehicles, which are still not fully understood. These gust effects on road vehicles have thus been experimentally examined here. This study was conducted on a small-scale road vehicle model, which to our knowledge is the first study of this type. Particular emphasis was placed on the aerodynamic forces and moments experienced by the road vehicle related to the strength and frequency of the Bora wind gusts, the vertical wind incidence angle, and the vehicle position on the bridge. In the experiments regarding the wind gust strength and frequency, the road vehicle model was placed in the upwind traffic lane at zero horizontal and vertical flow incidence angles. The effect of the vertical wind incidence angle and vehicle position was analyzed for the road vehicle model placed in the upwind, middle, and downwind traffic lanes of the bridge-deck section model, where the horizontal flow incidence angle was zero, while the vertical flow incidence angle was studied from 0° to 50°. The experiments were carried out in the Transient Flow Field Simulator of the NatHaz Modeling Laboratory at the University of Notre Dame, USA. The results reveal some important findings. Regarding the wind gust strength and frequency experiments, the aerodynamic loads rose linearly with increasing gust strength and were concurrently affected by vortex shedding and wind gusting phenomena. The steady aerodynamic loads were generally higher for a road vehicle closer to the upwind edge of the bridge decks. The wind gusting of the Bora can cause difficulties for the maneuvering of road vehicles and for their stability in the upwind traffic lane, while the risk for road vehicles in the downwind traffic lanes was predominantly a

consequence of the impinging shed vortices unique to bridge architecture and the aerodynamic form of vehicles.

Keywords: gusty Bora wind, aerodynamic loads on road vehicles, laboratory experiments.

1. INTRODUCTION

The Bora is a very strong, usually dry and always gusty wind that blows from the northeast across the coastal mountain ranges on the eastern coast of the Adriatic Sea, e.g. Yoshino (1976), Bajić (1988, 1989), Tutiš (1988), Vučetić (1991), Belušić and Klaić (2004, 2006). It more commonly occurs in winter when it can last from several hours up to several days, e.g. Jurčec (1981), Poje (1992), Enger and Grisogono (1998), Jeromel et al. (2009). Its mean velocity, usually not less than 5 m/s and often surpassing 30 m/s, is less significant than its gusts that can reach velocities up to five times the average, e.g. Petkovšek (1987), Grisogono and Belušić (2009), Večenaj et al. (2010), Belušić et al. (2013). There is no precise definition of the Bora, primarily due to its extreme spatial variability, e.g. Horvath et al. (2009), Večenaj et al. (2012). However, its basic characteristics are that it is a horizontal wind with an azimuth from the first quadrant lasting at least for three hours with a mean wind speed higher than 5 m/s and a standard deviation comparable to the mean value.

Bora wind gusts are a consequence of cold air cylinders rolling down the slope on the warm side of a mountain ridge. Along with the atmospheric turbulence and sliding cold air, the concurrent action of these three phenomena creates a complex wind flow and turbulence with characteristic Bora features, Figure 1.

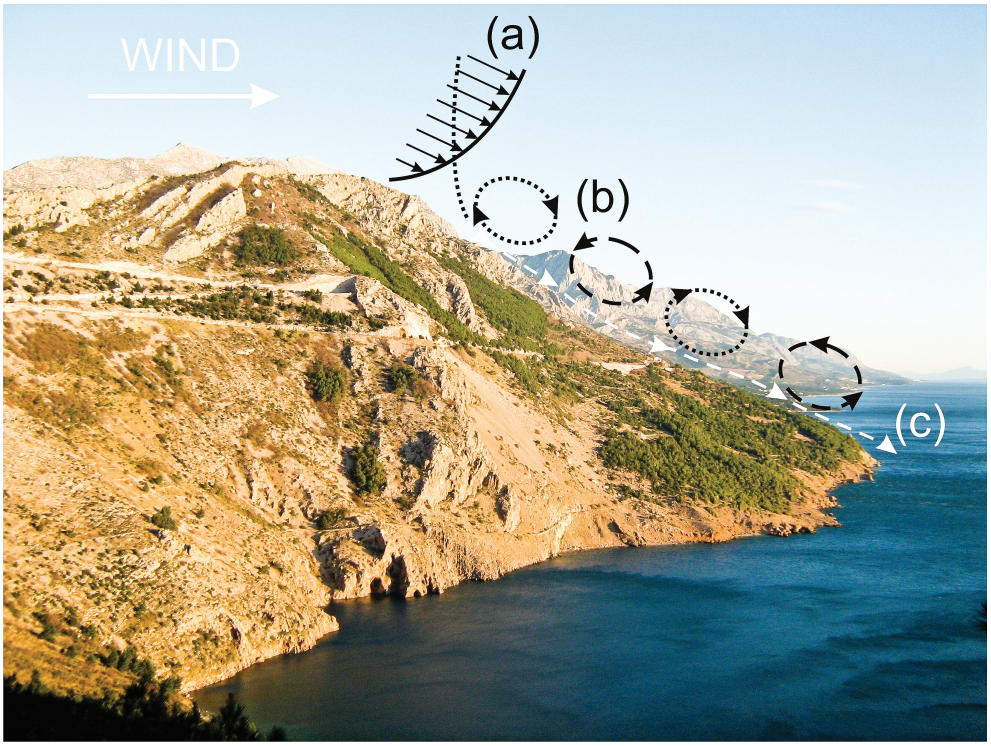

Figure 1. Elements of the gusty Bora wind: a) atmospheric wind flow and turbulence (the solid line is the mean velocity profile and the dotted line is the turbulence kinetic energy profile); b) air cylinders exerted by orographic wave breaking; c) sliding cold air. Photograph taken by Tomica Kozmar in the Dubci area, 40 km south of Split, Croatia, after Kozmar et al. (2012a)

Slika 1. Elementi mahovitog vjetra bure: a) atmosferski vjetar i turbulencija (puna crta je profil osrednjene vrijednosti brzine, isprekidana crta je profil kinetičke energije turbulencije), b) vrtlozi zraka nastali lomljenjem orografskog vala, c) klizajući hladan zrak. Fotografiju snimio Tomica Kozmar na području Dubaca, 40 km južno od Splita, Hrvatska, Kozmar i sur. (2012a)

The characteristics of the Bora wind have been previously analyzed in meteorology, climatology, and geophysics. However, the focus of these works was quite different from what is required for input information for environmental and structural aerodynamics. In other words, the existing data are of rather marginal relevance for engineering applications. This was therefore motivation for the joint work of geophysicists and engineers to address the Bora and other non-synoptic winds in a form suitable for engineering applications, e.g. Lepri et al. (2014, 2015, 2017), a special issue of *Wind and Structures* (Kozmar, 2017), Hangan and Kareem (2021).

There is a substantial body of knowledge on aerodynamic loads acting on road vehicles subjected to quasi-steady turbulent cross flows. In these quasi-steady conditions, three types of wind-induced vehicle accidents are possible, i.e. overturning, side-slip, and rotation. Baker (1986, 1987, 1991a,b,c) extensively studied the performance of high-sided vehicles in cross winds and proposed equations to account for the wind effects on vehicles. For high-sided vehicles like buses and trucks, overturning is more likely to occur than the other two types of accidents. A gust duration of only 2 s to 3 s was seen to be sufficient to blow over a vehicle, Baker and Robinson (1990). The wind speed at which the accident criteria are exceeded is a function of vehicle speed, wind direction, and the infrastructure. Meteorological data may be used to determine the time period, the accident wind speed, and the risk probability, Baker and Reynolds (1992). This brief survey reveals that quasi-steady cross winds may create a substantial risk for vehicles, while this issue is even more complex for transient winds like the Bora.

Preliminary studies on the effects of transient wind loads on vehicles have shown that the steady-state approach underestimates transient forces and moments, Ryan and Dominy (1998), while the aerodynamic forces exerted only by wind gusts may possibly be predicted by assuming the quasi-steady flow, Bearman and Mullarkey (1994). Currently, there is clearly a substantial lack of knowledge on this topic, a fact which provided motivation for the present work.

Laboratory experiments on the effects of the gusty Bora wind on road vehicles are reported here. Specifically, the aerodynamic loads on road vehicles on bridges were the subject of analysis because vehicles in this configuration are particularly sensitive to cross-wind loading. The aerodynamic forces and moments experienced by road vehicles were studied relating to the strength and frequency of the wind gusts of the Bora, the vertical wind incidence angle, and the vehicle position on the bridge. The study presents an overview of the experimental analysis performed so far and published as journal articles and conference contributions, Kozmar et al. (2009, 2011, 2012a,b, 2015). The contents of these previous publications were adopted or adapted for the purposes of the present study. However, respective references are not provided on each and every occasion in the present article to enhance readability by avoiding disruptions that could occur with excessive referencing.

2. METHODOLOGY

Experiments were carried out in the Transient Flow Field Simulator (TFFS) in the NatHaz Modeling Laboratory at the University of Notre Dame, USA. The TFFS test section equipped with four fans creating the airflows is presented in Figure 2.

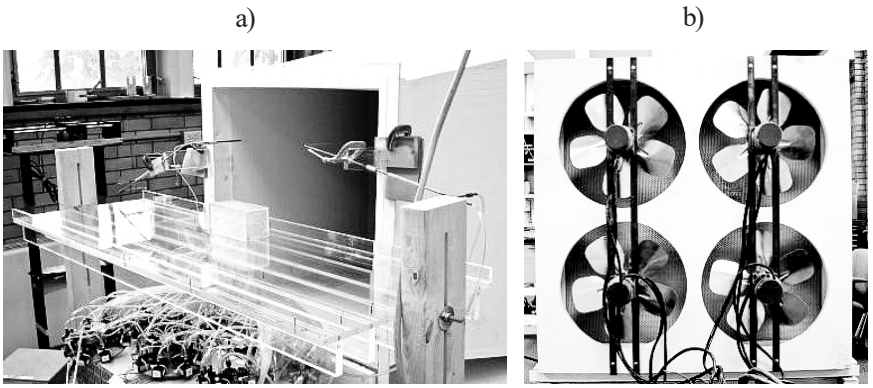

Figure 2. Transient Flow Field Simulator (TFFS) in the NatHaz Modeling Laboratory at the University of Notre Dame, USA. a) test section with a vehicle model on a bridge-deck section model; b) four fans creating the airflows, Kozmar et al. (2012a)

Slika 2. Simulator polja nestacionarnog strujanja zraka (TFFS) u sklopu NatHaz laboratorija Sveučilišta Notre Dame u SAD-u. a) ispitna sekcija s modelom vozila na modelu sekcije mosta, b) četiri ventilatora koji stvaraju strujanje zraka, Kozmar i sur. (2012a)

The TFFS is an open-circuit type wind tunnel with a 50 cm wide and 50 cm high rectangular open test section and a set of four fans that create transient flows. Its general purpose is to allow study of the effect of gusty winds on structural models. Upstream of the structural model, the air flows through a honeycomb, two sets of screens and a nozzle with a contraction ratio of 2:1. At the inlet of the test section, a maximal velocity of ~5 m/s can be achieved. The fans are connected to low-inertia BLM-N23-1000 brushless AC servomotors with a 1000 line differential quadrature encoder. The motors are controlled by a Galil DMC-2143 Ethernet system programmed using Labview and Matlab.

Instantaneous velocities in the x-direction were measured using a constant temperature hot-wire probe (DANTEC 54T30) and an eight-channel MINICTA anemometer system. x, y, and z are the main flow, lateral and vertical directions of the Cartesian coordinate system, respectively. The velocity signals were sampled using a 12-bit digitizer

National Instruments PCMCIA type DAQ-card 6024E. The calibrations of the hot-wire probe were conducted in a calibration tunnel by subjecting the probe to uniform flows at eleven different flow velocities.

SenSym transducers (model ASCX01DN) were used in Pitot-probe pressure measurements to determine u, which is the mean flow velocity in the x-direction. SenSym transducers were also used in pressure measurements on the vehicle model surface. The pressure transducers were placed outside the vehicle model and connected to pressure taps on the vehicle model surface using 300 mm long Tygon tubing.

The 114 mm long, 57 mm high, and 57 mm wide Plexiglas prism represents a generic van model at a simulation length scale of 1:40. This road vehicle model corresponds to a VW Transporter van in nature. Forty-five pressure taps were evenly distributed on the vehicle model surfaces with nine taps on each surface. Aerodynamic loads on the vehicle model were determined by integrating the pressures over the vehicle model surfaces.

The vehicle model was mounted on a 1 m long generic bridge-deck section model with three traffic lanes and barrier walls. In the experiments focusing on the wind gust strength and frequency, the vehicle model was placed in the center of the upwind traffic lane, Figure 3.

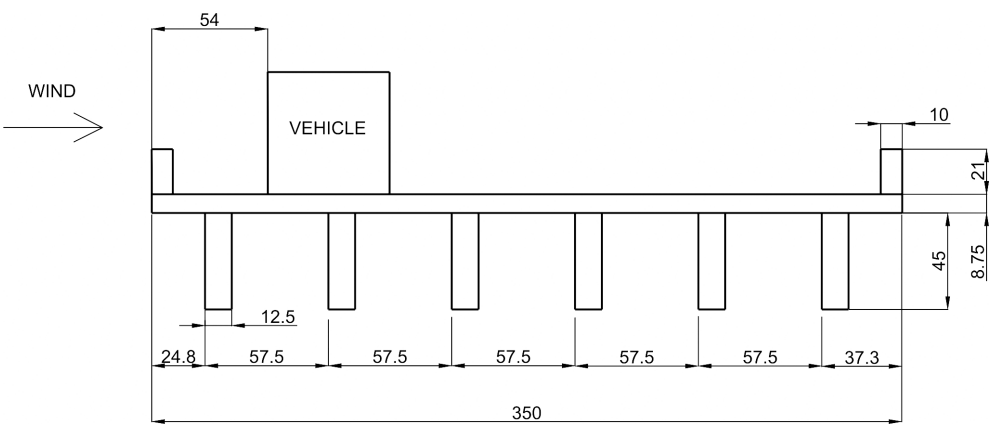

Figure 3. Vehicle model in the center of the upwind traffic lane of the bridge-deck section model with dimensions provided in mm on the model scale, Kozmar et al. (2012a)

Slika 3. Model vozila u središtu prometne trake uz naletni rub sekcije mosta s dimenzijama navedenim u mm na skali modela, Kozmar i sur. (2012a)

Another set of experiments was carried out to investigate the effect of the vertical wind incidence angle and vehicle position on the bridge on the aerodynamic loads experienced by Bora wind gusting. In these experiments, the vehicle model was placed in the center of the upwind, middle, and downwind traffic lanes, Figure 4.

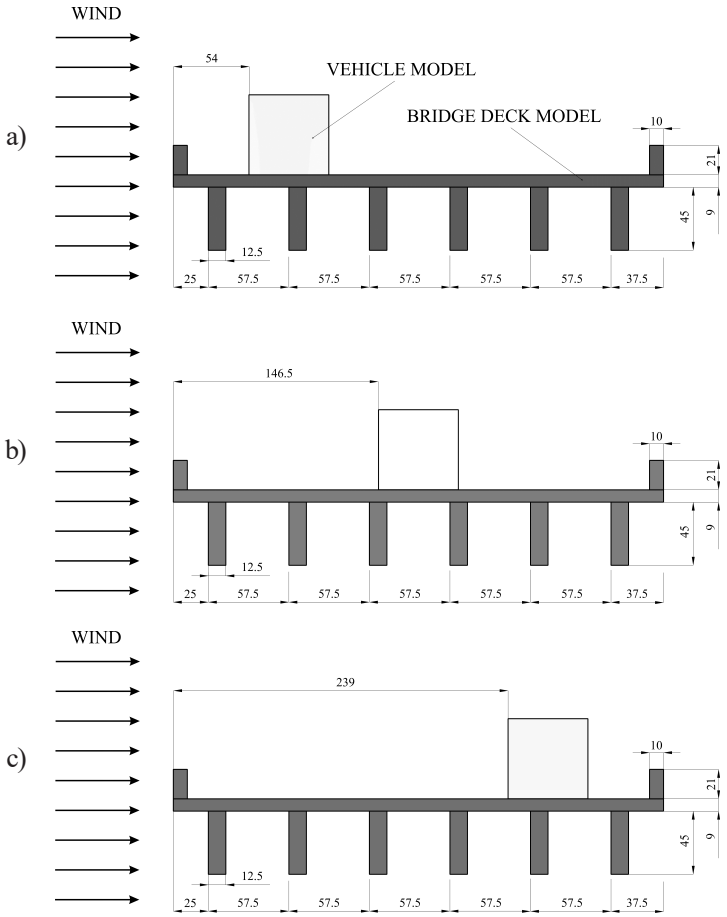

Figure 4. Experimental setup for the vehicle model on the bridge-deck section model: a) vehicle model in the upwind traffic lane; b) vehicle model in the middle traffic lane; c) vehicle model in the downwind traffic lane; all dimensions are provided in mm on the model scale, Kozmar et al. (2015)

Slika 4. Eksperimentalni postav modela vozila na modelu sekcije mosta: a) model vozila u prometnoj traci uz vjetar, b) model vozila u srednjoj prometnoj traci, c) model vozila u prometnoj traci niz vjetar; sve dimenzije su dane u mm na skali modela, Kozmar i sur. (2015)

The pedestrian pathway along the bridge is taken to be 1.45 m and a single traffic lane 3.7 m wide that gives a distance between the leading edge of the bridge deck and the vehicle center of 3.3 m, all in full-scale dimensions, i.e. 3.3 m is 82.5 mm on the model-scale calculated using the simulation length scale of 1:40. The 1.8 m full-scale height of the I-beams was selected, which is a common design of freeway bridges. All model parts were manufactured of Plexiglas on a 1:40 simulation length scale. The bridge-deck section model was placed 50 mm downstream of the nozzle exit and rigidly fixed to avoid flow disturbances.

Longitudinal turbulence intensity I_u at the position of the vehicle model (center of the cross section) was 8%, both during the gusts and 'regular' (weak) wind periods, and the maximal mean flow velocity was $\overline{u}$ = 4.5 m/s. Reynolds number (*Re*) effects were observed for *Re* < 14000. For *Re* > 14000, possible errors in the side force coefficient C_{FS} and the lift force coefficient C_{FL} are 16% and 3%, respectively, which is acceptable for the present study where the fundamental flow and loading phenomena were to be clarified. All subsequent experiments were accordingly conducted at *Re* > 14000.

The side force F_S and overturning (rolling) moment M_R of the vehicle were studied because they are generally considered important parameters when investigating the cross-wind loading of vehicles. The effects of Bora wind gusts were simulated by exposing the vehicle model to an airflow which consisted of intermittent switching between weak wind (smaller velocity) and wind gusts (larger velocity).

The horizontal flow incidence angle on the bridge-deck section and vehicle model was 0° in all experiments. The vertical flow incidence angle α was 0° in the experiments regarding the wind gust strength and frequency, while in the experiments regarding the effects of α and the vehicle position on the bridge deck, it was in the range of $0° < \alpha < 50°$, Figure 5.

Figure 5. Vehicle model on the bridge-deck section model at various vertical flow incidence angles, Kozmar et al. (2015)

Slika 5. Model vozila na modelu sekcije mosta pri različitim vertikalnim kutovima nastrujavanja zraka, Kozmar i sur. (2015)

By varying α, the experiments aimed to simulate the Bora wind loading of vehicles in the vicinity of hills of various slope angles.

3. RESULTS

The effect of Bora wind gust strength and frequency on the aerodynamic loading of a vehicle was studied first. The gust strength ratio was determined given the maximal possible flow velocity in the TFFS, and minimal flow velocity regarding the *Re* sensitivity. While it is possible in the TFFS facility to obtain a ratio of flow gust to 'regular' wind velocity equal to 1.3, in Bora wind events in nature this ratio can be as high as five, so the effect of even stronger wind gusts on vehicles remains to be studied in the future. The time history and details of five different flow velocity records (for the *u* flow velocity component in the main flow direction) characterized by the gust duration $\Delta t_G = 4$ s and the duration of 'regular' wind events $\Delta t_R = 4$ s are given in Figure 6 and Table 1. $\overline{u}_G$ is the mean flow velocity in the *x*-direction during gusts, $\overline{u}_R$ is the mean flow velocity in the *x*-direction during 'regular' (weak wind) periods, *t* is the time, Δt_G is the time duration of gusts, and Δt_R is the time duration of 'regular' wind events.

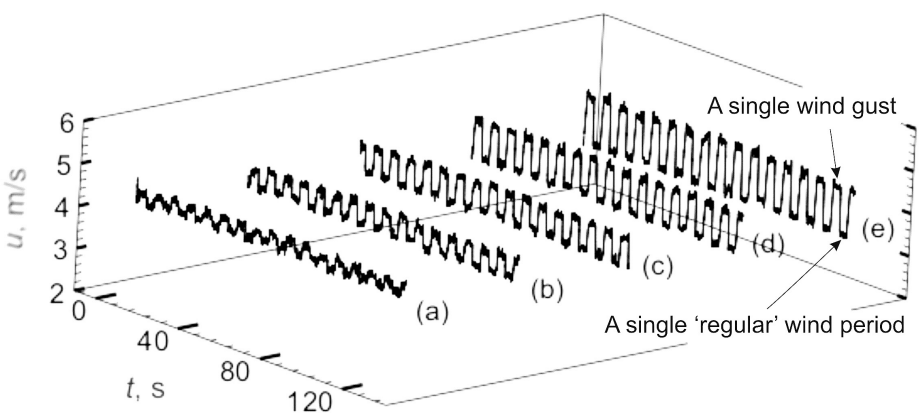

Figure 6. Velocity records for five gust strengths characterized by $\Delta t_R = 4$ s and $\Delta t_G = 4$ s, Kozmar et al. (2012a)

Slika 6. Zapisi brzine za pet jakosti udara bure karakteriziranih s $\Delta t_R = 4$ s i $\Delta t_G = 4$ s, Kozmar i sur. (2012a)

Table 1. Details of velocity time records shown in Figure 6 characterized by $\Delta t_R = 4$ s and $\Delta t_G = 4$ s, Kozmar et al. (2012a)

Tablica 1. Pojedinosti vremenskih zapisa brzine prikazanih na slici 6, karakteriziranih s $\Delta t_R = 4$ s i $\Delta t_G = 4$ s, Kozmar i sur. (2012a)

	(a)	(b)	(c)	(d)	(e)
$\overline{u}_R$, m/s	4.24	4.03	3.85	3.65	3.44
$\overline{u}_G$, m/s	4.45	4.45	4.45	4.45	4.46
$\overline{u}_G / \overline{u}_R$	1.05	1.10	1.16	1.22	1.30

The experiments were also conducted for $\Delta t_R = 3$ s and $\Delta t_G = 2$ s, and for $\Delta t_R = 2$ s and $\Delta t_G = 3$ s, Tables 2 and 3, respectively.

Table 2. Details of velocity time records characterized by $\Delta t_R = 3$ s and $\Delta t_G = 2$ s, Kozmar et al. (2012a)

Tablica 2. Pojedinosti vremenskih zapisa brzine karakteriziranih s $\Delta t_R = 3$ s i $\Delta t_G = 2$ s, Kozmar i sur. (2012a)

	(f)	(g)	(h)	(i)	(j)
$\overline{u}_R$, m/s	4.42	4.19	3.92	3.71	3.44
$\overline{u}_G$, m/s	4.62	4.64	4.58	4.59	4.56
$\overline{u}_G / \overline{u}_R$	1.05	1.11	1.17	1.24	1.33

Table 3. Details of velocity time records characterized by Δt_R = 2 s and Δt_G = 3 s, Kozmar et al. (2012a)

Tablica 3. Pojedinosti vremenskih zapisa brzine karakteriziranih s Δt_R = 2 s i Δt_G = 3 s, Kozmar i sur. (2012a)

	(k)	(l)	(m)	(n)	(o)
$\overline{u}_R$, m/s	4.34	4.12	3.91	3.67	3.41
$\overline{u}_G$, m/s	4.55	4.55	4.57	4.56	4.52
$\overline{u}_G / \overline{u}_R$	1.05	1.10	1.17	1.24	1.33

Each experiment consisted of twenty 'gust' events and twenty 'regular' wind events. The side force and overturning (rolling) moment coefficients, i.e. C_{FS} and C_{MR}, respectively, were normalized using $\overline{u}_R$. The sign convention was based on Coleman and Baker (1994). The spatial scale L is related to the time scale T using the $L = U \cdot T$ relation, where U is the flow velocity scale. The timescales are the spatial scales divided by appropriate flow velocity. The mean 'regular' wind velocity in nature can be taken as 16 m/s. In the TFFS, the mean 'regular' wind velocity was approximately 4 m/s and the simulation length scale was 1:40. The time scale 1:10 was thus accordingly adopted.

Figures 7-9 show the dimensionless power spectral density of the longitudinal flow velocity fluctuations $f \cdot S_u(f) / \sigma_u^2$ for the time records reported in Tables 1-3, respectively. f is the frequency, $S_u(f)$ is the power spectral density, and σ_u^2 is the variance.

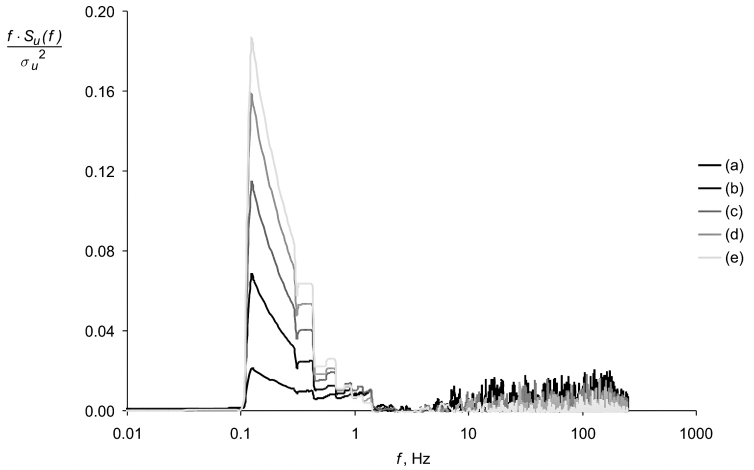

Figure 7. Power spectral density of the longitudinal velocity fluctuations of the flow velocity records presented in Table 1 (Δt_R = 4 s and Δt_G = 4 s), Kozmar et al. (2012a)

Slika 7. Spektralna gustoća snage uzdužnih pulzacija brzine strujanja zraka za eksperimente navedene u Tablici 1 (Δt_R = 4 s and Δt_G = 4 s), Kozmar i sur. (2012a)

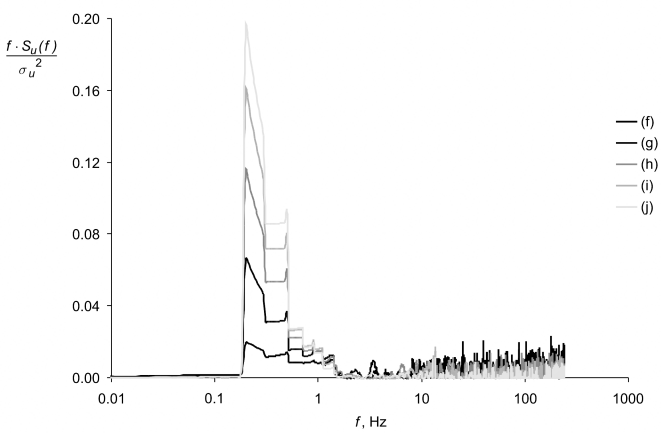

Figure 8. Power spectral density of the longitudinal velocity fluctuations of the flow velocity records presented in Table 2 (Δt_R = 3 s and Δt_G = 2 s), Kozmar et al. (2012a)

Slika 8. Spektralna gustoća snage uzdužnih pulzacija brzine strujanja zraka za eksperimente navedene u Tablici 2 (Δt_R = 3 s and Δt_G = 2 s), Kozmar i sur. (2012a)

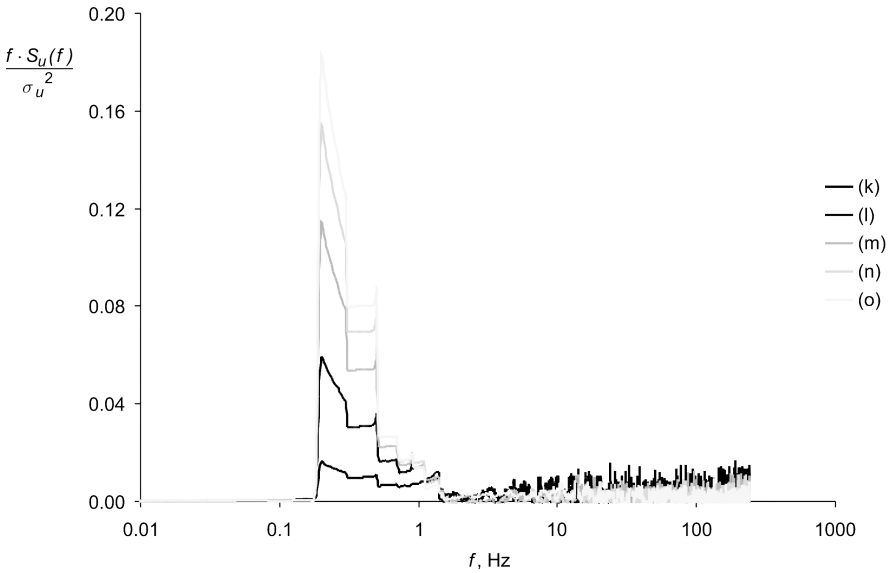

Figure 9. Power spectral density of the longitudinal velocity fluctuations of the time series presented in Table 3 (Δt_R = 2 s and Δt_G = 3 s), Kozmar et al. (2012a)

Slika 9. Spektralna gustoća snage uzdužnih pulzacija brzine strujanja zraka za eksperimente navedene u Tablici 3 (Δt_R = 2 s and Δt_G = 3 s), Kozmar i sur. (2012a)

The spectral peak can be observed at 0.125 Hz for the (a) to (e) records, and at 0.2 Hz for (f) to (o), which is the effect of intermittent switching between lower and higher flow velocity. These spectral peaks correspond to wind gusts from 50 s to 80 s duration in nature. Another important feature is the energy distribution during wind gusts as the energy of the spectral peaks increases when the wind gusting becomes stronger, i.e. at higher $\overline{u}_G/\overline{u}_R$ ratios. This trend was observed for all repetition rates of the wind gusting.

These flow features have important implications for the steady aerodynamic loading of vehicles, Figures 10 and 11. C_{FS}^{gust} is the mean side force during gusts and $C_{FS}^{regular}$ is the mean side force in 'regular' wind.

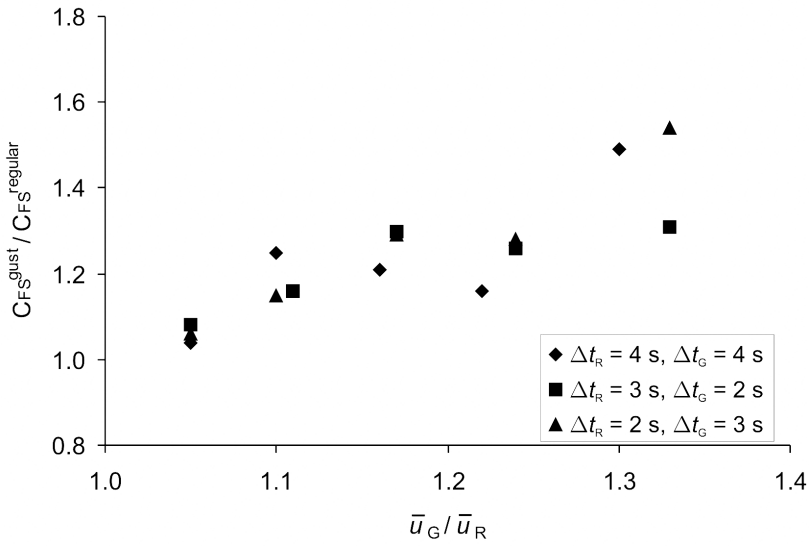

Figure 10. Mean side force experienced by a vehicle for various wind gust strengths and frequencies, Kozmar et al. (2012a)

Slika 10. Prosječna bočna sila vozila za različite jačine i frekvencije udara vjetra, Kozmar i sur. (2012a)

The mean side force ($C_{FS}^{gust} / C_{FS}^{regular}$ ratio) increases linearly with an increase in the gust strength ($\overline{u}_G / \overline{u}_R$), where both C_{FS}^{gust} and $C_{FS}^{regular}$ were normalized using the same mean flow velocity $\overline{u}_R$. The average increase in the mean side force is about 16% larger than the increase in the mean flow velocity for all repetition rates. For the same $\overline{u}_G / \overline{u}_R$ ratio, $C_{FS}^{gust} / C_{FS}^{regular}$ is within the ±12% margin.

Figure 11 shows an increase in the mean overturning moment around the vehicle center with an increase in the mean flow velocity.

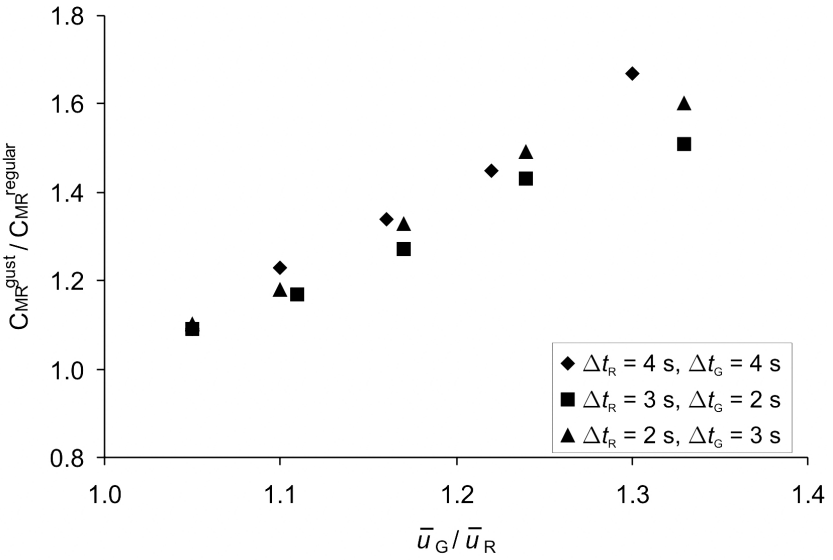

Figure 11. Mean overturning moment experienced by a vehicle for various wind gust strengths and frequencies, Kozmar et al. (2012a)

Slika 11. Prosječni moment prevrtanja vozila za različite jačine i učestalosti udara vjetra, Kozmar i sur. (2012a)

C_{MR}^{gust} is the mean overturning moment in wind gusts, and $C_{MR}^{regular}$ is the mean overturning moment in 'regular' wind. M_R was calculated by integrating the moments over the respective model surface around the center of gravity height using the pressure results over the vertical surfaces of the vehicle and its roof.

The mean overturning moment increases twice as strongly as the mean flow velocity, i.e. for a 10% increase in velocity, the overturning moment increases by 20%. For the same $\bar{u}_G / \bar{u}_R$ ratio, the recorded $C_{MR}^{gust} / C_{MR}^{regular}$ is within the ±10% margin.

The frequency of wind gusts does not have a considerable effect on the mean side force and mean overturning moment as the results indicate the same trends in all these configurations.

Unsteady aerodynamic loads are particularly relevant for the dynamic stability of vehicles. In order to investigate this complex phenomenon, the side force and overturning moment fluctuations of the vehicle were analyzed, Figures 12-17. $S_{FS}(f)$ is the power spectral density of the side force fluctuations, and σ_{FS}^2 is their variance. $S_{MR}(f)$ is the power spectral density and σ_{MR}^2 is the variance of the overturning moment fluctuations.

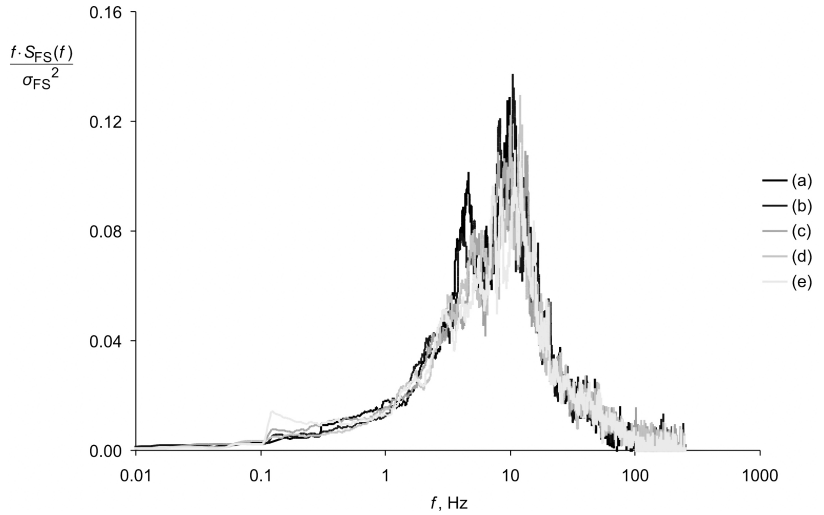

Figure 12. Power spectral density of the side force fluctuations for the time series presented in Table 1 (Δt_R = 4 s and Δt_G = 4 s), Kozmar et al. (2012a)

Slika 12. Spektralna gustoća snage pulzacija bočne sile za eksperimente navedene u Tablici 1 (Δt_R = 4 s and Δt_G = 4 s), Kozmar i sur. (2012a)

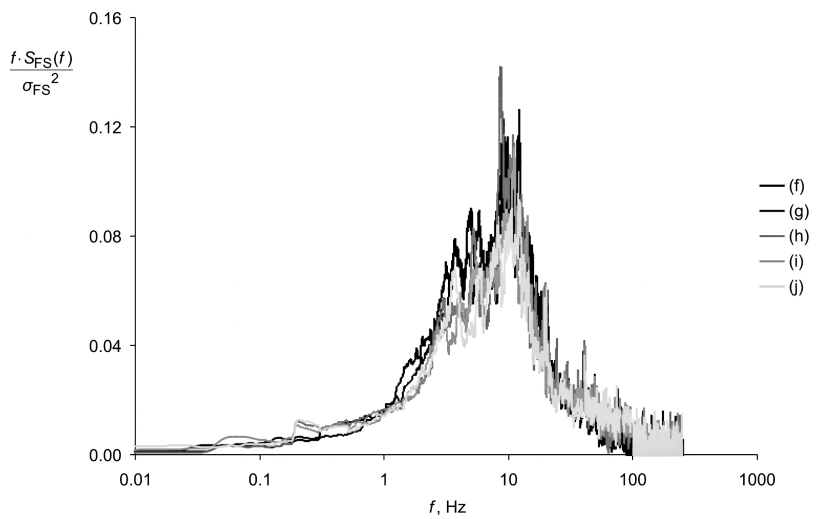

Figure 13. Power spectral density of the side force fluctuations for the time series presented in Table 2 (Δt_R = 3 s and Δt_G = 2 s), Kozmar et al. (2012a)

Slika 13. Spektralna gustoća snage pulzacija bočne sile za eksperimente navedene u Tablici 2 (Δt_R = 3 s and Δt_G = 2 s), Kozmar i sur. (2012a)

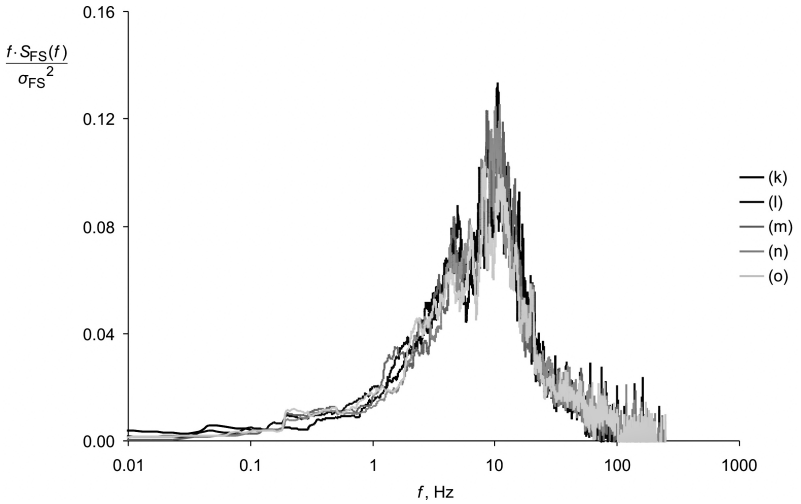

Figure 14. Power spectral density of the side force fluctuations for the time series presented in Table 3 (Δt_R = 2 s and Δt_G = 3 s), Kozmar et al. (2012a)

Slika 14. Spektralna gustoća snage pulzacija bočne sile za eksperimente navedene u Tablici 3 (Δt_R = 2 s and Δt_G = 3 s), Kozmar i sur. (2012a)

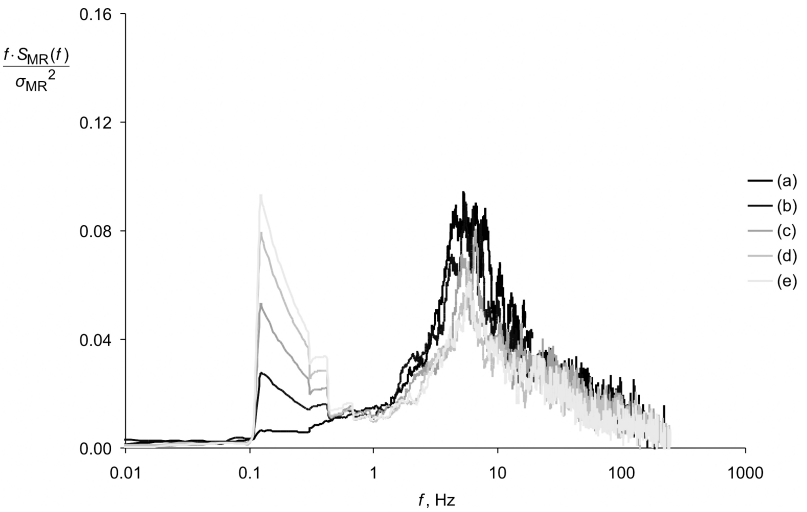

Figure 15. Power spectral density of the overturning moment fluctuations for the time series presented in Table 1 (Δt_R = 4 s and Δt_G = 4 s), Kozmar et al. (2012a)

Slika 15. Spektralna gustoća snage pulzacija momenta prevrtanja za eksperimente navedene u Tablici 1 (Δt_R = 4 s and Δt_G = 4 s), Kozmar i sur. (2012a)

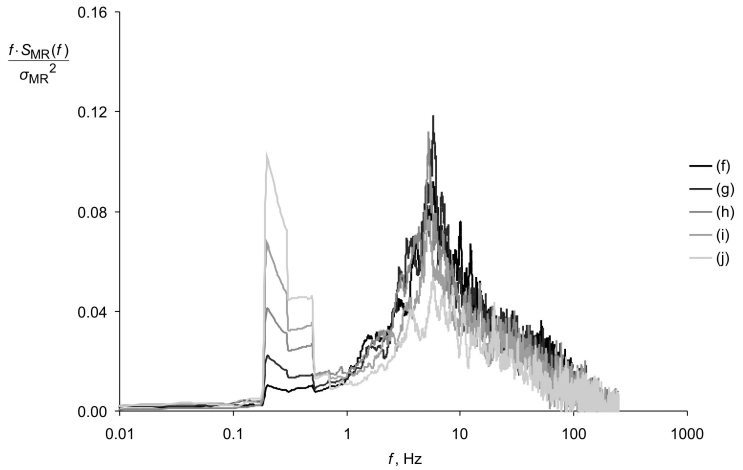

Figure 16. Power spectral density of the overturning moment fluctuations for the time series presented in Table 2 (Δt_R = 3 s and Δt_G = 2 s), Kozmar et al. (2012a)

Slika 16. Spektralna gustoća snage pulzacija momenta prevrtanja za eksperimente navedene u Tablici 2 (Δt_R = 3 s and Δt_G = 2 s), Kozmar i sur. (2012a)

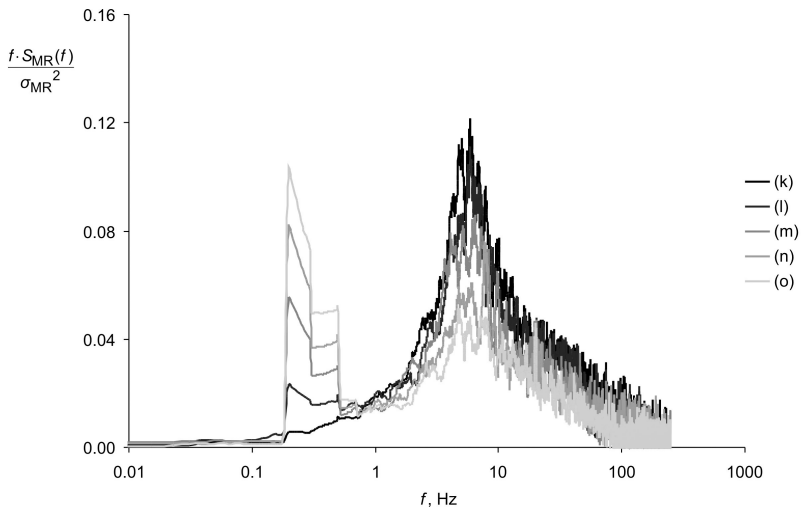

Figure 17. Power spectral density of the overturning moment fluctuations for the time series presented in Table 3 (Δt_R = 2 s and Δt_G = 3 s), Kozmar et al. (2012a)

Slika 17. Spektralna gustoća snage pulzacija momenta prevrtanja za eksperimente navedene u Tablici 3 (Δt_R = 2 s and Δt_G = 3 s), Kozmar i sur. (2012a)

For the F_S fluctuations, a distinct peak at 10 Hz due to buffeting vortices shed from the bridge deck is present in all configurations. The gust strength and frequency have negligible effects on the peak frequency and magnitude. The Strouhal number $St = fD/\overline{u} \sim 0.075$ was calculated using the peak frequency $f = 10$ Hz, $D \sim 0.03$ m (bridge-deck height including the barrier) and $\overline{u} = 4$ m/s, which is close to $St = 0.1$, a value which has commonly been accepted for the flow separation from bridge decks, Ryall et al. (2000).

Three spectral peaks are observed in the M_R fluctuations. These are low-frequency peaks at 0.125 Hz and 0.2 Hz (0.0125 Hz and 0.02 Hz full-scale) and the high-frequency peak at ~10 Hz (~1 Hz full-scale).

The low-frequency peak corresponds to the peak in the freestream wind spectrum. The high-frequency peak is a consequence of the vortex shedding from the bridge and the vehicle. This high-frequency peak is also observed in the F_S spectra. These results indicate that the M_R is concurrently affected by the vortex shedding and wind gusting phenomena. The low-frequency peak becomes stronger and the high-frequency peak weaker as the wind-gust strength increases. At the same time, the energy excited by the vortex shedding phenomenon decreases.

Another segment of work addressed the effect of α and the vehicle position on the bridge deck on the aerodynamic loads acting on the vehicle. In these experiments, the effects of Bora wind gusts were simulated by subjecting the vehicle and bridge-deck section models to an airflow which consisted of intermittent switching between 'regular' wind and wind gusts each 3 s. A portion of this velocity time record is shown in Figure 18.

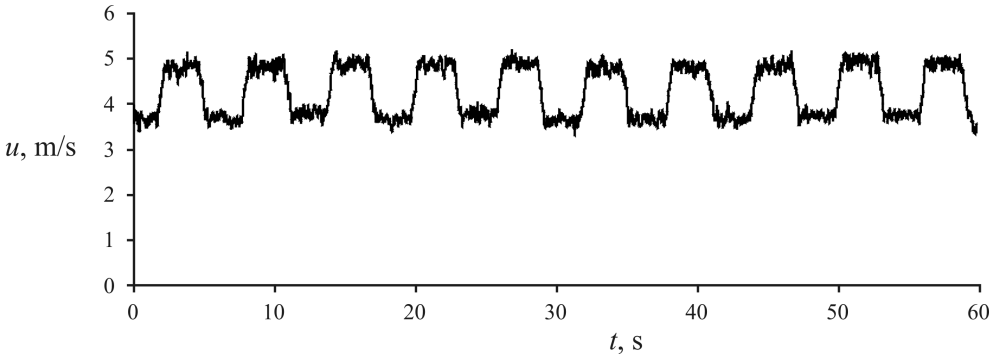

Figure 18. A portion of the studied velocity time record, Kozmar et al. (2015)

Slika 18. Dio vremenskog zapisa brzine, Kozmar i sur. (2015)

Steady aerodynamic loads, i.e. F_S and M_R, of the vehicle in the upwind and middle traffic lanes of the bridge deck subjected to Bora gusting were analyzed at various α, Figures 19 and 20. F_S and M_R were normalized using their respective values at $\alpha = 10^o$.

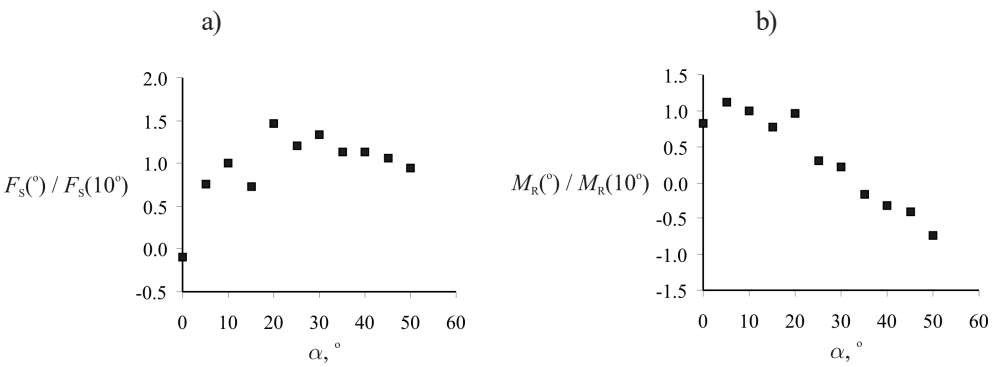

Figure 19. F_S and M_R of the vehicle in the upwind traffic lane at α = 0°, 5°, 10°, 15°, 20°, 25°, 30°, 35°, 40°, 45°, 50°; the horizontal flow incidence angle is 0°, Kozmar et al. (2015)

Slika 19. F_S i M_R vozila u prometnoj traci uz vjetar pri α = 0°, 5°, 10°, 15°, 20°, 25°, 30°, 35°, 40°, 45°, 50°; horizontalni kut nastrujavanja zraka je 0°, Kozmar i sur. (2015)

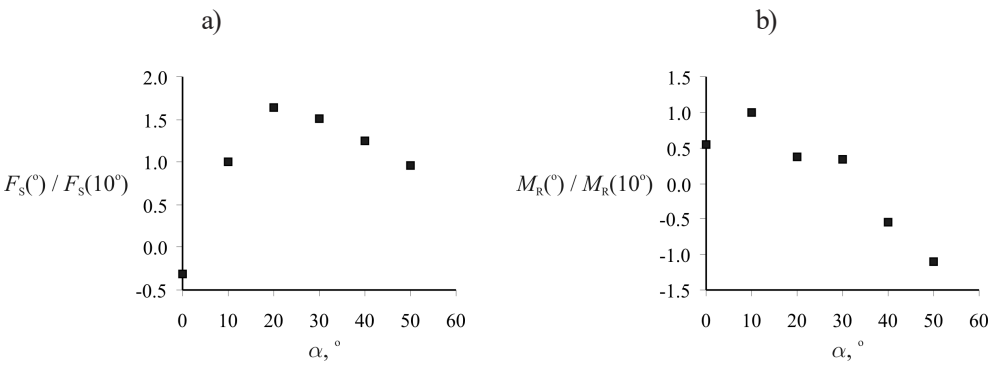

Figure 20. F_S and M_R of the vehicle in the middle traffic lane at α = 0°, 10°, 20°, 30°, 40°, 50°; the horizontal flow incidence angle is 0°, Kozmar et al. (2015)

Slika 20. F_S i M_R vozila u srednjoj prometnoj traci pri α = 0°, 10°, 20°, 30°, 40°, 50°; horizontalni kut nastrujavanja zraka je 0°, Kozmar i sur. (2015)

The trends observed for a vehicle in the upwind and middle traffic lanes are similar. F_S is minimal at $\alpha = 0^o$ because the barrier wall at the upwind leading edge of the bridge-deck section shelters the vehicle. With an increasing α, the vehicle becomes more exposed to the flow and the F_S reaches its maximum at $\alpha \sim 20^o$. With a further rise in α, the F_S decreases.

Small wind incidence angles around $\alpha = 10^o$ are critical in the context of the M_R, a trend which is present for both vehicle positions on the bridge deck. With a further gain in α, the M_R decreases. This trend at small α is due to: a) slight negative pressures on the upwind vehicle surface close to the ground due to the flow separating from the barrier wall and a consequent flow recirculation between the barrier wall and the upwind vehicle surface; or b) negative pressures on the vehicle top surface due to the flow separation. The higher risk for vehicles in these configurations is at $\alpha < 30^o$.

In order to analyze the unsteady aerodynamic loading of vehicles on bridges subjected to the Bora wind, S_{FS}, S_{MR} and the respective fluctuating (rms) aerodynamic coefficients $C_{FS,rms}$ and $C_{MR,rms}$ were studied.

Figures 21, 22, 23 show S_u in the freestream flow, and S_{FS} and S_{MR} along with their respective $C_{FS,rms}$ and $C_{MR,rms}$, respectively, all for the vehicle in the upwind traffic lane.

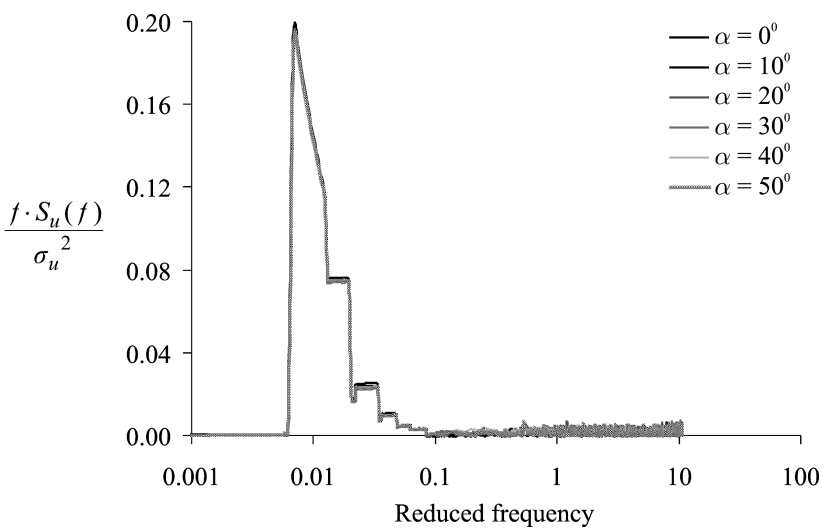

Figure 21. Power spectral density of the longitudinal flow velocity fluctuations, Kozmar et al. (2015)

Slika 21. Spektralna gustoća snage uzdužnih pulzacija brzine strujanja zraka, Kozmar i sur. (2015)

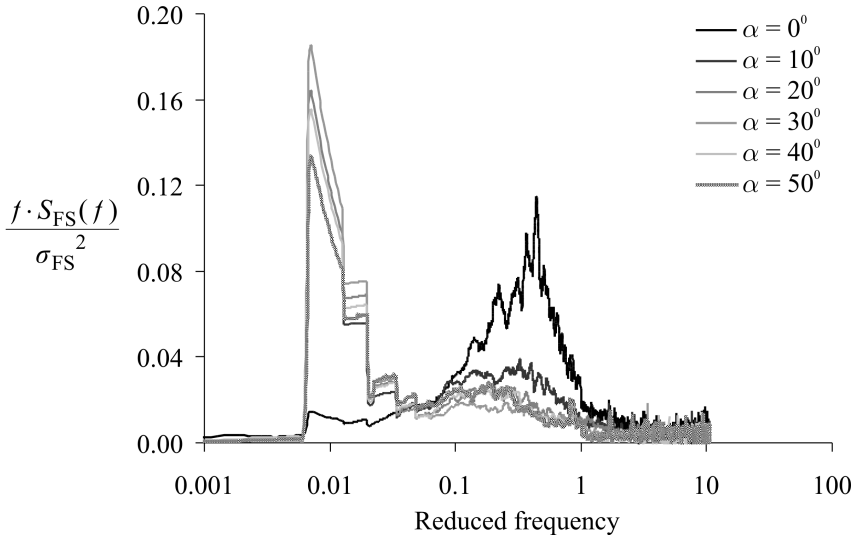

α, °	0	10	20	30	40	50
$C_{FS,rms}$, -	0.37	0.47	0.49	0.54	0.44	0.38

Figure 22. Power spectral density and $C_{FS,rms}$ of the side force fluctuations, Kozmar et al. (2015)
Slika 22. Spektralna gustoća snage i $C_{FS,rms}$ pulzacija bočne sile, Kozmar i sur. (2015)

α, °	0	10	20	30	40	50
$C_{MR,rms}$, -	0.22	0.22	0.19	0.16	0.14	0.15

Figure 23. Power spectral density and $C_{MR,rms}$ of the overturning moment fluctuations, Kozmar et al. (2015)
Slika 23. Spektralna gustoća snage i $C_{MR,rms}$ pulzacija momenta prevrtanja, Kozmar i sur. (2015)

In the velocity power spectra, there is a low-frequency peak which is a consequence of intermittent switching between lower and higher flow velocity. In the power spectra of the unsteady aerodynamic loads experienced by the vehicle, two peaks can be observed. The low-frequency peak at the same frequency as the characteristic frequency of the freestream wind gusting is due to the impact of the wind gusts. The high-frequency peak is attributed to the vortices shed from the bridge and their interactions with the vehicle model.

With an increasing α, the effects of shed vortices decrease, as exhibited by a weaker high-frequency peak in the power spectra of the unsteady aerodynamic loads experienced by the vehicle. $C_{FS,rms}$ reaches a maximum at $\alpha = 30^{o}$, while $C_{MR,rms}$ is maximal at $\alpha = 0^{o}$.

Another important aspect of the Bora cross-wind gusting of vehicles is the position of the vehicle on the bridge deck. To analyze this issue, steady aerodynamic loads for a vehicle placed in the upwind, middle, and downwind traffic lanes at vertical and horizontal wind incidence angles of 0^{o} are shown in Figure 24. The F_S and M_R are normalized using their respective results recorded for the vehicle in the upwind traffic lane.

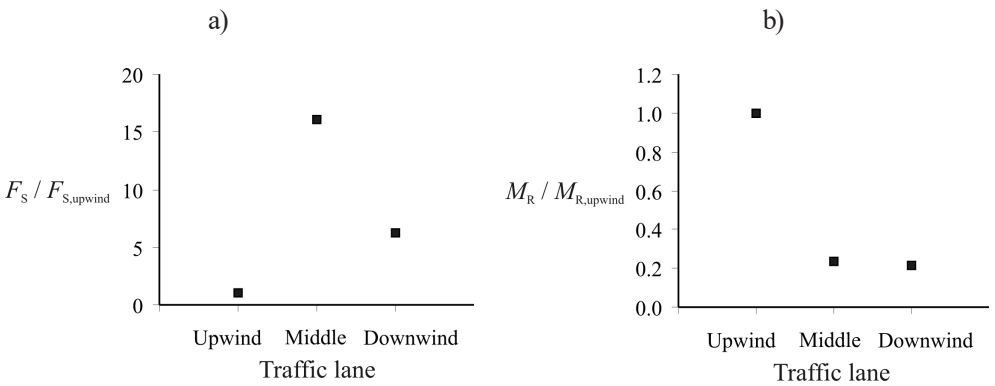

Figure 24. F_S and M_R of the vehicle in the upwind, middle, and downwind traffic lanes of the bridge-deck section, Kozmar et al. (2015)

Slika 24. F_S and M_R vozila u prometnim trakama uz vjetar, sredinu i niz vjetar na sekciji mosta, Kozmar i sur. (2015)

F_S is maximal in the middle traffic lane, while the M_R is maximal in the upwind traffic lane. These results indicate that in regard to steady aerodynamic loading, vehicles on bridges are more vulnerable when closer to the upwind edge of the bridge decks.

Figures 25, 26, 27 show S_u in the freestream flow, and S_{FS} and S_{MR} along with their respective $C_{FS,rms}$ and $C_{MR,rms}$ for a vehicle in the upwind, middle, and downwind traffic lanes, respectively, at horizontal and vertical flow incidence angles of 0^{o}.

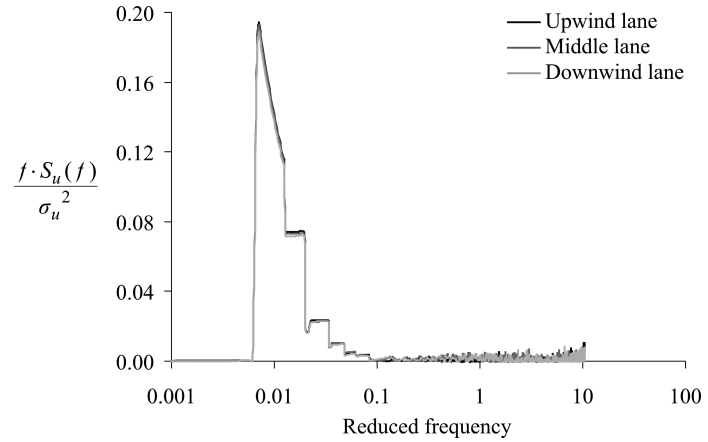

Figure 25. Power spectral density of longitudinal flow velocity fluctuations depending on the position of the vehicle on the bridge-deck section, Kozmar et al. (2015)

Slika 25. Spektralna gustoća snage uzdužnih pulzacija brzine strujanja zraka ovisno o položaju vozila na sekciji mosta, Kozmar i sur. (2015)

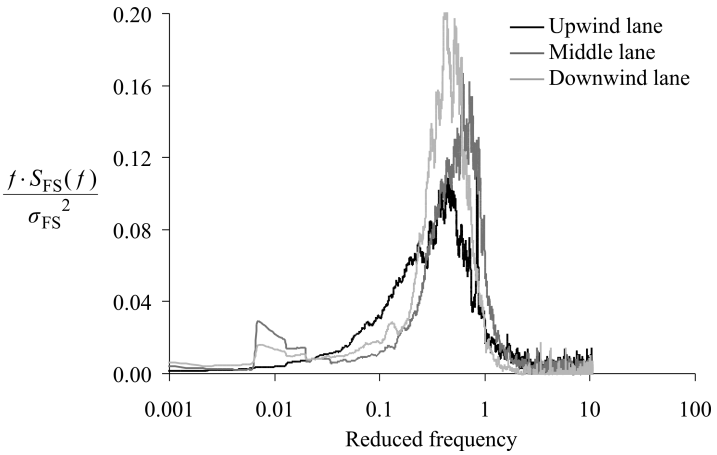

Traffic lane	Upwind	Middle	Downwind
$C_{FS,rms}$, -	0.31	0.45	0.42

Figure 26. Power spectral density and $C_{FS,rms}$ of the side force fluctuations depending on the vehicle position on the bridge-deck section, Kozmar et al. (2015)

Slika 26. Spektralna gustoća snage i $C_{FS,rms}$ pulzacija bočne sile ovisno o položaju vozila na sekciji mosta, Kozmar i sur. (2015)

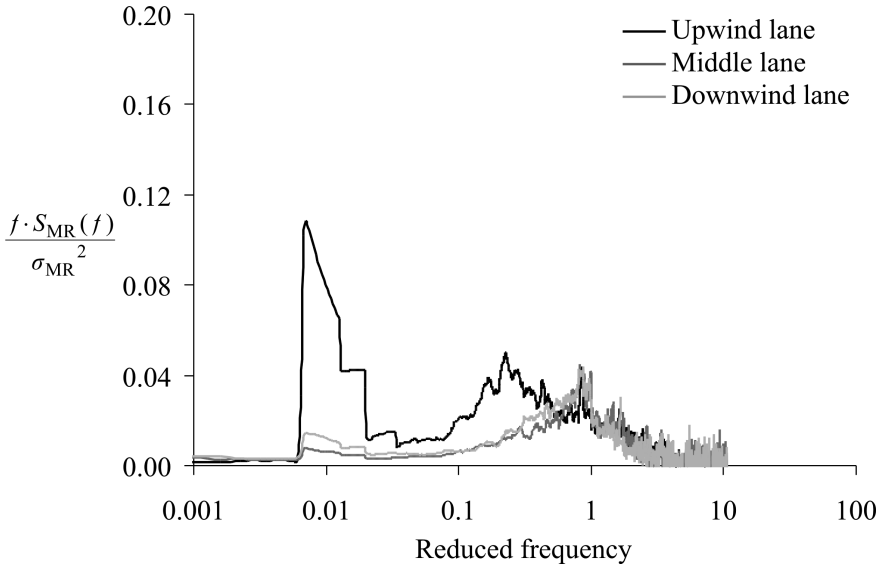

Traffic lane	Upwind	Middle	Downwind
$C_{MR,rms}$, -	0.24	0.20	0.18

Figure 27. Power spectral density and $C_{MR,rms}$ of the overturning moment fluctuations depending on the vehicle position on the bridge-deck section, Kozmar et al. (2015)

Slika 27. Spektralna gustoća snage i $C_{MR,rms}$ pulzacija momenta prevrtanja ovisno o položaju vozila na sekciji mosta, Kozmar i sur. (2015)

As the vehicle is placed in the downstream traffic lanes, the high-frequency peak in the F_S fluctuations due to shed vortices becomes stronger. The low-frequency peak in the F_S fluctuations due to wind gusting is small for all three traffic lanes.

The low-frequency M_R fluctuations due to wind gusting are the strongest in the upwind traffic lane and negligible in the downwind traffic lanes. This indicates a weakening of the wind gusting effects on the M_R fluctuations when the vehicle is placed further downstream of the bridge-deck leading edge. The high-frequency M_R fluctuations due to shed vortices have nearly the same amplitude in all three traffic lanes, while they are slightly shifted to higher frequencies in the two downwind traffic lanes.

The $C_{FS,rms}$ coefficient is larger in the two downwind traffic lanes compared to the upwind traffic lane which is a consequence of an increase in the high-frequency peak due to shed vortices. This indicates a more dominant role of shed vortices in the F_S fluc-

tuations when the vehicle is placed further downstream of the bridge-deck leading edge. This is because of the reattachment of the flow that separated at the bridge-deck leading edge, a flow which subsequently hits the vehicle.

These unsteady aerodynamic loads reveal that the wind gusting frequency of local atmospheric winds can create difficulties in vehicle maneuvering and stability, particularly in the upwind traffic lane. The vulnerability of vehicles in the downwind traffic lanes is predominantly a consequence of shed vortices, which develop characteristics for a particular bridge architecture and the aerodynamic form of vehicles.

4. CONCLUSIONS

The Bora is a very strong and gusty downslope wind. It creates substantial aerodynamic loading and occasional dynamic instability of vehicles. Bora wind effects on road vehicles are currently not fully understood, which provided motivation for this work. In the present study, the experimental analysis of Bora wind loads on road vehicles is presented, and provides the authors' most relevant findings on this topic so far.

The experiments were carried out in the Transient Flow Field Simulator of the NatHaz Modeling Laboratory at the University of Notre Dame, USA. A vehicle model on the bridge-deck section model was subjected to an airflow which simulated Bora wind gusts. The analysis is based on the side force and overturning moment of the vehicle because these are the key parameters regarding aerodynamic loads acting on vehicles. These parameters were studied for various strengths and frequencies of Bora wind gusts, vertical wind incidence angles, and vehicle positions on the bridge deck.

In the experiments regarding the wind gust strength and frequency, the vehicle model was placed in the upwind traffic lane at zero horizontal and vertical flow incidence angles, where the flow perpendicularly impinged on the side surface of the vehicle model. The effect of the vertical wind incidence angle and vehicle position was analyzed for the vehicle model placed in the upwind, middle, and downwind traffic lanes of the bridge-deck section model. In these experiments, the horizontal flow incidence angle was zero, while the vertical flow incidence angle was studied from 0° to 50°. By varying the vertical flow incidence angle, these experiments aimed to simulate Bora wind loads on vehicles in the vicinity of hills characterized by various slope angles.

Regarding the wind gust strength and frequency experiments, the aerodynamic loads increase linearly with an increase in the gust strength. The average growth in the mean side force is ~16% higher than the increase in the mean flow velocity. The mean overturning moment increases twice as much as the mean flow velocity. The gust

strength and frequency have negligible effects on the peak frequency and magnitude. There is a peak in the side force spectra at frequencies corresponding to the energy contents exerted by the vortices shed from the bridge deck. In the overturning moment fluctuations, the low-frequency peak corresponds to the peak in the freestream wind spectrum, while the high-frequency peak is a consequence of the vortex shedding from the bridge deck and the vehicle. These results indicate that the overturning moment of the vehicle is concurrently influenced by the vortex shedding and wind gusting phenomena.

In the context of Bora wind loads acting on vehicles at various vertical wind incidence angles and vehicle positions on the bridge deck, steady aerodynamic loads on the vehicle are generally higher for vehicles closer to the upwind edge of the bridge decks.

The effect of the shed vortices on the side force fluctuations is dominant in the downstream traffic lanes, while the overturning moment fluctuations are at a maximum in the upwind traffic lane. These unsteady aerodynamic loads reveal that Bora wind gusting can create difficulties in vehicle maneuvering and stability in the upwind traffic lane, while the risk for vehicles in the downwind traffic lanes is predominantly a consequence of shed vortices, which depend on the particular bridge architecture and the aerodynamic form of the vehicles.

5. ACKNOWLEDGEMENTS

The first author acknowledges the support of the Fulbright Foundation and the University of Zagreb, Croatia. Support for the second author was partially provided by the Global Center of Excellence, Tokyo Polytechnic University, funded by the Japanese Ministry of Education, Culture, Sports, Science and Technology (MEXT) in the framework of the project on load effects in transient flow conditions. Special thanks go to Mr. Brent Bach for manufacturing the experimental models.

6. REFERENCES

Bajić A (1988). The strongest Bora event during ALPEX SOP, *Rasprave-Papers* 23**,** 1-12.

Bajić A (1989). Severe Bora on the northern Adriatic. Part I: Statistical analysis, *Rasprave-Papers* 24, 1-9.

Baker CJ (1986). A simplified analysis of various types of wind-induced road vehicle accidents, *Journal of Wind Engineering and Industrial Aerodynamics* 22(1), 69-85.

Baker CJ (1987). Measures to control vehicle movement at exposed sites during windy periods, *Journal of Wind Engineering and Industrial Aerodynamics* 25(2), 151-161.

Baker CJ (1991a). Ground vehicles in high cross winds. 2. Unsteady aerodynamic forces, *Journal of Fluids and Structures* 5(1), 91-111.

Baker CJ (1991b). Ground vehicles in high cross winds. 3. The interaction of aerodynamic forces and the vehicle system, *Journal of Fluids and Structures* 5(2), 221-241.

Baker CJ (1991c). Ground vehicles in high cross winds. 1. Steady aerodynamic forces, *Journal of Fluids and Structures* 5(1), 69-90.

Baker CJ, Robinson CG (1990). The assessment of wind tunnel testing techniques for ground vehicles in cross winds, *Journal of Wind Engineering and Industrial Aerodynamics* 33(1-2), 429-438.

Baker CJ, Reynolds S (1992). Wind-induced accidents of road vehicles, *Accident Analysis and Prevention* 24(6), 559-575.

Bearman PW, Mullarkey SP (1994). Aerodynamic Forces on Road Vehicles due to Steady Side Winds and Gusts, Vehicle Aerodynamics Conference, Loughborough, United Kingdom.

Belušić D, Klaić, ZB (2004). Estimation of Bora wind gusts using a limited area model, *Tellus A: Dynamic Meteorology and Oceanography* 56(4), 296-307.

Belušić D, Klaić ZB (2006). Mesoscale dynamics, structure and predictability of a severe Adriatic Bora case, *Meteorologische Zeitschrift* 15(2), 157-168.

Belušić D, Hrastinski M, Večenaj Ž, Grisogono B (2013). Wind regimes associated with a mountain gap at the northeastern Adriatic Coast, *Journal of Applied Meteorology and Climatology* 52(9), 2089-2105.

Coleman SA, Baker CJ (1994). An experimental study of the aerodynamic behavior of high sided lorries in cross winds, *Journal of Wind Engineering and Industrial Aerodynamics* 53(3), 401-429.

Enger L, Grisogono B (1998). The response of bora-type flow to sea surface temperature, *Quarterly Journal of the Royal Meteorological Society* 124(548), 1227–1244.

Grisogono B, Belušić D (2009). A review of recent advances in understanding the meso- and micro-scale properties of the severe Bora wind, *Tellus A* 61(1), 1-16.

Hangan H, Kareem A (2021). The Oxford Handbook of Non-synoptic Wind Storms Hazards, Oxford University Press, Oxford, United Kingdom.

Horvath K, Ivatek-Šahdan S, Ivančan-Picek B, Grubišić V (2009). Evolution and Structure of Two Severe Cyclonic Bora Events: Contrast between the Northern and Southern Adriatic, *Weather and Forecasting* 24(4), 946-964.

Jeromel M, Malačič V, Rakovec J (2009). Weibull distribution of bora and sirocco winds in the northern Adriatic Sea, *Geofizika* 26(1), 85-100.

Jurčec V (1981). On mesoscale characteristics of Bora conditions in Yugoslavia, *Pure and Applied Geophysics* 119**,** 640-657.

Kozmar H, Butler K, Kareem A (2009). Aerodynamic loads on a vehicle exposed to cross-wind gusts: An experimental study, 7th Asia-Pacific Conference on Wind Engineering, Taipei, Taiwan.

Kozmar H, Butler K, Kareem A (2011). Effects of cross-wind gust strength on vehicle aerodynamics, 13th International Conference on Wind Engineering, Amsterdam, The Netherlands.

Kozmar H, Butler K, Kareem A (2012a). Transient cross-wind aerodynamic loads on a generic vehicle due to bora gusts, *Journal of Wind Engineering and Industrial Aerodynamics* 111, 73-84.

Kozmar H, Butler K, Kareem A (2012b). Aerodynamic loads on vehicles due to the gusty bora wind, 7th International Congress of Croatian Society of Mechanics, Zadar, Croatia.

Kozmar H, Butler K, Kareem A (2015). Downslope gusty wind loading of vehicles on bridges, *Journal of Bridge Engineering* 20(11), 04015008-1-04015008-11.

Kozmar H (2017). Characteristics of downslope windstorms for engineering applications [Special issue], *Wind and Structures* 24(6).

Lepri P, Kozmar H, Večenaj Ž, Grisogono B (2014). A summertime near-ground velocity profile of the Bora wind, *Wind and Structures* 19(5), 505-522.

Lepri P, Večenaj Ž, Kozmar H, Grisogono B (2015). Near-ground turbulence of the Bora wind in summertime, *Journal of Wind Engineering and Industrial Aerodynamics* 147, 345-357.

Lepri P, Večenaj Z, Kozmar H, Grisogono B (2017). Bora wind characteristics for engineering applications, *Wind and Structures* 24(6), 579-611.

Petkovšek Z (1987). Main Bora gusts - a model explanation, *Geofizika* 4, 41-50.

Poje D (1992). Wind persistence in Croatia, *International Journal of Climatology* 12(6), 569-586.

Ryall MJ, Parke GAR, Harding JE (2000). The Manual of Bridge Engineering, Thomas Telford, London, United Kingdom.

Ryan A, Dominy RG (1998). Aerodynamic forces induced on a passenger vehicle in response to a transient cross-wind gust at a relative incidence of 30^{o}, *SAE Transactions 107(6): Journal of Passenger Cars*, 958-966.

Tutiš V (1988). Bora on the Adriatic Coast during ALPEX SOP on 27 to 30 April 1982, *Rasprave-Papers* 23, 45-56.

Večenaj Ž, Belušić D, Grisogono B (2010). Characteristics of the near-surface turbulence during a bora event, *Annales Geophysicae* 28(1), 155-163.

Večenaj Ž, Belušić D, Grubišić V, Grisogono B (2012). Along-coast features of bora related turbulence, *Boundary-Layer Meteorology* 143, 527-545.

Vučetić V (1991). Statistical analysis of severe Adriatic Bora, *Croatian Meteorological Journal* 26, 41-51.

Yoshino MM (1976). Local Wind Bora, University of Tokyo Press, Tokyo, Japan.

EKSPERIMENTALNO MODELIRANJE UDARA BURE NA CESTOVNA VOZILA

Sažetak

Bura je vrlo jak i mahovit zavjetrinski vjetar koji puše iz smjera sjeveroistoka preko obalnih planinskih lanaca na istočnoj obali Jadranskog mora. Pričinjava značajne poteškoće za inženjersku infrastrukturu, promet i život općenito. Dok su učinci kvazistacionarnog turbulentnog atmosferskog graničnog sloja na cestovna vozila trenutno prilično poznati, bura stvara nestacionarna aerodinamička opterećenja na vozila, koja još uvijek nisu u potpunosti shvaćena. Stoga su utjecaji udara bure na cestovna vozila eksperimentalno ispitani. Istraživanje je provedeno na modelu cestovnog vozila, što je prema našim saznanjima prva analiza ove vrste. Poseban je naglasak na aerodinamičnim silama i momentima vozila ovisno o jačini i učestalosti udara bure, kutu nastrujavanja vjetra i položaju vozila na mostu. U eksperimentima koji se odnose na jačinu i frekvenciju udara bure, model vozila je postavljen u prometnu traku neposredno uz naletni rub sekcije mosta, pri čemu su horizontalni i vertikalni kutovi nastrujavanja jednaki nuli. Utjecaj vertikalnog kuta nastrujavanja i položaja vozila je analiziran za model vozila postavljen uz vjetar, niz vjetar i u srednjoj prometnoj traci. Pritom je horizontalni kut nastrujavanja jednak nuli, dok je utjecaj vertikalnog kuta nastrujavanja proučavan od 0° do 50°. Eksperimenti su provedeni u simulatoru polja nestacionarnog strujanja zraka u sklopu NatHaz laboratorija Sveučilišta Notre Dame u SAD-u. Rezultati su otkrili neka važna saznanja. S obzirom na jačinu i frekvenciju udara bure, aerodinamička opterećenja se linearno povećavaju s povećanjem jačine udara bure i na njih istodobno utječu pojave odvajanja vrtloga od sekcije mosta i udara vjetra. Osrednjena aerodinamička opterećenja su općenito veća kod vozila smještenih bliže naletnom bridu sekcije mosta. Udari bure mogu stvoriti poteškoće kod upravljanja vozilom i njegovom stabilnosti u prometnom traku uz naletni brid sekcije mosta, dok je rizik za vozila u drugim prometnim trakama uglavnom posljedica odvajanja vrtloga od naletnog ruba sekcije mosta, što je karakteristično za aerodinamičke oblike mosta i vozila.

Ključne riječi: Mahoviti vjetar bura, aerodinamička opterećenja cestovnih vozila, laboratorijski eksperimenti.

Hrvoje Kozmar

Faculty of Mechanical Engineering and Naval Architecture, University of Zagreb, Ivana Lučića 5, 10000 Zagreb, Croatia

Ahsan Kareem

NatHaz Modeling Laboratory, University of Notre Dame, IN 46556, Notre Dame, USA

Rad 549. Technical sciences 21(2022)

Nakladnik
HRVATSKA AKADEMIJA ZNANOSTI I UMJETNOSTI
Trg Nikole Šubića Zrinskog 11, 10000 Zagreb

Za nakladnika
Akademik Dario Vretenar, glavni tajnik

Grafička urednica i urednica na portalu Hrčak
Nina Ivanović

Digitalni identifikator objekta (DOI)
Kristina Polak Bobić

Naklada
200 primjeraka

Tisak
Stega tisak

Zagreb, veljača 2022.